From: ZBS7-Lage <ZBS7-Lage@rki.de>
To: nCoV-Lage <nCoV-Lage@rki.de>
Date: 8/12/2021 3:57:56 PM
Subject: AW: [Aufgabe ID 4089] Daten zu verlдngerter Virusausscheidung bei Delta Variante
Attachments: Shedding Infectiousness s41467-020-20568-4.pdf
SARS-CoV-2 viral loaddynamics, duration of viral sheddingand infectiousness 2020.07.25.20162107v1.full.pdf
Shedding Review fpubh-09-652842.pdf
Shedding journal.pbio.3001333.pdf
shedding eabi5273.full.pdf
Shedding Delta 2021.07.28.21261295v1.full.pdf

Liebes Lagezentrum,

in Rucksprache mit ZBS1 und in Absprache mit Abt. 1 hatten wir folgende Antwort fur die diskutierte Frage:

_____

Die Kinetik der Virusausscheidung folgt auch bei der Delta-Variante dem von SARS-CoV-2 bekannten Muster (Cevik et al 2020; Yan et al 2021; Jones et al 2021; Kissler et al 2021; sowie unsere Hinweise zur Testung auf SARS-CoV-2). Es gibt jedoch Hinweise auf eine initial hohere Viruslast. Der weitere Verlauf der Infektion scheint in den meisten Fallen analog den bisher bekannten Verlaufen zu erfolgen. Allerdings sind Falle protrahierter Ausscheidung auch uber den Tag 14 hinaus beschrieben (Chia et al 2021). Dies gilt allerdings auch fur die initiale Variante (van Kampen et al 2021).

Durch die bereits im Februar 2021 beim Entlassmanagement erfolgten Anpassungen auf mind. 14 Tage mit abschlie?endem Antigentest zur Detektion von hohen Viruslasten zu diesem Zeitpunkt ist zunachst eine weitere Beobachtung der Datenlage gerechtfertigt. Wir schlagen Wiedervorlage der Fragestellung Ende September 2021 zur Berucksichtigung der zwischenzeitlich verfugbar werdenden Literatur vor. (Literatur in der Anlage)"

Zur Frage der ggf. gebotenen Anpassung von Quarantanezeiten im Zusammenhang mit der Delta-Variante (Inkubationszeit) befasst sich aktuell FG36 (siehe Protokoll KS vom 11.08.21)

_____

Gerne kann dieser Punkt auch im Krisenstab nochmal diskutiert werden.

Vielen Dank und viele Gru?e,
Michaela Niebank

-----Ursprungliche Nachricht-----
Von: Schmid, Bernhard Im Auftrag von nCoV-Lage
Gesendet: Donnerstag, 12. August 2021 13:37

An: Lang, Katharina <LangK@rki.de>; Nitsche, Andreas <NitscheA@rki.de>; Michel, Janine <MichelJ@rki.de>
Cc: nCoV-Lage <nCoV-Lage@rki.de>; ZBS1-Diagnostik <ZBS1-Diagnostik@rki.de>; ZBS7-Lage <ZBS7-Lage@rki.de>
Betreff: WG: [Aufgabe ID 4089] Daten zu verlangerter Virusausscheidung bei Delta Variante

Liebe Kolleginnen und Kollegen,

wir mochten uns hiermit nach dem Stand der Bearbeitung der Aufgabe ID 4089, Frist morgen DS, erkundigen.

Vielen Dank und viele Gru?e,
Bernhard Schmid, LZ Aufgaben

-----Ursprungliche Nachricht-----
Von: Stern, Daniel Im Auftrag von nCoV-Lage
Gesendet: Donnerstag, 5. August 2021 16:14
An: Lang, Katharina <LangK@rki.de>; Nitsche, Andreas <NitscheA@rki.de>; Michel, Janine <MichelJ@rki.de>
Cc: nCoV-Lage <nCoV-Lage@rki.de>; ZBS7-Lage <ZBS7-Lage@rki.de>; ZBS1-Diagnostik <ZBS1-Diagnostik@rki.de>
Betreff: [Aufgabe ID 4089] Daten zu verlangerter Virusausscheidung bei Delta Variante

Lieber Katharina, Lieber Andi, Liebe Janine,

Aus dem Protokoll der Krisenstabssitzung hat sich eine Aufgabe mit der Bitte um Ubernahme ergeben:

* Gibt es Daten zu einer langeren Virusausscheidung bei Delta?

ToDo: Fr. Lang nimmt Frage mit ins Fachgebiet.

ToDo: Evtl. konnte sich ZBS1 das ansehen. Klarung, ob eine retrospektive Betrachtung aus klinischen Proben moglich ist.

Bei der Erledigung von Erlassen: Beantwortung sollte immer durch das Lagezentrum erfolgen!

Aufgabe ID 4089

Federfuhrende RKI-Organisationseinheit: ZBS7

Weitere RKI-Organisationseinheit/en: ZBS1

Bearbeitende/r: Lang, Nitsche, Michel

Thema: Daten zu verlangerter Virusausscheiden bei Delta

Beschreibung:

Dokumentenordner:

Frist: 13.08.2021 DS

Bei Erledigung: bitte E-Mail an nCoV-Lage@rki.de <mailto:nCoV-Lage@rki.de>

Im Betreff bitte die Aufgaben ID angeben.

Anmerkung: falls Sie den Eindruck haben, dass die Aufgabe falsch zugewiesen wurde oder der Auftrag nicht verstandlich ist, bitten wir um Ruckmeldung!

Vielen Dank und viele Gru?e,

Daniel

i.A. Daniel Stern

Lagezentrum COVID-19

Robert Koch-Institut

Seestr. 10

13353 Berlin

Tel.: 030 18754 3063

E-Mail: nCoV-Lage@rki.de

Internet: www.rki.de

Twitter: @rki_de

Das Robert Koch-Institut ist ein Bundesinstitut im Geschaftsbereich des Bundesministeriums fur Gesundheit

nature COMMUNICATIONS

ARTICLE

https://doi.org/10.1038/s41467-020-20568-4 OPEN

Duration and key determinants of infectious virus shedding in hospitalized patients with coronavirus disease-2019 (COVID-19)

Jeroen J. A. van Kampen[1]✉, David A. M. C. van de Vijver[1], Pieter L. A. Fraaij[1,2], Bart L. Haagmans[1], Mart M. Lamers[1], Nisreen Okba[1], Johannes P. C. van den Akker[3], Henrik Endeman[3], Diederik A. M. P. J. Gommers[3], Jan J. Cornelissen[4], Rogier A. S. Hoek[5,6], Menno M. van der Eerden[5], Dennis A. Hesselink[6,7], Herold J. Metselaar[6,8], Annelies Verbon[9], Jurriaan E. M. de Steenwinkel[9], Georgina I. Aron[1], Eric C. M. van Gorp[1], Sander van Boheemen[1], Jolanda C. Voermans[1], Charles A. B. Boucher[1], Richard Molenkamp[1], Marion P. G. Koopmans[1,10], Corine Geurtsvankessel[1,10] & Annemiek A. van der Eijk[1,10]

Key questions in COVID-19 are the duration and determinants of infectious virus shedding. Here, we report that infectious virus shedding is detected by virus cultures in 23 of the 129 patients (17.8%) hospitalized with COVID-19. The median duration of shedding infectious virus is 8 days post onset of symptoms (IQR 5–11) and drops below 5% after 15.2 days post onset of symptoms (95% confidence interval (CI) 13.4–17.2). Multivariate analyses identify viral loads above 7 $\log_{10}$ RNA copies/mL (odds ratio [OR] of 14.7 (CI 3.57-58.1; $p < 0.001$) as independently associated with isolation of infectious SARS-CoV-2 from the respiratory tract. A serum neutralizing antibody titre of at least 1:20 (OR of 0.01 (CI 0.003-0.08; $p < 0.001$) is independently associated with non-infectious SARS-CoV-2. We conclude that quantitative viral RNA load assays and serological assays could be used in test-based strategies to discontinue or de-escalate infection prevention and control precautions.

[1] Department of Viroscience, Erasmus MC, Rotterdam, The Netherlands. [2] Department of Pediatrics, Subdivision Infectious Diseases and Immunology, Erasmus MC - Sophia, Rotterdam, The Netherlands. [3] Department of Intensive Care, Erasmus MC, Rotterdam, The Netherlands. [4] Department of Hematology, Erasmus MC, Rotterdam, The Netherlands. [5] Department of Pulmonary Medicine, Erasmus MC, Rotterdam, The Netherlands. [6] Erasmus MC Transplant Institute, Rotterdam, The Netherlands. [7] Department of Internal Medicine, Division of Nephrology and Transplantation, Erasmus MC, Rotterdam, The Netherlands. [8] Department of Gastroenterology and Hepatology, Erasmus MC, Rotterdam, The Netherlands. [9] Department of Medical Microbiology and Infectious Diseases, Erasmus MC, Rotterdam, The Netherlands. [10] These authors contributed equally: Marion P. G. Koopmans, Corine Geurtsvankessel, Annemiek A. van der Eijk. ✉email: j.vankampen@erasmusmc.nl

Coronavirus disease-2019 (COVID-19) is a new clinical entity caused by severe acute respiratory syndrome coronavirus 2 (SARS-CoV-2)[1,2]. In particular, persons with underlying diseases, such as diabetes mellitus, hypertension, cardiovascular disease, and respiratory disease, are at increased risk for severe COVID-19, and case fatality rates increase steeply with age[3].

Understanding the kinetics of infectious virus shedding in relation to potential for transmission is crucial to guide infection prevention and control strategies[4]. Long-term shedding of viral RNA has been reported in COVID-19 patients, even after full recovery, putting serious constraints on timely discharge from the hospital or de-escalation of infection prevention and control practices[5–7]. Detection of viral RNA by reverse transcriptase-polymerase chain reaction (RT-PCR) is the gold standard for COVID-19 diagnosis and this technique is used in test-based strategies to discontinue or de-escalate infection prevention and control precautions[8–10]. However, there is no clear correlation between detection of viral RNA and detection of infectious virus using cell culture[5,11,12]. Detection of infectious virus, also called live virus or replication-competent virus, by demonstration of in vitro infectiousness on cell lines is regarded as a more informative surrogate of viral transmission than detection of viral RNA[8–10]. In a COVID-19 hamster model, the window of transmission correlated well with the detection of infectious virus using cell culture but not with viral RNA[13]. Key questions in COVID-19, like in any other infectious disease, are how long a person sheds infectious virus and what the determinants are of infectious virus shedding[5,11,12,14,15].

Two studies reported that infectious virus could not be detected in respiratory tract samples obtained more than 8 days after onset of symptoms despite continued detection of high levels of viral RNA[5,12]. For one patient, infectious virus shedding up to 18 days after onset of symptoms was reported[11]. Shedding of infectious SARS-CoV-2 has not been studied in larger groups of patients nor in patients with severe or critical COVID-19. Here, we show that patients with critical COVID-19 may shed infectious virus for longer periods of time compared to what has been reported for in patients with mild COVID-19. In addition, we show that infectious virus shedding drops to undetectable levels below a viral RNA load threshold and once serum neutralizing antibodies are present, which suggests that quantitative viral RNA load assays and serological assays could be used in test-based strategies to discontinue or de-escalate infection prevention and control precautions.

Results

We included 129 hospitalized individuals that had been diagnosed with COVID-19 by RT-PCR and for whom at least one virus culture from a respiratory tract sample was available (Table 1). Of these, 89 patients (69.0%) had been admitted to the intensive care and the remaining 40 patients (31.0%) were admitted to the medium care. Mechanical ventilation was only performed at the intensive care (81 or 91.0% of patients). Supplemental oxygen was given to 8 (9.0%) of the intensive care patients and to 35 (87.5%) medium care patients. Thirty patients were immunosuppressed (23%) of whom 19 (14.7%) were nonseverely immunocompromised and 11 (8.5%) were severely immunocompromised.

We tested 690 respiratory samples from the 129 patients for the presence of infectious virus using cell culture and determined the viral RNA load with RT-qPCR (Fig. 1). Infectious SARS-CoV-2 was isolated from 62 respiratory tract samples (9.0%) of 23 patients (17.8%). The median time of infectious virus shedding was 8 days post onset of symptoms (IQR 5–11, range 0–20) and probit analysis showed a probability of ≤5% for isolating infectious SARS-CoV-2 when the duration of symptoms was 15.2 days (95% CI 13.4–17.2) or more (Fig. 2A). The median viral load was significantly higher in culture positive samples than in culture negative samples (8.14 versus 5.88 Log_{10} RNA copies/mL, $p < 0.0001$) and the probability of isolating infectious SARS-CoV-2 was less than 5% when the viral load was below 6.63 Log_{10} RNA copies/mL (95% CI 6.24–6.91) (Fig. 2B).

For 27 patients, neutralizing antibody titers from 112 serum samples that were obtained on the same day as a respiratory tract sample were available in our diagnostic database (Table 2). The probability of isolating infectious virus was less than 5% when the neutralizing antibody titer was 1:80 or higher (Fig. 2C). In addition to these neutralizing antibody measurements, we performed RT-PCRs to detect SARS-CoV-2 subgenomic messenger RNA in the 112 corresponding respiratory tract samples. Detection of the subgenomic RNAs outlasted the detection of infectious virus (Supplementary Figs. 1 and 2), and predicted poorly if virus cultures were positive (positive predictive value of 37.5%). In addition, quantitative assessment of subgenomic RNA using cycle threshold (CT) values had no added value over measuring viral genomic RNA loads or serological response to predict infectious virus shedding (Supplementary Fig. 3).

Finally, the key parameters were compared using multivariate generalized estimating equations (Table 3). For this, timepoints for which all three data types (RT-qPCR, virus culture and serum neutralizing antibody titer) were available were included ($n = 112$). A viral load exceeding 7 Log_{10} RNA copies/mL, less than 7 days of symptoms, absence of serum neutralizing antibodies and being immunocompromised were all associated with a positive virus culture in univariate analysis. After submitting all these variables into a multivariate analysis, we found that only a viral load above 7 Log_{10} RNA copies/mL and absence of serum neutralizing antibodies were independently associated with isolation of infectious SARS-CoV-2 from the respiratory tract.

Discussion

In this study we assessed the duration and key determinants of infectious SARS-CoV-2 shedding in patients with severe and critical COVID-19. Such information is critical to design test-based and symptom-based strategies to discontinue infection prevention and control precautions. Both strategies only allow for discontinuation of infection prevention and control precautions after partial resolution of symptoms. Symptom-based strategies use as additional criterion that a certain time interval should have passed since onset of symptoms, while test-based strategies use negative SARS-CoV-2 RT-PCR results as main additional criterion.

The duration of infectious virus shedding found in this study was longer than has been reported previously[5,11,12]. Wölfel and colleagues showed for patients with mild COVID-19 that infectious virus could not be detected after more than eight days since onset of symptoms[5]. Bullard and colleagues obtained similar results, but disease severity was not reported[12]. Shedding of infectious virus up to 18 days after onset of symptoms has been reported for a single case of mild COVID-19[11]. The patients in this study had severe or critical COVID-19 and detection of infectious virus was common after eight days or more since onset of symptoms. For a single patient, infectious virus was detected up to 20 days after onset of symptoms. Higher viral loads have been reported for severe COVID-19 cases compared to mild cases, which may in part explain the longer duration of shedding found in this study[16–20]. Our findings imply that symptom-based strategies to discontinue infection prevention and control precautions should take diseases severity into account. For example, the CDC currently use a minimum disease duration of 10 days in their symptom-based strategy as the statistically estimated likelihood of recovering replication-competent virus approaches zero after ten days of symptoms[8,21]. Based on our findings, a longer disease duration could be considered for severely-ill patients.

High viral RNA loads were independently associated with shedding of infectious virus, but, upon seroconversion, shedding of

Table 1 Patient characteristics.

Characteristic	All	Intensive care	Ward	p value (ICU vs ward)
Number[a]	129	89 (69.0%)	40 (31.0%)	
Male	86 (66.7%)	65 (73.0%)	21 (52.5%)	0.04
Age (median—IQR)	65 (57–72)	66 (57–72)	63 (57–74)	0.90
Immunocompromised[b]				
Moderate	19 (14.7%)	10 (11.2%)	9 (22.5%)	0.04
Severe	11 (8.5%)	5 (5.6%)	6 (15.0%)	
Clinical parameters				
Mechanical ventilation	81 (62.8%)	81 (91.0%)	0	
Supplemental oxygen	43 (33.3%)	8 (9.0%)	35 (87.5%)	
Died	14 (10.9%)	11 (12.3%)	3 (7.5%)	
Duration of illness[c]				
Median (IQR)	18 (13–21)	18 (13–22)	15 (12–18)	0.009
Tests per patient, total (mean per person)				
Culture	690 (5.3)	601 (6.8)	89 (2.2)	
PRNT	112 (0.9)	82 (0.9)	30 (0.8)	
PCR	688 (5.3)	599 (6.7)	89 (2.2)	

[a]Disease severity classification according to NIH criteria (https://www.covid19treatmentguidelines.nih.gov/overview/management-of-covid-19/): 81/129 (62.5%) critical disease, 43/129 (33.3%) severe disease, 5/129 (3.9%) moderate disease.
[b]Immunocompromised level was scored as described previously[25]. Patients with severe immunosuppression ($n = 11$): Lung transplantation, or other solid organ transplantation and treatment for rejection within the last 3 months ($n = 3$); Underlying disease treated with daily corticosteroid dosages (based on prednisone) >30 mg for >14 days and/or immunomodulating biologicals ($n = 4$); Allogeneic hematopoietic stem cell transplantation within the last 12 months, or allogeneic hematopoietic stem cell transplantation with with graft-versus-host-disease treated with immunosuppressive drugs, or acute leukemia ($n = 4$). Patients with nonsevere immunosuppression ($n = 19$): Untreated auto-immune disease or underlying disease treated with immunosuppressive drugs (excluding treatment with daily corticosteroid dosages (based on prednisone) >30 mg for >14 days and/or treatment with immunomodulating biologicals) ($n = 10$); At least 1 year after solid organ transplantation (excluding lung transplantation) and no rejection ($n = 3$); Hematological malignancies (excluding acute leukemia and leukemia treated with induction therapy or chemotherapy resulting in neutropenia for >7 days) ($n = 4$); Other nonsevere immunodeficiencies ($n = 2$).
[c]As of April 17th 2020. PRNT = plaque-reduction neutralization titer. Respiratory tract samples for virus culture and PCR were obtained from the lower respiratory tract (sputum) on the intensive care unit (538/690 samples, 78%) and from the upper respiratory tract (swabs) on the intensive care unit as well as on the medium care unit (152/690 samples, 22%). A total of 127 out of the 690 respiratory tract samples that were submitted for virus culture (18.4%) were obtained from immunocompromised patients. For categorical variables a two-sided Chi-square test was used and for continuous variables a two-sided student's *t*-test was used. No adjustments were made for multiple comparisons.

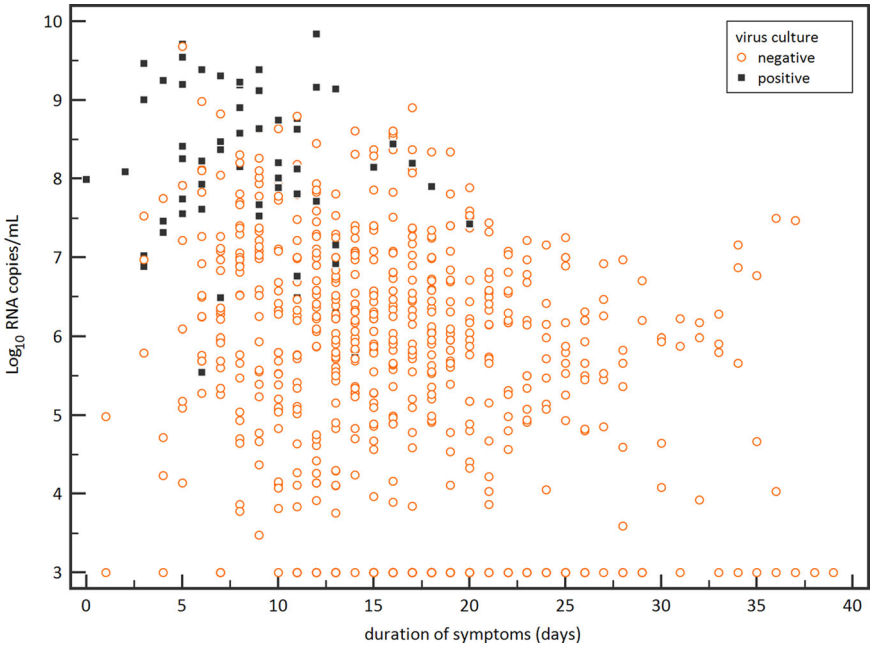

Fig. 1 Viral loads and duration of symptoms for infectious virus shedding. Viral RNA loads (Log_{10} RNA copies/mL) in the respiratory samples versus the duration of symptoms (days). Black boxes represent virus culture positive samples and open red circles represent the virus culture negative samples.

infectious virus dropped rapidly to undetectable levels. Infectious virus could not be isolated from respiratory tract samples once patients had a serum neutralizing antibody titer of at least 1:80. These results warrant the use of quantitative viral RNA load assays and serological assays in test-based strategies to discontinue or de-escalate infection prevention and control precautions. The probability of isolating infectious virus was less than 5% when viral RNA load was below 6.63 Log10 RNA copies/mL, which is strikingly similar compared to the cutoff of 6.51 Log10 RNA copies/mL reported by Wölfel et al.[5]. In addition, Bullard and colleagues used cycle threshold (ct) values as quantitative measure for viral RNA load and reported that infectious virus could not be isolated from diagnostic samples when ct values were above 24[12]. Together, these results indicate that viral RNA load cutoffs could be used in test-based strategies to discontinue infection prevention and control precautions. In addition, we report here a very strong association between neutralizing antibody response and shedding of infectious virus with an odds ratio of 0.01 for isolating infectious virus after seroconversion. Antibody responses were measured with a plaque-reduction neutralization test (PRNT)[22]. Neutralization assays, which are the gold standard in coronavirus serology, are labor-intensive and require a biosafety level 3 laboratory. We have recently cross-validated various commercial immunoassays using our PRNT50% as gold standard. Some commercial assays showed good agreement with our PRNT50%: For example, the

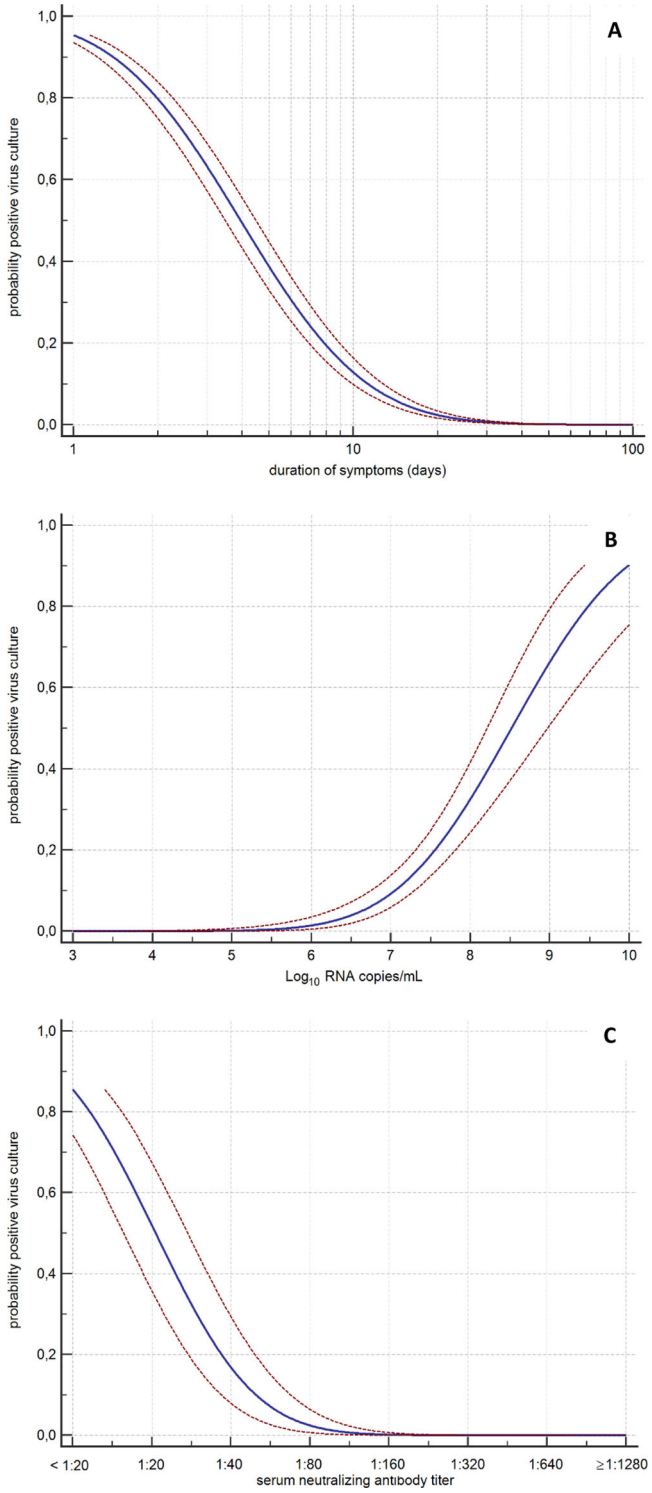

Fig. 2 Probabilities of infectious virus shedding. Probit analyses of the detection of infectious virus in respiratory samples with cell culture for duration of symptoms in days (**A**) ($n = 690$ samples), viral RNA load in Log10 copies per mL (**B**) ($n = 688$ samples), and serum neutralizing antibody titer (**C**) ($n = 112$ samples). Blue line represent the probit curve and the dotted red lines represent the 95% confidence interval. Serum neutralizing antibody titers are expressed as plaque-reduction neutralization titers 50% as described previously[27].

Table 2 Serum neutralizing antibody titers and isolation of infectious virus from the respiratory tract.

Serum neutralizing antibody titer	Total number samples	Number culture positive samples (%)	Number culture negative samples (%)
<1:20	31	27 (87%)	4 (13%)
1:20	10	4 (40%)	6 (60%)
1:40	7	2 (29%)	5 (71%)
1:80	2	0 (0%)	2 (100%)
1:160	4	0 (0%)	4 (100%)
1:320	11	0 (0%)	11 (100%)
1:640	9	0 (0%)	9 (100%)
1:1280	14	0 (0%)	14 (100%)
1:2560	16	0 (0%)	16 (100%)

Serum neutralizing antibody titers against SARS-CoV-2 were determined using a plaque-reduction neutralization assay[17]. Neutralizing antibodies (titers of 1:20 or higher) were detected in 72.3% (81/112) of the serum samples. For six patients, infectious SARS-CoV-2 was isolated from the respiratory tract despite the presence of neutralizing SARS-CoV-2 antibodies in the serum sample pairs. In four of these six patients, infectious virus was not isolated in the consecutive respiratory tract samples obtained after a virus culture positive sample (sampled from day +1, +1, +4, and +4 in respect to virus culture positive sample). For one patient, infectious virus was not isolated in the respiratory tract sample obtained one day after the virus culture positive respiratory tract sample, while the respiratory tract sample obtained 2 days after the virus culture positive respiratory tract sample was positive for infectious SARS-CoV-2. All respiratory tract samples obtained thereafter tested negative for infectious virus. For one patient, no follow-up respiratory tract samples were available.

Wantai SARS-CoV-2 Ig total ELISA has a sensitivity of 99% (95% CI 97–100%) and a specificity of 99% (95% CI 96–100%)[23]. These commercial immunoassays require less stringent biosafety measures and are amenable to high throughput use resulting in a broad application of our results to guide infection prevention strategies and discharge management for clinical cases being hospitalized.

Detection of viral subgenomic RNA correlated poorly with shedding of infectious virus. These RNAs are produced only in actively infected cells and are not packaged into virions. Subgenomic RNAs were still detected when virus cultures turned negative. This could indicate that active replication continues in severely-ill symptomatic COVID-19 patients after seroconversion and after shedding of infectious virus has stopped. Possibly, infectious virions are produced but are directly neutralized by antibodies in the respiratory tract. On the other hand, the half-life of viral subgenomic RNAs is not known in COVID-19 and these RNAs may still be detected once replication has stopped.

Our study has some limitations. Firstly, virological data were obtained from diagnostic samples only and samples were not prospectively collected at predefined timepoints. However, as many aspects of COVID-19 were still unclear, a sampling-rich diagnostic approach was applied in our institution with regular virological monitoring of confirmed COVID-19 patients. This approach resulted in a large high quality dataset from a considerable number of patients including patients with a immunocompromised status. The strikingly similar viral RNA load cutoff for a 5% probability of a positive virus culture found by us and by Wölfel et al. underpins the validity of the results[5]. Secondly, we used in vitro cell cultures as a surrogate marker for infectious virus shedding. The success of SARS-CoV-2 isolation is dependent on which cell lines is used[24]. Vero cells are currently regarded as the gold standard to detect infectious SAR-CoV-2, but the true limit of detection is unknown. Notwithstanding the above, experimental evidence from a COVID-19 hamster model showed that transmission of SARS-CoV-2 correlated well with detection of infectious SARS-CoV-2 from respiratory tract samples using in vitro Vero cell cultures while detection of viral RNA did not[13]. More data from experimental models, and epidemiological and modeling

Table 3 Univariate and multivariate analysis of key determinants for infectious virus shedding.

Variable	Positive virus culture ($n = 33$)	Negative virus culture ($n = 79$)	Univariate odds ratio (95% CI)	Multivariate odds ratio (95% CI)
Viral RNA load				
>10^7 RNA copies/mL	29 (87.9%)	22 (27.8%)	18.8 (5.5–64.2), $p < 0.001$	14.7 (3.7–58.1), $p < 0.001$
Duration of symptoms				
<7 days	20 (60.6%)	17 (21.5%)	5.6 (1.7–18.1), $p = 0.004$	2.1 (0.4–11.7), $p = 0.31$
Serum neutralizing antibody titer				
1:20 or higher	6 (18.2%)	75 (94.9%)	0.01 (0.003–0.05), $p < 0.001$	0.01 (0.002–0.08), $p < 0.001$
Immunocompromised				
Yes	10 (30.3%)	10 (12.7%)	3.00 (0.8–11.0), $p = 0.098$	2.0 (0.7–5.3), $p = 0.22$

Results of the univariate and multivariate generalized estimating equation analysis. The analyses were limited to the samples for which a viral RNA load and a serum neutralizing antibody titer were available from samples taken at the same day.

studies on transmission, which take viral RNA load and antibody response into account, are needed for further validation of this approach. It should be noted that, besides the infectious viral load, additional factors determine virus transmissibility. Finally, our study only included hospitalized symptomatic adults with severe or critical COVID-19 and important differences were noted in our study compared to what has been reported for in mild COVID-19. Thus, further studies are needed on the determinants and duration of infectious virus shedding in specific patient groups.

In conclusion, infection prevention and control guidelines should take into account that patients with severe or critical COVID-19 may shed infectious virus for longer periods of time compared to what has been reported for in patients with mild COVID-19. Infectious virus shedding drops to undetectable levels when viral RNA load is low and serum neutralizing antibodies are present, which warrants the use of quantitative viral RNA load assays and serological assays in test-based strategies to discontinue or de-escalate infection prevention and control precautions.

Methods

Samples and patients. Between March 8, 2020 and April 8, 2020, diagnostic respiratory samples of COVID-19 patients from the Erasmus MC that were send to our laboratory for SARS-CoV-2 PCR were also submitted for virus culture. From these patients, results from SARS-CoV-2 PCRs on diagnostic respiratory samples and results from SARS-CoV-2 neutralizing antibody measurements on serum samples were extracted from our diagnostic laboratory information management system (LabTrain version 3, bodegro, the Netherlands). The following information was extracted from the electronic patient files (HiX version 6.1, ChipSoft, the Netherlands): date of onset of symptoms, disease severity (hospitalized on ICU with mechanical ventilation, hospitalized on ICU with oxygen therapy, hospitalized to ward with oxygen therapy, hospitalized to ward without oxygen therapy), information to classify patients as immunocompetent, nonseverely immunocompromised (excluding diabetes mellitus), or severely immunocompromised as described previously[25], disease severity score according to the NIH classification (https://www.covid19treatmentguidelines.nih.gov/overview/management-of-covid-19/), and whether the patients were still alive or not as of April 17, 2020. Excel 2016 (Microsoft Corp, USA) was used as data collection software.

Sample processing and analysis. Swabs from the upper respiratory tract were collected in tubes containing 4 mL virus transport medium (Dulbecco's modified eagle's medium (DMEM, Lonza) supplemented with 40% FBS, 20 mM 4-(2-hydroxyethyl)-1-piperazineethanesulfonic acid (HEPES), NaCO3, 10 µg/ml amphotericin B, 1000 U/mL penicillin, 1000 µg/mL streptomycin). Supernatant was passed through a 45-µm filter and used for PCR analysis and virus culture. For sputum samples, 6 mL sample processing medium (DMEM supplemented with 17 mM HEPES, $NaCO_3$, 1000 U/mL penicillin, 1000 µg/mL streptomycin, 12.5 µg/ml amphotericin B) was added until the final volume was 6 mL. Subsequently, samples were vortexed, centrifugated, passed through a 45-µm filter, and 1 part FBS was added to 1.5 parts supernatant. Subsequently, processed samples were used for PCR analysis and virus culture.

Real-time RT-PCR detection of SARS-CoV-2 was performed using an in-house assay[26] or using the SARS-CoV-2 test on a cobas® 6800 system (Roche Diagnostics). Subsequently, cycle threshold (ct) values were converted to Log_{10} RNA copies/mL using calibration curves based on quantified E-gene in vitro RNA transcripts[5]. SARS-CoV-2 subgenomic RNAs were detected with RT-PCR[5].

Respiratory samples were cultured on Vero cells, clone 118, using 24-wells plates with glass coverslips[27]. Cells were inoculated with 200 µL sample per well and centrifugated for 15 min at 3500 × *g*. After centrifugation, inoculum was discarded, virus culture medium (Iscove's modified Dulbecco's medium (IMDM; Lonza) supplemented with 2 mM L-glutamine (Lonza), 100 U/mL penicillin (Lonza), 100 µg/mL streptomycin (Lonza), 2.5 µg/mL amphotericin B (department of hospital pharmacy, Erasmus MC), and 1% heat-inactivated fetal bovine serum (Sigma)) was added, and samples were cultured at 37 °C and 5% CO_2 for 7 days. Each sample was cultured in triplicate: Two replicates were fixed with ice-cold acetone after 24 and 48 h, respectively irrespective if cytopathic effect (CPE) was visible. The fixed samples were further analyzed with immunofluorescence (see below). The remaining replicate was scored for CPE on a daily basis for 7 days. When CPE was visible, the sample was fixed with ice-cold acetone and further analyzed with immunofluorescence (see below). Virus cultures were regarded as negative if no CPE was visible during 7 days. For immunofluorescence read-out, the fixed cells were washed with phosphate buffer saline (PBS), and incubated for 30 min at 37 °C with 25 µL 1000-fold diluted polyclonal rabbit SARS-CoV anti-nucleoprotein antibodies (Sino Biological, catalogue number 40143-T62). After incubation, samples were washed with three times with PBS and once with deionized water. Subsequently, cells were incubated for 30 min at 37 °C with 25 µL 2000-fold diluted Alexa Fluor 488-labeled polyclonal goat anti-rabbit IgG (Invitrogen, catalogue number A-11070). Subsequently, cells were washed three times with PBS. Finally, cells were incubated for 1 min with 25 µL Evan's Blue (counterstain), washed twice with deionized water, air dried and analyzed with a fluorescence microscope.

Serum neutralizing antibodies titers against SARS-CoV-2 (German isolate; GISAID ID EPI_ISL 406862; European Virus Archive Global #026V-03883) were determined using a plaque-reduction neutralization test[22]. A plaque-reduction neutralization titer 50% (PRNT50%) of 1:20 or more was considered to be positive and a PRNT50% below 1:20 negative.

Medical ethical approval. All patient samples and data used in this study were collected in the context of routine clinical patient care. Additional analyses were performed only on surplus of patient material collected in the context of routine clinical patient care. The institutional review board of the Erasmus MC (Rotterdam, The Netherlands) approved the use of these data and samples (METC-2015-306). METC-2015-306 is a generic protocol to study viral diseases. Informed consent for COVID-19 research was waived by the privacy knowledge office of the Erasmus MC (Rotterdam, The Netherlands). Instead, patients had the right to opt-out against the use of their surplus patient material and their medical data for research. The opt-out system of the Erasmus MC was checked for all patients included in this study, and none of the patients included in this study opted-out against the use of their surplus patient material and their medical data for research.

Statistical analysis. Categorical and continuous variables were compared using the Chi-square test the student's *t*-test, respectively. Generalized estimating equations were used to identify factors that are associated with a virus culture positive respiratory tract sample. The continuous data in the generalized estimating equations were dichotomized using various cutoff values. In the main paper we present the results of the best fitting generalized estimating equations using the levels of dichotomizing that had the best fit according to the quasi-likelihood under the independence criterion (QIC)[28]. Sensitivity analysis is shown in Supplementary Table 1 and Supplementary Table 2. All variables having a p value < 0.1 in univariate analysis were submitted into a multivariate general estimating equation to account for repeated measurements obtained from the same patient during hospitalization[29]. For this analysis we used the geepack package version 1.3-1 and R version 4.0.0[29]. Probit analyses were performed with MedCalc version 19.2.3 (MedCalc Software Ltd).

Role of the funding source. This work partially was funded through EU COVID-19 grant RECOVER 101003589. The study sponsors were involved neither in the study design, the collection, analysis and interpretation of the data, writing of the report, nor in the decision to submit the paper for publication. The corresponding author had full access to all the data in the study and had final responsibility for the decision to submit for publication.

Reporting summary. Further information on research design is available in the Nature Research Reporting Summary linked to this article.

Data availability

All relevant data are available from the authors upon request. Source data are provided with this paper.

Received: 30 June 2020; Accepted: 1 December 2020;
Published online: 11 January 2021

References

1. Huang, C. et al. Clinical features of patients infected with 2019 novel coronavirus in Wuhan, China. *Lancet* **395**, 497–506 (2020).
2. Zhu, N. et al. China Novel Coronavirus Investigating and Research Team. A Novel Coronavirus from Patients with Pneumonia in China, 2019. *N. Engl. J. Med.* **382**, 727–733 (2020).
3. Docherty, A. B. et al. ISARIC4C investigators. Features of 20 133 UK patients in hospital with covid-19 using the ISARIC WHO Clinical Characterisation Protocol: prospective observational cohort study. *BMJ* **369**, m1985 (2020).
4. Anderson, R. M. et al. Epidemiology, transmission dynamics and control of SARS: the 2002–2003 epidemic. *Philos. Trans. R. Soc. Lond. B Biol. Sci.* **359**, 1091–1105 (2004).
5. Wölfel, R. et al. Virological assessment of hospitalized patients with COVID-2019. *Nature* https://doi.org/10.1038/s41586-020-2196-x (2020).
6. Ling, Y. et al. Persistence and clearance of viral RNA in 2019 novel coronavirus disease rehabilitation patients. *Chin. Med. J. (Engl.)*. **133**, 1039–1043 (2020).
7. Lan, L. et al. Positive RT-PCR test results in patients recovered from COVID-19. *JAMA* https://doi.org/10.1001/jama.2020.2783 (2020).
8. CDC. *Discontinuation of Transmission-Based Precautions and Disposition of Patients with COVID-19 in Healthcare Settings (Interim Guidance)*. https://www.cdc.gov/coronavirus/2019-ncov/hcp/disposition-hospitalized-patients.html (2020).
9. ECDC. *Guidance for discharge and ending isolation in the context of widespread community transmission of COVID-19—first update 8 April 2020*. https://www.ecdc.europa.eu/sites/default/files/documents/covid-19-guidance-discharge-and-ending-isolation-first%20update.pdf (2020)
10. WHO. *Clinical management of COVID-19*. WHO Reference Number: WHO/2019-nCoV/clinical/2020.5. https://www.who.int/publications/i/item/clinical-management-of-covid-19 (2020).
11. Liu, W. D. et al. Prolonged virus shedding even after seroconversion in a patient with COVID-19. *J. Infect.* **S0163-4453**, 30190–30190 (2020).
12. Bullard, J. et al. Predicting infectious SARS-CoV-2 from diagnostic samples. *Clin. Infect. Dis.* **71**, 2663–2666 (2020).
13. Sia, S. F. et al. Pathogenesis and transmission of SARS-CoV-2 in golden hamsters. *Nature* https://doi.org/10.1038/s41586-020-2342-5 (2020).
14. Munster, V. J., Koopmans, M., van Doremalen, N., van Riel, D. & de Wit, E. A novel coronavirus emerging in China—key questions for impact assessment. *N. Engl. J. Med.* **382**-, 692–694 (2020).
15. Wang, W. et al. Detection of SARS-CoV-2 in different types of clinical specimens. *JAMA* https://doi.org/10.1001/jama.2020.3786 (2020).
16. Liu, Y. et al. Viral dynamics in mild and severe cases of COVID-19. *Lancet Infect. Dis.* **20**, 656–657 (2020).
17. Zheng, S. et al. Viral load dynamics and disease severity in patients infected with SARS-CoV-2 in Zhejiang province, China, January-March 2020: retrospective cohort study. *BMJ* **369**, m1443 (2020).
18. Lui, G. et al. Viral dynamics of SARS-CoV-2 across a spectrum of disease severity in COVID-19. *J. Infect.* **81**, 324–327 (2020).
19. He, X. et al. Temporal dynamics in viral shedding and transmissibility of COVID-19. *Nat. Med.* **26**, 672–675 (2020).
20. Xu, T. et al. Clinical features and dynamics of viral load in imported and non-imported patients with COVID-19. *Int. J. Infect. Dis.* **94**, 68–71 (2020).
21. CDC. *Symptom-Based Strategy to Discontinue Isolation for Persons with COVID-19—Decision Memo*. https://www.cdc.gov/coronavirus/2019-ncov/community/strategy-discontinue-isolation.html (2020).
22. Okba, N. M. A. et al. Severe acute respiratory syndrome coronavirus 2-specific antibody responses in coronavirus disease 2019 patients. *Emerg. Infect. Dis.* **26**, 1478–1488 (2020).
23. GeurtsvanKessel, C. H. et al. An evaluation of COVID-19 serological assays informs future diagnostics and exposure assessment. *Nat. Commun.* **3436**, 1–5 (2020).
24. Hoffmann, M. et al. SARS-CoV-2 cell entry depends on ACE2 and TMPRSS2 and is blocked by a clinically proven protease inhibitor. *Cell* **181**, 271–280.e8 (2020).
25. Fraaij, P. L. et al. Viral shedding and susceptibility to oseltamivir in hospitalized immunocompromised patients with influenza in the Influenza Resistance Information Study (IRIS). *Antivir. Ther.* **20**, 633–642 (2015).
26. Corman, V. M. et al. Detection of 2019 novel coronavirus (2019-nCoV) by real-time RT-PCR. *Euro. Surveill.* **25**, 23–30 (2020).
27. Kuiken, T. et al. Experimental human metapneumovirus infection of cynomolgus macaques (Macaca fascicularis) results in virus replication in ciliated epithelial cells and pneumocytes with associated lesions throughout the respiratory tract. *Am. J. Pathol.* **164**, 1893–1900 (2004).
28. Hanley, J. A., Negassa, A., Edwardes, M. D. D. & Forrester, J. E. Statistical analysis of correlated data using generalized estimating equations: an orientation. *Am. J. Epidemiol.* **157**, 364–375 (2003).
29. Højsgaard, S., Halekoh, U. & Yan, J. The R package geepack for generalized estimating equations. *J. Stat. Softw.* **15**, 11 (2005).

Acknowledgements

We gratefully acknowledge EVA-g and Christian Drosten for provision of the quantified E-gene transcript. Bibi Slingerland, Ga-Lai Chong, Rose Willemze, Jordy Dekker, George Sips, Stephanie Popping, Daphne Mulders, Alex de Ries, and Jeroen Ijpelaar gratefully acknowledged for their technical and analytical contributions. John T. Brooks (CDC) is acknowledged for his helpful discussions on COVID-19 disease severity classification. This work was partially funded through EU COVID-19 grant RECOVER 101003589.

Author contributions

J.J.A.v.K. conceived and designed the study, supervised the study, wrote the first draft of the manuscript. D.A.M.C.v.d.V., P.L.A.F., C.G., A.E., M.K., R.M., and C.B. contributed to the conception and design of the study. G.I.A. performed the virus cultures. C.G. and J.J.A.v.K. supervised the virus culture experiments. B.H. and M.M.L. provided intellectual input for virus culture experiments and analyses. N.O. performed the virus neutralization tests. B.L. and C.G. supervised virus neutralization tests. R.M., S.v.B., and J.C.V. supervised and interpreted the molecular analyses. D.A.M.C.v.d.V. performed the statistical analyses. P.L.A.F. and J.J.A.v.K. supervised the clinical data analyses. J.P.C.v.d.A., H.E., D.A.M.P.J.G., J.J.C., R.A.S.H., M.M.v.d.E., D.A.H., H.J.M., A.V., J.E.M.d.S., and E.C.M.v.G. were involved in COVID-19 patient care, data, and specimen collection. All authors discussed the results and implications and commented on the manuscript at all stages.

Competing interests

The authors declare no competing interests.

Additional information

Supplementary information is available for this paper at https://doi.org/10.1038/s41467-020-20568-4.

Correspondence and requests for materials should be addressed to J.J.A.v.K.

Peer review information *Nature Communications* thanks Joshua Schiffer and Clemens-Martin Wendtner for their contribution to the peer review of this work. Peer reviewer reports are available.

Reprints and permission information is available at http://www.nature.com/reprints

Publisher's note Springer Nature remains neutral with regard to jurisdictional claims in published maps and institutional affiliations.

SARS-CoV-2 viral load dynamics, duration of viral shedding and infectiousness – a living systematic review and meta-analysis

Author: Muge Cevik[1,2], Matthew Tate[3], Ollie Lloyd[2,4], Alberto Enrico Maraolo[5], Jenna Schafers[2], Antonia Ho[6]

Affiliations:

1. Division of Infection and Global Health Research, School of Medicine, University of St Andrews, UK
2. NHS Lothian Infection Service, Regional Infectious Diseases Unit, Western General Hospital, Edinburgh, U.K.
3. Respiratory Medicine, University Hospital Wishaw, Wishaw, UK
4. Edinburgh Medical School, College of Medicine & Veterinary Medicine, University of Edinburgh, UK
5. First Division of Infectious Diseases, Cotugno Hospital, AORN dei Colli, Naples, Italy.
6. MRC-University of Glasgow Centre for Virus Research, University of Glasgow, Glasgow, UK

Corresponding author:

Dr Muge Cevik
Division of Infection and Global Health Research,
School of Medicine, University of St Andrews, Fife, KY16 9TF
Telephone number: +447732800814
Email address: mc349@st-andrews.ac.uk

Keywords: SARS-CoV-2, COVID-19, viral shedding, viral dynamics, infectiousness

ABSTRACT

Background Viral load kinetics and the duration of viral shedding are important determinants for disease transmission. We aim i) to characterise viral load dynamics, duration of viral RNA, and viable virus shedding of SARS-CoV-2 in various body fluids and ii) to compare SARS-CoV-2 viral dynamics with SARS-CoV-1 and MERS-CoV.

Methods: Medline, EMBASE, Europe PMC, preprint servers and grey literature were searched to retrieve all articles reporting viral dynamics and duration of SARS-CoV-2, SARS-CoV-1 and MERS-CoV shedding. We excluded case reports and case series with < 5 patients, or studies that did not report shedding duration from symptom onset. PROSPERO registration: CRD42020181914.

Findings: Seventy-nine studies on SARS-CoV-2, 8 on SARS-CoV-1, and 11 on MERS-CoV were included. Mean SARS-CoV-2 RNA shedding duration in upper respiratory tract, lower respiratory tract, stool and serum were 17.0, 14.6, 17.2 and 16.6 days, respectively. Maximum duration of SARS-CoV-2 RNA shedding reported in URT, LRT, stool and serum was 83, 59, 35 and 60 days, respectively. Pooled mean duration of SARS-CoV-2 RNA shedding was positively associated with age (p=0.002), but not gender (p = 0.277). No study to date has detected live virus beyond day nine of illness despite persistently high viral loads. SARS-CoV-2 viral load in the upper respiratory tract appears to peak in the first week of illness, while SARS-CoV-1 and MERS-CoV peak later.

Conclusion: Although SARS-CoV-2 RNA shedding in respiratory and stool can be prolonged, duration of viable virus is relatively short-lived. Thus, detection of viral RNA cannot be used to infer infectiousness. High SARS-CoV-2 titres are detectable in the first week of illness with an early peak observed at symptom onset to day 5 of illness. This review underscores the importance of early case finding and isolation, as well as public education on the spectrum of illness. However, given potential delays in the isolation of patients, effective containment of SARS-CoV-2 may be challenging even with an early detection and isolation strategy.

Funding: No funding was received.

INTRODUCTION

Viral load kinetics and the duration of viral shedding are important determinants for disease transmission. They determine the duration of infectiousness which is a critical parameter to inform effective control measures and disease modelling. While a number of studies have evaluated SARS-CoV-2 shedding, viral load dynamics and duration of viral shedding reported across studies so far have been heterogenous.[1] In several case series with serial respiratory sampling, peak viral load was observed just before, or at the time of symptom onset.[2-4] Viral ribonucleic acid (RNA) shedding was reported to be persistent in the upper respiratory tract and in faeces, for over one month after illness onset.[1] However, the duration of SARS-CoV-2 RNA detection has not been well characterised. A comprehensive understanding of viral load dynamics, length of viral shedding, and how these relate to other factors, such as age and disease severity is lacking.

The aim of this systematic review and meta-analysis was to i) characterise the viral load dynamics of SARS-CoV-2, duration of viral RNA shedding by reverse transcriptase polymerase chain reaction (RT-PCR) and viable virus shedding in various body fluids and ii) compare SARS-CoV-2 viral dynamics with that of SARS-CoV-1 and MERS-CoV.

METHODS

Search Strategy

We retrieved all articles reporting viral dynamics and/or the duration of shedding of SARS-CoV-2, SARS-CoV-1 or MERS-CoV in various specimens through systematic searches of major databases including Medline, EMBASE, Europe PMC, pre-print databases (MedRxiv, BioRxiv) and the grey literature from 1 January 2003 to 6th June 2020 using Medical Subject Headings (MeSH) terms (Supplementary Material). We also manually screened the references of included original studies to obtain additional studies. Studies prior to 2003 were excluded since the first recognised case of SARS-CoV-1 was identified in March 2003.

This systematic review was registered in PROSPERO on 29th April 2020 (CRD42020181914) and will be updated in three monthly intervals as a living systematic review.

Study Selection

Studies were eligible if they met the following inclusion criteria: (1) report on SARS-CoV-2, SARS-CoV-1 or MERS-CoV infection and (2) report viral load kinetics, duration of viral shedding or viable virus. We excluded: (1) review papers; (2) animal studies; (3) studies on environmental sampling; (4) case reports and case series with < 5 participants, due to likely reporting bias; (5) papers where the starting point of viral shedding was not clear or reported from post-discharge and (6) modelling studies with no original data.

Data Extraction

Two authors (MT and OL) screened and retrieved articles according to the eligibility criteria. Four reviewers (MT, OL, JS, MC) performed full text review and final article selection. From each study, the following variables were extracted as a minimum: name of first author, year of publication, city and country, sample size, median age, sex ratio, time from symptom onset to viral clearance detected by RT-PCR and culture in different specimens, and longest reported time to viral clearance. If these data were not reported, we also contacted the authors to request the data. If available, we extracted data on peak viral load, clinical outcome, and reported factors associated with duration of viral shedding.

Risk of bias in included studies

Two authors (OL and JS) independently assessed study quality and risk of bias using the Joanna Briggs Institute (JBI) Critical Appraisal Checklist tools,[5] which comprise standardised checklists, for the different study designs included in this review. Any disagreements regarding grading of quality were resolved through discussion with a third author (MC).

Meta-Analysis

For every study included, mean duration of viral shedding and 95% confidence interval (CI) were calculated. The random-effects model (DerSimonian or Laird) was applied to estimate a pooled effect size. Forest plots illustrated the detailed representation of all studies based on the effect size and 95% CI. If not reported, means and standard deviations were derived from sample size, median, interquartile range (IQR), minimum and maximum values.[6] Heterogeneity between studies were quantified by the I^2 index and Cochran's Q test. Publication bias was not assessed as usual

appraisal methods are uninformative when meta-analysed studies do not include a test of significance. A weighted meta-regression using an unrestricted maximum likelihood model was performed to assess the impact of potential moderators on the pooled effect size (P-values <0.05 were considered significant). All statistical analyses were performed using Comprehensive Meta-Analysis (CMA) version 3 software (Biostat, Englewood, mNJ).

RESULTS

The systematic search identified 1486 potentially relevant articles. Three hundred and fifty articles were retrieved for full text review. After reviewing the eligibility criteria, a total of 79 studies on SARS-CoV-2, eight on SARS-CoV-1, and 11 on MERS-CoV were included (Figure 1).

Summary of SARS-CoV-2 studies

Of the 79 papers included, 58 studies were conducted in China (Table 1). Six studies included outpatient or community cases, the remainder comprised hospitalised patients only. Six studies reported viral load dynamics exclusively in children.[7-12] Two additional studies included children, but data on viral load dynamics were presented in aggregate with adults.[13,14] One study reported findings in renal transplant patients.[15]

Median duration of viral shedding

In total, 61 studies reported median or maximum viral RNA shedding in at least one body fluid and six studies provided duration of shedding stratified by illness severity only. Of those, 43 (3229 individuals) reported duration of shedding in upper respiratory tract (URT), seven (260 individuals) in lower respiratory tract (LRT), 13 (586 individuals) in stool, and 2 studies (108 individuals) in serum samples were eligible for quantitative analysis. Means viral shedding durations were 17.0 days (95% CI, 15.5-18.6), 14.6 days (95% CI, 9.3-20.0), 17.2 days (95% CI, 14.4-20.1) and 16.6 days (95% CI, 3.6-29.7), respectively (Figures 2 to 5). Maximum duration of RNA shedding reported in URT, LRT, stool and serum was 83, 59, 35 and 60 days, respectively.

Studies reporting duration of viral shedding in URT and stool samples were eligible for meta-regression analysis. Pooled mean viral shedding duration was positively associated with age

(slope: +0.304; 95% CI, +0.115 to +0.493; p = 0.002 Fig 6), but not gender (p = 0.277, Supplementary Fig 3). When adjusted for the proportion of male subjects in a multivariable analysis, mean age was positively associated with the mean duration of viral shedding in URT specimens (p = 0.003). There was a positive but non-significant association between mean age and duration of shedding in stool (p=0.37) (Supplementary Fig 4).

Peak viral load

The majority of studies evaluating SARS-CoV-2 viral load in serial URT samples demonstrated peak viral loads within the first week of symptom onset. [2,4,8,16-24] The highest viral loads were reported either soon after or at the time of symptom onset[2,8,16,23,24] or at day 3-5 of illness[4,18,20,22] followed by a consistent decline.

Five studies that evaluated viral load dynamics in LRT samples observed a peak viral load in the second week of illness.[4,18,20,23,25] In contrast, the dynamics of SARS-CoV-2 shedding in stool is more erratic, with highest viral loads reported on day 7,[18] 2-3 weeks,[24,25] and up to 5-6 weeks after symptom onset.[23] While several studies reported significantly higher viral titres in stool compared to respiratory samples,[8,25] Huang *et al.* reported lower viral load in stool than in both LRT and URT samples early in the disease course.[23]

Severity and association with duration of viral shedding

In total, 20 studies evaluated duration of viral RNA shedding based on disease severity. The majority (n=13) reported longer duration of viral shedding in patients with severe illness than those with non-severe illness, [18,25-36] while five studies reported similar shedding durations according to disease severity in URT samples [17,19,37-39] and one study in stool samples. [40] Only one study reported shorter viral shedding in moderate to severe illness compared to mild to moderate illness.[41] Six studies have performed comparative analysis based on severity of illness;[18,25,27,28,38,39] the majority (n=5) demonstrated significantly longer duration of shedding among the severe illness group compared to the non-severe patients and only one study observed no difference.[39] (Table 2).

Other factors associated with prolonged shedding

All but one study[42] (n=10) that examined the impact of age on SARS-CoV-2 shedding identified an association between older age and prolonged viral RNA shedding.[25,26,28,33,37-39,43-45] Three studies identified age as an independent risk factor for delayed viral clearance.[25,26,38] Male sex was also associated with prolonged shedding,[25,38,46] and the association remained significant even when patients were stratified based on illness severity.[25,38] Corticosteroid treatment was associated with delayed viral clearance in four studies,[33,38,47,48] and one study that recruited 120 critically ill patients, found no difference between corticosteroid and control groups.[49]

In a phase 2 open-label study evaluating interferon beta-1b, lopinavir–ritonavir, and ribavirin a shorter duration of viral shedding was seen with combination treatment compared to the control.[50] None of the antiviral regimens (chloroquine, oseltamivir, arbidol, and lopinavir/ritonavir) independently improved viral RNA clearance.[28,51] In a retrospective study of 284 patients, lopinavir/ritonavir use was associated with delayed viral clearance even after adjusting for confounders.[28]

Asymptomatic SARS-CoV-2 shedding

Twelve studies reported on viral load dynamics and/or duration of viral shedding among patients with asymptomatic SARS-CoV-2 infection (Table 3); two demonstrated lower viral loads among asymptomatic patients compared to symptomatic patients,[8,52] while four studies found similar initial viral loads. [13,14,53,54] However, Chau *et al* reported significantly lower viral load in asymptomatic patients during the follow up compared to symptomatic patients.[53] Faster viral clearance was observed in asymptomatic individuals in five out of six studies.[13,28,53,55,56] The exception Yongchen *et al*., found longer shedding duration among asymptomatic cases, but the difference was not significant.[36]

Live virus detection

We identified 11 studies that attempted to isolate live virus. All eight studies that attempted virus isolation in respiratory samples successfully cultured viable virus within the first week of illness, [9,17,20,54,57-60] No live virus was isolated from any respiratory samples taken after day 8 of symptoms

in three studies,[20,57,58] or beyond day 9 in two studies[17,54] despite persistently high viral RNA loads. One study demonstrated the highest probability of positive culture on day 3 of symptoms.[57] Arons *et al*. cultured viable virus 6 days before typical symptom onset, however onset of symptom was unclear.[54]

The success of viral isolation correlated with viral load quantified by RT-PCR. No successful viral culture was obtained from samples with a viral load below 10^6 copies/ml, [20] Ct values >24,[57] or >34,[54,58] with culture positivity declining with increasing Ct values.[58] Several other studies cultured live virus from RT-PCR positive specimens; however, they did not correlate these results with viral load titres.[9,59,60]

Only one study reported the duration of viable virus shedding in respiratory samples; the median time to clearance from URT and LRT samples was 3.5 and 6 days, respectively.[20] Arons *et al*. cultured viable virus in one out of three asymptomatic cases from the respiratory tract.[54]

Of 3 studies attempting to isolate viable virus from stool,[20,61] culture was successful in two of three RNA-positive patients in one study, but the time points from symptom onset were not reported.[62] Andersson *et al.* failed to culture virus from 27 RT-PCR positive serum samples.[63]

Summary of SARS-CoV-1 and MERS studies

Eight studies on SARS-CoV-1 were included; the majority of studies did not report mean or median duration of viral shedding thus, were not eligible for quantitative analysis. The maximum duration of viral shedding reported was 8 weeks in URT,[64,65] 52 days in LRT,[61,64] 6-7 weeks in serum,[66] and 126 days in stool samples.[61,64,67-69] Dialysis patients had longer viral shedding in stool compared to non-dialysis patients.[68] Studies that have evaluated SARS-CoV-1 kinetics found low viral load in the initial days of illness, increasing after the first week of illness in URT samples, peaking at day 10,[70] or day 12-14,[67] and declining after week 3-4.[65] High viral loads correlated with severity of illness[65] and poor survival.[65] While Chen *et al.* identified an association between younger age and lower viral titers, [65] Leong *et al*. found no difference.[69] Viable SARS-CoV-1 was isolated from stool and respiratory samples up to 4 weeks, and urine specimens up to day 36.[64,66] All attempts to isolate virus from RT-PCR–positive stool specimens collected >6weeks after

disease onset failed.[61] The isolation probability for stool samples was approximately 5 to 10 times lower compared to respiratory specimens.[64]

We identified 11 studies on MERS-CoV. Three studies (324 subjects) reporting MERS-CoV shedding in URT and four studies (93 subjects) in LRT were included in the quantitative analysis. The mean shedding duration was 15.3 days (95% CI, 11.6 – 19.0) and 16.6 days (95% CI, 14.8 – 18.4), respectively (Supplementary Figures 1 and 2). Only one study reported duration of viral shedding in serum with a median of 14 days and max of 38 days.[71] In a small study, mortality rates were higher in patients with viraemia.[72] In URT and LRT specimens, prolonged shedding was associated with illness severity[73,74] and survival[75] with the shortest duration observed in asymptomatic patients.[73] Peak viral loads were observed between days 7 to 10 and higher viral loads was observed among patients with severe illness and fatal outcome.[71,73,74,76,77] Differences in viral loads between survivors and fatal cases was more pronounced in the second week of illness (P< .0006).[77] The proportion of successful viable culture was 6% in respiratory samples with a viral load values below 10^7copies/ml.[78]

Qualitative analysis

All but 11 studies (6 cohort studies, 2 cross-sectional studies, and 1 RCT on SARS-CoV-2 and 2 cohort studies on MERS-CoV) were case series, the majority of which recruited non-consecutive patients and therefore prone to possible selection bias. (Supplementary Table 1)

DISCUSSION

This systematic review and meta-analysis provide comprehensive data on the viral dynamics of SARS-CoV-2 including the duration of RNA shedding and viable virus isolation. Our findings suggest that while patients with SARS-CoV-2 may have prolonged RNA shedding, median time to live virus clearance from upper and lower respiratory tract samples were 3.5 days and 6 days respectively. No live virus isolated beyond day nine of symptoms despite persistently high viral RNA loads, thus emphasising that the infectious period cannot be inferred from the duration of viral RNA detection. This finding is supported by several studies demonstrating a relationship

between viral load and viability of virus, with no successful culture from samples below a certain viral load threshold.

SARS-CoV-2 viral load appears to peak in the URT within the first week of illness, and later in the LRT. In contrast, peaks in SARS-CoV-1 and MERS-CoV viral loads in the URT occurred at days 10-14 and 7-10 days of illness, respectively. Combined with viable isolation in respiratory samples within the first week of illness, patients with SARS-CoV-2 infection are likely to be most infectious in the first week of illness. Several studies report viral load peaks during the prodromal phase of illness or at the time of symptom onset, [2,4,8,16-23] providing a rationale for the efficient spread of SARS-CoV-2. This is supported by the observation in contact tracing studies that the highest risk of transmission occurs during the prodromal phase or early in the disease course.[79,80] No secondary cases were identified beyond 5 days after the symptom onset.[81] Although modelling studies estimated potential viral load peak before symptom onset, we did not identify any study that confirms pre-symptomatic viral load peak.[16]

Emerging evidence suggests a correlation between virus persistence and disease severity and outcome. [18,25,27-29,38] This is consistent with the viral load dynamics of influenza, MERS-CoV, and SARS-CoV-1 whereby severity of illness was also associated with prolonged viral shedding.[73,74,82] However, more studies are needed to understand the duration of viable virus in patients with severe illness.

Similar to SARS-CoV-1, SARS-CoV-2 can be detected in stool for prolonged periods, with high viral loads detected even after 3 weeks of illness. A clear difference between SARS-CoV and MERS-CoV is the detection of viral RNA in stool. In SARS-CoV-1, RNA prevalence in stool samples was high, with almost all studies reporting shedding in stool. Although viable SARS-CoV-1 was isolated up to 4 weeks of illness, faecal-oral transmission was not considered to be a primary driver of infection. Whereas in MERS-CoV, none of the studies reported duration of viral shedding in stool and RNA detection was low.[77,83] To date, only a few studies demonstrated viable SARS-CoV-2 in stool.[62,84] Thus, the role of faecal shedding in viral transmission remains unclear.

Although viral loads at the start of infection appear to be comparable between asymptomatic and symptomatic patients infected with SARS-CoV-2, most studies demonstrate faster viral clearance

among asymptomatic individuals. This suggests similar transmission potential among both groups at the onset of infection, but a shorter period of infectiousness in asymptomatic patients. This is in keeping with viral kinetics observed with other respiratory viruses such as influenza and MERS-CoV, in which people with asymptomatic infection have a shorter duration of viral shedding than symptomatic individuals. [73,85] However, there are limited data on the shedding of infectious virus in asymptomatic individuals to quantify their transmission potential.

We identified a systematic review of SARS CoV-2 viral load kinetics that included studies published up until 12 May 2020.[86] This review included many studies that did not meet our eligibility criteria, including 26 case reports and 13 case series involving <5 individuals; these are prone to significant selection bias, reporting atypical cases with prolonged viral shedding. Additionally, the review included studies that reported viral shedding duration from the time of hospital admission or initial PCR positivity, rather than symptom onset. Furthermore, no meta-analysis of the duration of viral shedding was performed.

This is the first study that has comprehensively examined and compared SARS-CoV-2, SARS-CoV-1 and MERS-CoV viral dynamics and performed a meta-analysis of viral shedding duration. Our study has limitations. First, some patients in the included studies received a range of treatments, including steroids and antivirals, which may have modified the shedding dynamics. Second, most of the included studies are case series, which are particularly vulnerable to selection bias. Third, our meta-analysis identified substantial study heterogeneity, likely due to differences in study population, follow up and management approaches. Further, shedding duration is reported as median ± IQR for most studies, but meta-analysis necessitates conversion to mean ± SD.[6] The validity of this conversion is based on the assumption that duration of viral shedding is normally distributed, which may not apply to some studies.

In conclusion, although SARS-CoV-2 RNA shedding can be prolonged in respiratory and stool samples, the duration of viable virus is short-lived, with culture success associated with viral load levels. No study has reported live SARS-CoV-2 beyond day nine. Most studies detected the SARS-CoV-2 viral load peak within the first week of illness. These findings highlight that isolation practices should be commenced with the start of first symptoms including mild and atypical

298 symptoms that precede more typical COVID-19 symptoms. This systematic review underscores
299 the importance of early case finding and isolation, as well as public education on the spectrum of
300 illness. However, given potential delays in the isolation of patients, effective containment of
301 SARS-CoV-2 may be challenging even with an early detection and isolation strategy.[87]

302

303 **Authors contributions:**

304 M. Cevik: conceptualisation, methodology, investigation, data curation, writing – original draft. M.
305 Tate: investigation, data curation, writing – original draft; O Lloyd: investigation, data curation,
306 writing – review and editing; A. E. Maraolo: formal analysis, writing – original draft; J. Schafers:
307 investigation, data curation, writing – review and editing; A Ho: conceptualisation, methodology,
308 data curation, writing – original draft, supervision.

309

310 **Financial support and sponsorship**

311 No financial support received

312

313 **Conflicts of interest**

314 All authors have nothing to disclose.

315 **Table 1: Summary of included studies**

316

Study	Geographical location	Study setting	Study design	Number of patients	Age Median (IQR)	Male sex N (%)	Specimen types
SARS-CoV-2							
Andersson et al. [63]	Oxford, UK	Hospital	Case series	167	56 (46-76)	89 (53)	Serum
Arons et al.[54]	King's County, USA	Care home	Cross-sectional	46	78.6 ± 9.5*	NR	URT
Bullard et al.[57]	Manitoba, Canada	Hospital	Case series	90	45 (30-59)	44 (49)	Respiratory samples (not specified)
Cai et al.[7]	Shanghai/ Hefei/ Qingdao, China	Hospital	Case series	10	6	4 (40)	LRT, blood, stool, urine
Cai et al.[26]	Shenzhen, China	Hospital	Case series	298	47 (33-61)	149 (50)	URT
Chang et al.[88]	Bejing, China	Hospital	Case series	16	35.5 (24-53)	11 (69)	URT
Chau et al.[53]	Ho Chi Minh City, Vietnam	Hospital	Case series	30	29 (16-60)	15 (50)	URT
Chen et al.[27]	Shanghai, China	Hospital	Case series	249	51 (36-64)	126 (51)	URT
Chen et al. [89]	Wuhan, China	Hospital	Case series	25	51.4 ±16.6*	11 (44)	URT
Chen et al.[28]	Guangzhou, China	Hospital	Case series	284	48 (33-62)	131 (46)	URT
Chen et al. [29]	Wuhan, China	Hospital	Case series	42	51	15 (36)	URT, stool, urine
Corman et al.[90]	Germany	Hospital	Case series	18	NR	12 (67)	Blood
Fan et al.[30]	Shenyang, China	Hospital	Case series	55	46.8	30 (55)	URT, sputum
Fang et al.[31]	Xiangtan, China	Hospital	Case series	32	41	16 (50)	URT, stool, blood
Fu et al.[91]	Huazhong, China	Hospital	Case series	50	64 (37-87)	27 (54)	URT
Han et al.[8]	Chongqing, South Korea	Hospital	Case series	12	6.5 (0.007-16)	5 (42)	URT, stool
He et al.[16]	Guangzhou, China	Hospital	Case series	94	46	47 (50)	URT
Hu et al.[37]	Qingdao, China	Hospital	Case series	59	46 (33-57)	28 (47)	URT
Hu et al.[55]	Nanjing, China	Hospital	Case series	24	32.5 (21-57)	8 (33)	URT
Huang et al.[51]	Guangzhou, China	Hospital	Case series	27	NR	12 (44)	URT

Huang et al.[23]	Wenzhou, China	Hospital	Case series	33	47 (range 2-84)	17 (52)	URT, LRT, stool
Huang et al.[92]	Wuhan, China	Hospital	Retrospective cohort	200	58± 17*	115 (48)	URT
Hung et al.[50]	Hong Kong	Hospital	RCT	127	52 (32-62)	68 (54)	URT, stool
Kim et al.[4]	Soeul/ Incheon/ Seongna, South Korea	Hospital	Case series	28	40 (28-54)	15 (54)	URT, LRT
Kujawski et al.[17]	6 states, USA	Hospital /Outpatient	Case series	12	53 (range 21-68)	8 (75)	URT, LRT, stool, blood, urine
L'Huillier et al.[9]	Geneva, Switzerland	Hospital	Case series	23	12 (3.8-14.5)	NR	URT
La Scola et al.[58]	France	Hospital	Case series	155	NR	NR	URT, LRT
Lavezzo et al.[14]	Vo', Italy	Community	Cross-sectional	Only sample # reported	Mixed	Mixed	URT
Le et al.[59]	Hanoi, Vietnam	Hospital	Case series	12	29.5*	3 (25)	URT
Li et al.[93]	Wuhan China	Hospital	Case series	36	57.5 (52-65)	23 (64)	URT
Liang et al.[49]	Wuhan, China	Hospital	Case series	120	61.5 (47-70)	68 (57)	URT
Ling et al.[47]	Shanghai, China	Hospital	Case series	66	44 (16-778)	38 (58)	URT, stool, blood, urine
Liu et al. [94]	Wuhan, China	Hospital	Case series	238	55 (38.3-65)	138 (58)	URT
Liu et al.[32]	Nanchang, China	Hospital	Case series	76	48.3	48 (63)	URT
Lo et al.[95]	Macau, China	Hospital	Case series	10	54 (27-64)	3 (30)	URT, LRT, stool, urine
Lou B et al.[96]	Zhejiang, China	Hospital	Case series	80	55 (45-64)	50 (69)	LRT
Pongpirul et al.[97]	Bangkok, Thailand	Hospital	Case series	11	61 (28-74)	6 (55)	URT
Qian et al.[98]	Ningbo, China	Hospital	Case series	24	NR	NR	URT
Quan et al.[99]	Wuhan/Shenzhen/ Xiangyang, China	Hospital	Case series	23	60.3 ±15.3*	23 (100)	Prostatic secretions all negative (URT)

Sakurai et al.[43]	Aichi, Japan	Hospital	Case series	90	59.5 (36-68)	53 (59)	URT
Seah et al.[100]	Singapore	Hospital	Case series	17	NR	NR	Tears
Shastri et al.[46]	Mumbai, India	Reference lab	Case series	68	37 (range 3-75)	48 (71)	URT
Shi et al.[33]	Wuhan, China	Hospital	Case series	246	58 (47-67)	126 (51)	URT
Song et al.[101]	Nanjing, China	Hospital	Case series	13	22 – 67 (range only)	13 (100)	URT, semen, testicular sample
Song et al. [102]	Beijing, China	Hospital/Outpatient	Case series	21	37 (21-59.5)	8 (38)	URT
Talmy et al.[44]	Ramat Gan, Israel	Outpatient	Case series	119	21 (19-25)	84 (71)	URT
Tan et al. [34]	Chongqing, China	Hospital	Case series	142	NR	NR	URT
Tan et al.[18]	Chongqing, China	Hospital	Case series	67	49 (10-77)	35 (52)	URT, LRT, stool, blood, urine
Tan et al.[10]	Changsha, China	Hospital	Case series	10	7 (1-12)	3 (30)	URT, stool
Tian et al. [41]	Beijing, China	Hospital/Outpatient	Case series	75	41.5 (range 0.8 – 88)*	42 (56)	Respiratory tract sample (not specified further)
To et al.[19]	Hong Kong, China	Hospital	Case series	23	62 (37-75)	13 (57)	URT, stool, blood, urine
To et al. [60]	Hong Kong, China	Hospital	Prospective Cohort	12	62.5 (37-75)	7 (58)	URT (saliva)
Tu et al. [103]	Anhui, China	Hospital	Case series	40	Viral shedding <10 days: 40.86 ± 8.26 Viral shedding ≥10 days: 45.5 ± 14.60	21 (53)	URT
Wang et al.[104]	Henan, China	Hospital	Case series	18	39 (29-55)	10 (56)	URT
Wang et al.[105]	Jinhua, China	Hospital	Case series	17	42 ±17*	10 (59)	URT, stool
Wölfel et al.[20]	Munich, Germany	Hospital	Case series	9	NR	NR	URT, blood, urine
Wu et al.[106]	Hainan, China	Hospital	Case series	91	50 (range 21-83)*	52 (57)	URT, stool

Wu et al.[11]	Qingdao, China	Hospital	Case series	74	6 (0.1-15.08 range)	44 (59)	Stool
Wu et al.[40]	Zhuhai, China	Hospital	Case series	74	43.8*	35 (47)	Stool
Wyllie et al.[21]	New Haven, USA	Hospital	Case series	44	61 (23-92 range)*	23 (52)	URT (saliva)
Xiao et al. [45]	Wuhan, China	Hospital	Case series	56	55 (42-68)	34 (61)	URT
Xiao et al.[62]	Guangzhou, China	Hospital	Case series	28			Stool
Xu et al. [38]	Shenzhen/ Zheijang, China	Hospital	Retrospective Cohort	113	52 (42-63)	66 (58)	URT
Xu et al.[107]	Shenyang, China	Hospital	Case series	14	48 ± 13.4*	7 (50)	URT, LRT, serum, conjunctiva
Xu et al. [12]	Guangzhou, China	Hospital	Case series	10	6.6	6 (60)	URT, rectal swab
Yan et al.[39]	Hubei, China	Hospital	Case series	120	52 (35-63)	54 (45)	URT
Yang et al.[56]	Wuhan, China	Hospital	Case series	78 (45 symptomatic)	Symptomatic: 56 (34-63) Asymptomatic: 37 (26-45)	Symptomatic:31 (40) Asymptomatic: 11 (33)	URT
Yang et al.[108]	Shenzhen, China	Hospital	Case series	213	52 (range 2-86)	108 (51)	URT, LRT
Yongchen et al.[36]	Nanjing, Xuzhou, China	Hospital	Case series	21	37	13 (62)	URT, stool
Young et al.[22]	Singapore	Hospital	Case series	18	47	9 (50)	URT, stool, blood, urine
Zha et al.[48]	Wuhu, China	Hospital	Case series	31	39 (32-54)	20 (65)	URT
Zhang et al.[24]	Beijing, China	Hospital	Case series	23	48 (40-62)	12 (52)	URT, stool, blood, urine
Zhang et al. [13]	Shenzhen, China	Hospital	Case series	56	Mixed	Mixed	URT, stool
Zheng et al.[25]	Zhejiang, China	Hospital	Retrospective Cohort	96	53 (33.4-64.8)	NR	LRT, stool, blood, urine
Zhou et al.[42]	Wuhan, China	Hospital	Case series	41	58 (48-62)	22 (54)	URT
Zhou et al. [35]	Wuhan, China	Hospital	Case series	191	56 (46-67)	119 (62)	URT
Zhou et al.[52]	Guangzhou, China	Hospital	Case series	31	45 (33-60) 37 (28-57)	4 (44) 6 (27)	URT
Zhu et al. [15]	Wuhan, China	Hospital	Case series	10	49.5	8 (80)	URT

Zou et al.[2]	Zhuhai, China	Hospital/outpatient	Case series	18	59 (range 26-76)	9 (50)	URT
SARS-CoV-1							
Chan et al.[64]	Hong Kong, China	Hospital	Case series	415	11.3 ± 4.1* 37.1 ± 11.2*	132 (33)	URT, LRT, stool, urine
Chen et al.[65]	Taiwan	Hospital	Case series	108	Stratified	95	URT
Cheng et al.[67]	Hong Kong, China	Hospital	Case series	1041	NR	NR	URT, LRT, stool, urine
Kwan et al.[68]	Hong Kong, China	Hospital	Case series	12 dialysis 33 controls	Dialysis: 58 (range 34-74);* Controls: 57 (range 34-75)	6 (50)	URT, stools, urine
Liu et al.[61]	Beijing, China	Hospital	Case series	56	31 (male) 34 (female)	31 (55)	LRT, stool
Leong et al.[69]	Singapore	Hospital	Case series	64	35.2 (17-63 range)*	16 (25)	URT, stool, blood, urine
Peiris et al. [70]	Hong Kong, China	Hospital	Case series	75	39.8 (SD 12.2)	0.92	URT
Xu et al.[109]	Beijing, China	Hospital	Case series	54	NR	NR	LRT, blood, urine
MERS-CoV							
Al Hosani et al.[73]	Abu Dhabi, UAE	Hospital/community	Case series	65	20 -59	43 (66)	LRT
Al-Jasser et al.[110]	Riyadh, Saudi Arabia	Hospital	Case series	167	46.71*	142 (57)	URT
Alkendi et al.[111]	Tawam/Al Ain, UAE	Hospital	Case series	58	43.5	41 (71)	URT
Arabi et al.[75]	Saudi Arabia	Hospital	Cohort	330	58 (44-69)	225 (68)	URT
Corman et al.[77]	Riyadh, Saudi Arabia	Hospital	Case series	37	69 (24–90)*	27 (39)	URT, LRT, stool, blood, urine
Hong et al.[76]	Seoul, South Korea	Hospital	Case series	30	49*	19 (63)	Blood
Min et al.[71]	Seoul/others, South Korea	Hospital	Case series	14	62	6 (35)	LRT, serum
Muth et al.[78]	Riyadh, Saudi Arabia	Hospital	Case series	32	66 (24-90)	24 (75)	LRT
Oh et al.[74]	Seoul, South Korea	Hospital	Case series	17	NR	NR	URT, LRT, serum
Park et al.[112]	Seoul, South Korea	Hospital	Case series	17	NR	NR	URT, LRT

Shalhoub et al.[72]	Jeddah, Saudi Arabia	Hospital	Retrospective cohort	32	65	14 (44)	LRT, serum

Abbreviations: UK, United Kingdom, USA; United States of America; UAE, United Arab Emirates; RCT, randomised controlled trial; URT, upper respiratory tract; LRT, lower respiratory tract; NR, not reported.

* Mean ± standard deviation (or range if stated).

333 **Table 2: Severity of illness and viral dynamics**

Study	Classification of severity	Median duration - days (IQR)	Viral dynamics in severe patients compared to non-severe patients	P-value
Chen *et al.*[27]	ICU vs. non-ICU patients	11	Median time to viral clearance significantly longer in ICU vs. non-ICU patients (HR=3.17, 95% CI, 2.29-4.37)	Only HR provided
Chen *et al* [28]	China CDC guideline (version 7)	12 (8-16)	Shedding duration varies by severity: asymptomatic 6 days; mild 10 days; moderate 12 days; serious 14 days; critical 32 days	<0.0001
Tan *et al.*[18]	China CDC guideline (version 6)	NP: 12 Any sample: 22	Viral shedding significantly longer in severe patients: any sample 23 vs. 20 days (note NP: 14 vs. 11 days – non-significant)	p=0.023 (any sample)
Xu *et al.*[38]	WHO criteria	17 (13-32)	Higher proportion of severe patients had shedding >21 days (34.2% vs.16.2%)	0.49
Yan *et al.* [39]	China CDC guideline (version 6)	23 (18-32)	No difference in shedding duration (general 23 days vs. severe 26 days vs. critical 28 days)	0.51
Zheng *et al.*[25]	China CDC guideline (version 6)	Resp: 18 (13-29)	Shedding duration significantly longer in severe patients (21 vs 14 days) in respiratory samples. No difference in shedding duration in stool/serum	p=0.04

334 Abbreviations: IQR, interquartile range; ICU, intensive care unit; HR, hazard ratio; CDC, Centers

335 for Disease Control and Prevention; WHO, World Health Organization.

336

337

338

339

340

341

342

343 **Table 3: SARS-CoV-2 viral dynamics in asymptomatic patients compared to symptomatic**
344 **patients**

	Median duration – days (IQR)	Viral dynamics in asymptomatic patients compared to symptomatic patients	P-value
Arons *et al.* [54]	NR	No difference in viral load	NS
Chau *et al.* [53]	NR	Initial viral load similar. Asymptomatic patients had significantly lower viral load during the follow up compared to symptomatic patients and faster viral clearance in asymptomatic, compared to symptomatic individuals	0.027
Chen *et al.* [28]	6 (3.5-10)	Significantly shorter duration of viral shedding among asymptomatic cases (median 6 days, IQR 3.5-10), with increasing shedding duration associated with increasing illness severity	<0.0001
Han *et al.* [8]	NR	Symptomatic children had higher initial RNA load in nasopharyngeal swab specimens than asymptomatic children (9.01 vs. 6.32 $\log_{10}$ copies/mL; p = 0.048).	0.048
Hu *et al.* [55]	6 (2-12)	Asymptomatic patients had shorter duration of viral shedding compared to pre-symptomatic patients (median duration of SARS-CoV-2 positivity was 6.0 (2.0 - 12.0) compared to 12.0 (12.0 - 14.0))	NR
Lavezzo *et al.* [14]	NR	No difference in viral load	NS
Le *et al.* [59]	9	NR	N/A
Sakurai *et al.* [43]	9 (6-11)	NR	N/A
Yang et al. [56]	8 (3-12)	Significantly shorter duration of viral shedding from nasopharynx swabs was observed among asymptomatic compared to symptomatic patients	P= .001
Yongchen *et al.* [36]	18 (5-28)	Longer shedding duration among asymptomatic cases (median 18 days, range 5-28), compared to non-severe (10 days, range 2-21) and severe (14 days, range 9-33) cases	NS
Zhang *et al.* [13]	9.63	Initial viral load similar, viral clearance occurred earlier in the asymptomatic (9.6 days) and symptomatic individuals (9.7 days, compared to pre-symptomatic group (13.6 days)	
Zhou *et al.* [52]	NR	Significantly higher viral load in symptomatic (n=22) compared to asymptomatic (n=9) patients (median cycle threshold (Ct) value 34.5 vs. 39.0, respectively) but duration of shedding was similar	

345 Abbreviations: IQR, interquartile range; RNA, ribonucleic acid; NR, not reported; NS, non-
346 significant; N/A, not applicable

Figure 1. Flowchart describing study selection

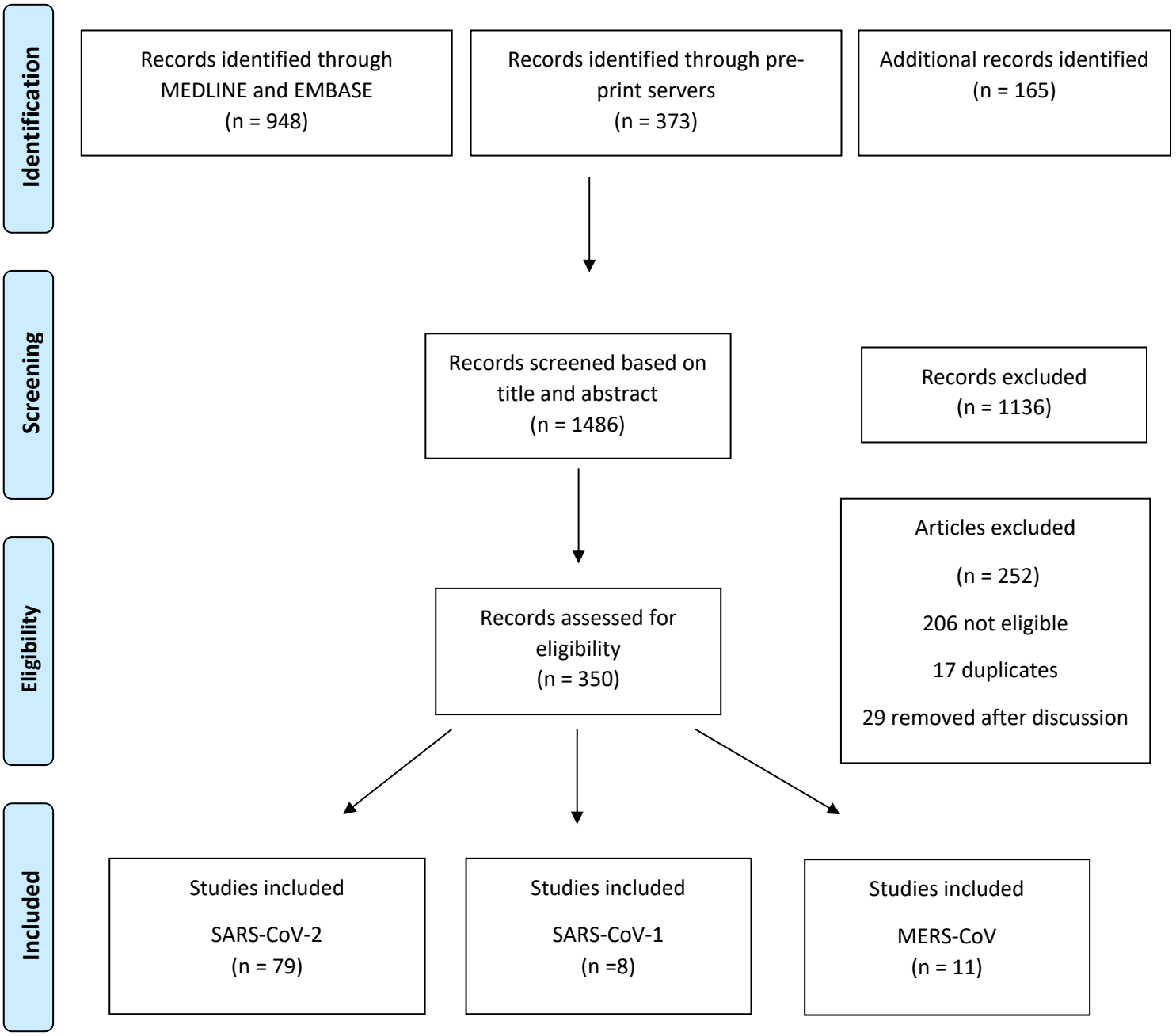

From: Moher D, Liberati A, Tetzlaff J, Altman DG, The PRISMA Group (2009). *P*referred *R*eporting *I*tems for *S*ystematic Reviews and *M*eta-*A*nalyses: The PRISMA Statement. PLoS Med 6(6): e1000097. doi:10.1371/journal.pmed1000097

For more information, visit www.prisma-statement.org.

Figure 2: Pooled mean duration (days) of SARS-CoV-2 shedding from the upper respiratory tract (random-effects model).

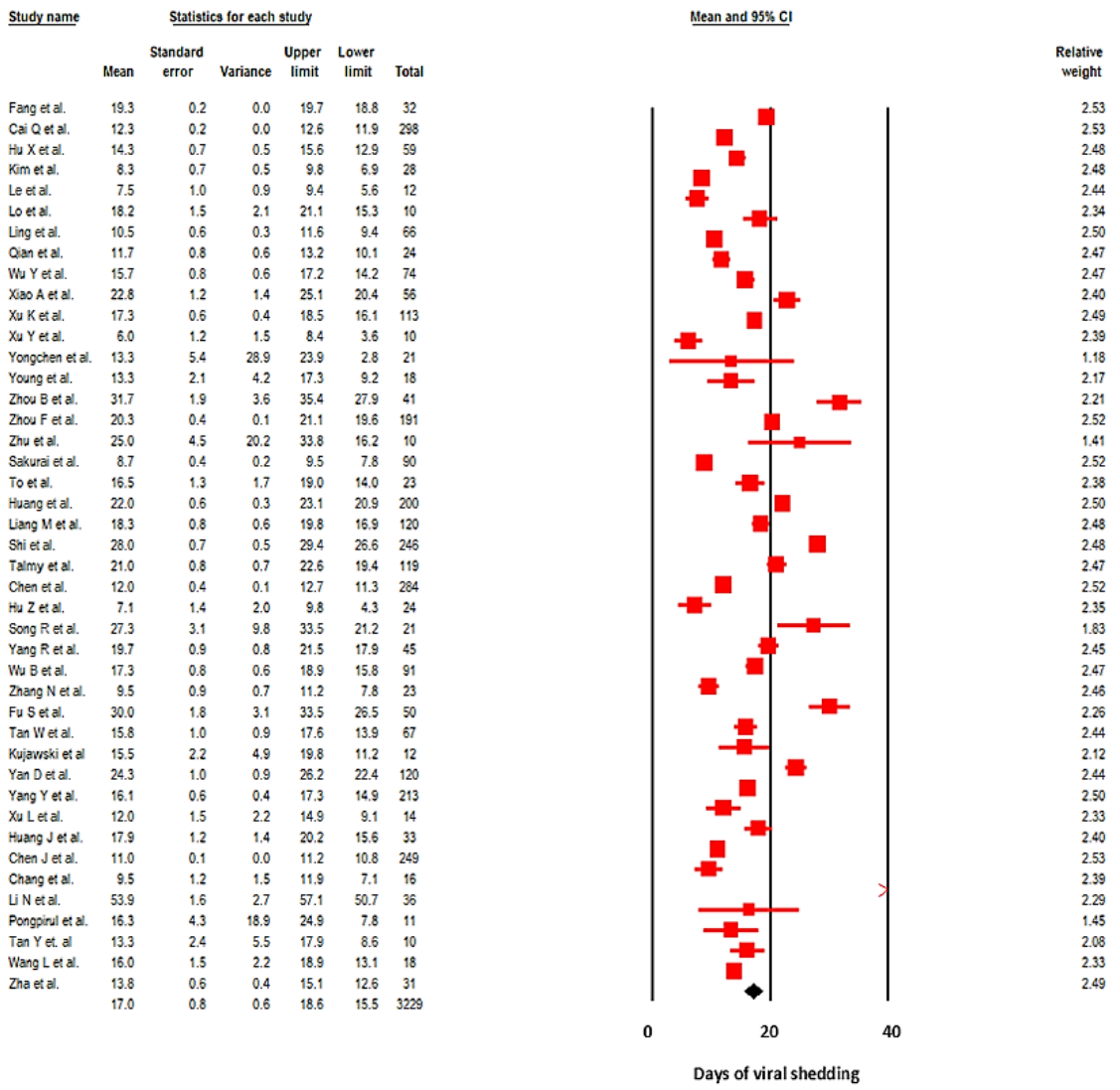

Note: the overall effect is plotted as a black square.

Test for heterogeneity: Q-value = 4076,08, df(Q) = 42, $p < 0.001$, $I^2 = 99\%$.

Figure 3: Pooled mean duration (days) of SARS-CoV-2 shedding from the lower respiratory tract (random-effects model).

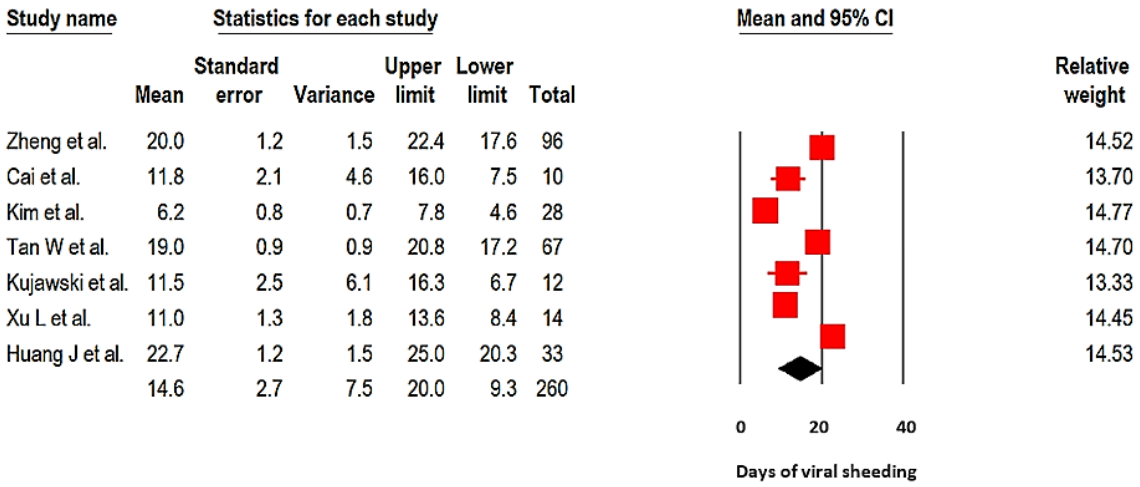

Note: the overall effect is plotted as a black square.

Test for heterogeneity: Q-value = 203.3, df(Q) = 6, $p < 0.001$, $I^2 = 97\%$.

Figure 4. Pooled mean duration (days) of SARS-CoV-2 shedding in the blood (random-effects model).

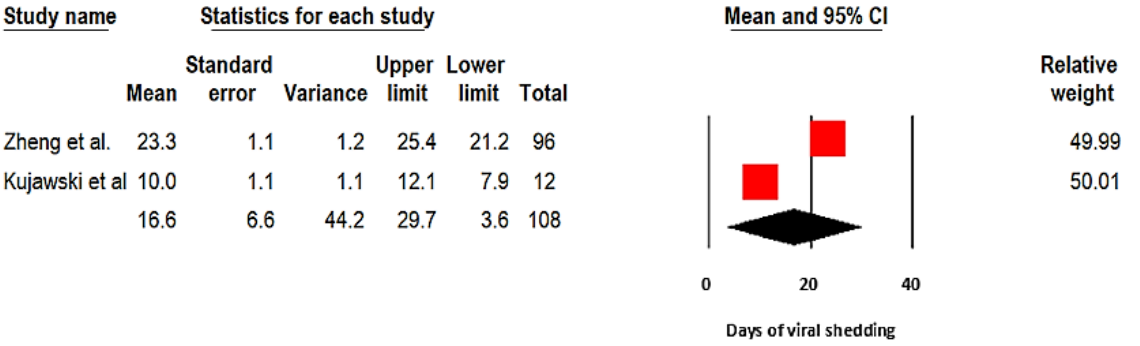

Note: the overall effect is plotted as a black square.

Test for heterogeneity: Q-value = 77,6, df(Q) = 1, $p < 0.001$, $I^2 = 99\%$.

Figure 5. Pooled mean duration (days) of SARS-CoV-2 shedding from the stool (random-effects model).

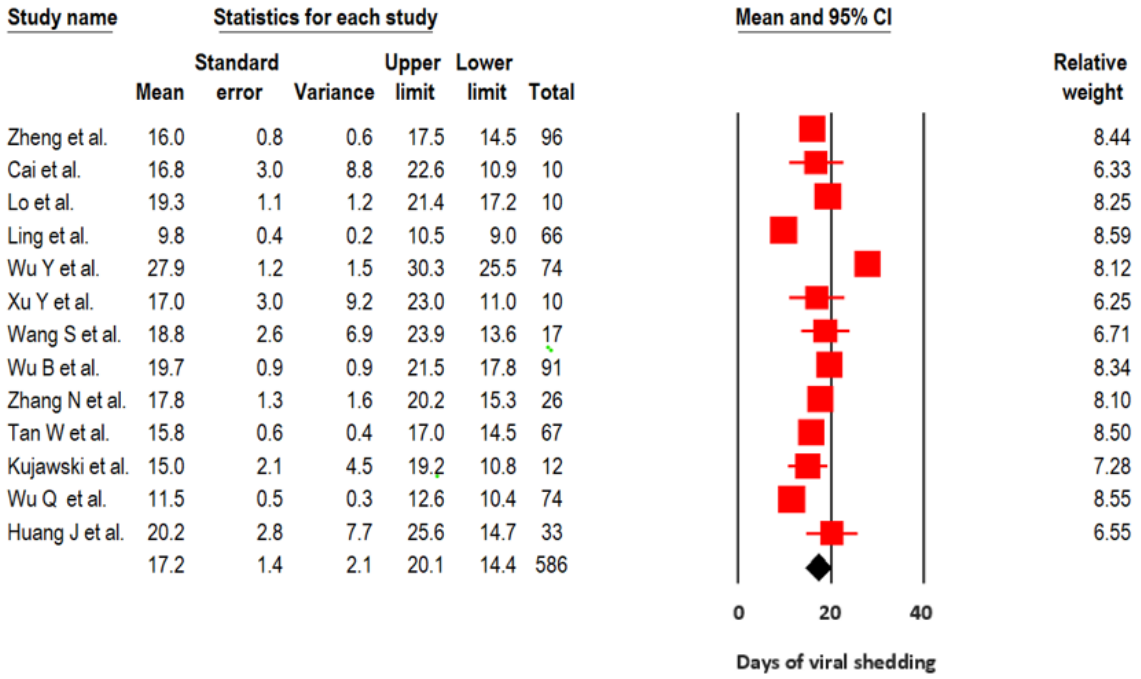

Note: the overall effect is plotted as a black square.

Test for heterogeneity: Q-value = 356.0, df(Q) = 12, $p < 0.001$, $I2 = 96.6\%$.

Figure 6. Meta-regression bubble plot of the impact of age on mean SARS-CoV-2 shedding from the upper respiratory tract

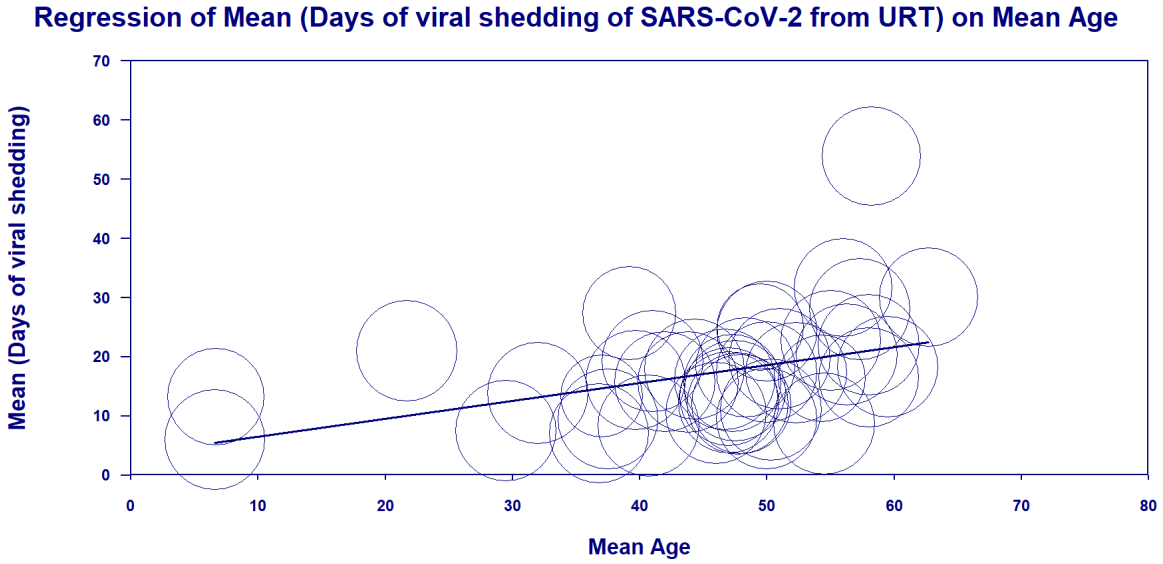

URT: upper respiratory tract.

Note: the plot was built upon 41 studies (no data on mean age from the study of Qian et al.[98]). A random-effects model was used.

References:

1. Cevik M, Bamford CGG, Ho A. COVID-19 pandemic-a focused review for clinicians. *Clin Microbiol Infect* 2020; **26**(7): 842-7.
2. Zou L, Ruan F, Huang M, et al. SARS-CoV-2 Viral Load in Upper Respiratory Specimens of Infected Patients. *New England Journal of Medicine* 2020; **382**(12): 1177-9.
3. Wolfel R, Corman VM, Guggemos W, et al. Virological assessment of hospitalized patients with COVID-2019. *Nature* 2020.
4. Kim ES, Chin BS, Kang CK, et al. Clinical Course and Outcomes of Patients with Severe Acute Respiratory Syndrome Coronavirus 2 Infection: a Preliminary Report of the First 28 Patients from the Korean Cohort Study on COVID-19. *J Korean Med Sci* 2020; **35**(13): e142.
5. Institute TJB. The Joanna Briggs Institute Critical Appraisal tools for use in JBI systematic reviews–checklist for case series. , 2017.
6. Wan X, Wang W, Liu J, Tong T. Estimating the sample mean and standard deviation from the sample size, median, range and/or interquartile range. *BMC Medical Research Methodology* 2014; **14**(1): 135.
7. Cai J, Xu J, Lin D, et al. A Case Series of children with 2019 novel coronavirus infection: clinical and epidemiological features. *Clinical Infectious Diseases* 2020; **28**: 28.
8. Han MS, Seong M-W, Kim N, et al. Early Release - Viral RNA Load in Mildly Symptomatic and Asymptomatic Children with COVID-19, Seoul - Volume 26, Number 10—October 2020 - Emerging Infectious Diseases journal - CDC.
9. L'Huillier A, Torriani G, Pigny F, Kaiser L, Eckerle I. Shedding of infectious SARS-CoV-2 in symptomatic neonates, children and adolescents. 2020.
10. Tan Y-p, Tan B-y, Pan J, Wu J, Zeng S-z, Wei H-y. Epidemiologic and clinical characteristics of 10 children with coronavirus disease 2019 in Changsha, China. *Journal of Clinical Virology* 2020; **127**: 104353.
11. Wu Q, Xing Y, Shi L, et al. Epidemiological and Clinical Characteristics of Children with Coronavirus Disease 2019. 2020.
12. Xu Y, Li X, Zhu B, et al. Characteristics of pediatric SARS-CoV-2 infection and potential evidence for persistent fecal viral shedding. *Nature Medicine* 2020; **26**(4): 502-5.
13. Zhang Z, Xiao T, Wang Y, et al. Early viral clearance and antibody kinetics of COVID-19 among asymptomatic carriers. *medRxiv* 2020: 2020.04.28.20083139.
14. Lavezzo E, Franchin E, Ciavarella C, et al. Suppression of a SARS-CoV-2 outbreak in the Italian municipality of Vo'. *Nature* 2020: 1-.
15. Zhu L, Gong N, Liu B, et al. Coronavirus Disease 2019 Pneumonia in Immunosuppressed Renal Transplant Recipients: A Summary of 10 Confirmed Cases in Wuhan, China. *Eur Urol* 2020; **18**: 18.
16. He X, Lau EHY, Wu P, et al. Temporal dynamics in viral shedding and transmissibility of COVID-19. *Nature Medicine*; **26**(5): 672-5.
17. Kujawski SA, Wong KK, Collins JP, et al. Clinical and virologic characteristics of the first 12 patients with coronavirus disease 2019 (COVID-19) in the United States. *Nature Medicine* 2020; **26**(6): 861-8.
18. Tan W, Lu Y, Zhang J, et al. Viral Kinetics and Antibody Responses in Patients with COVID-19. 2020.
19. To KK-W, Tsang OT-Y, Leung W-S, et al. Temporal profiles of viral load in posterior oropharyngeal saliva samples and serum antibody responses during infection by SARS-CoV-2: an observational cohort study. *The Lancet Infectious Diseases* 2020; **20**(5): 565-74.
20. Wolfel R, Corman VM, Guggemos W, et al. Virological assessment of hospitalized patients with COVID-2019. *Nature* 2020; **581**(7809): 465-9.
21. Wyllie AL, Fournier J, Casanovas-Massana A, et al. Saliva is more sensitive for SARS-CoV-2 detection in COVID-19 patients than nasopharyngeal swabs.

22. Young BE, Ong SWX, Kalimuddin S, et al. Epidemiologic Features and Clinical Course of Patients Infected With SARS-CoV-2 in Singapore. *JAMA* 2020; **03**: 03.
23. Huang J, Mao T, Li S, et al. Long period dynamics of viral load and antibodies for SARS-CoV-2 infection: an observational cohort study. *medRxiv* 2020: 2020.04.22.20071258.
24. Zhang N, Gong Y, Meng F, Bi Y, Yang P, Wang F. Virus shedding patterns in nasopharyngeal and fecal specimens of COVID-19 patients. 2020.
25. Zheng S, Fan J, Yu F, et al. Viral load dynamics and disease severity in patients infected with SARS-CoV-2 in Zhejiang province, China, January-March 2020: retrospective cohort study. *BMJ* 2020; **369**.
26. Cai Q, Huang D, Ou P, et al. COVID-19 in a designated infectious diseases hospital outside Hubei Province, China. *Allergy* 2020; **n/a**(n/a).
27. Chen J, Qi T, Liu L, et al. Clinical progression of patients with COVID-19 in Shanghai, China. *Journal of Infection* 2020; **80**(5): e1-e6.
28. Chen X, Zhang Y, Zhu B, et al. Associations of clinical characteristics and antiviral drugs with viral RNA clearance in patients with COVID-19 in Guangzhou, China: a retrospective cohort study.
29. Chen Y, Chen L, Deng Q, et al. The presence of SARS-CoV-2 RNA in the feces of COVID-19 patients. *Journal of Medical Virology* 2020; **03**: 03.
30. Fan L, Liu C, Li N, et al. Medical treatment of 55 patients with COVID-19 from seven cities in northeast China who fully recovered: a single-center, retrospective, observational study.
31. Fang Z, Zhang Y, Hang C, Ai J, Li S, Zhang W. Comparisons of viral shedding time of SARS-CoV-2 of different samples in ICU and non-ICU patients. *Journal of Infection* 2020; **21**: 21.
32. Liu Y, Yan L-M, Wan L, et al. Viral dynamics in mild and severe cases of COVID-19. *Lancet Infect Dis* 2020; **20**(6): 656-7.
33. Shi J, Cheng C, Yu M, et al. Systemic Inflammatory Cytokines Associate With SARS-COV-2 Viral Shedding Time in Covid-19 Inpatients. *ResearchSquare* 2020.
34. Tan L, Kang X, Ji X, et al. Validation of Predictors of Disease Severity and Outcomes in COVID-19 Patients: A Descriptive and Retrospective Study. *Med* 2020.
35. Zhou F, Yu T, Du R, et al. Clinical course and risk factors for mortality of adult inpatients with COVID-19 in Wuhan, China: a retrospective cohort study. *Lancet* 2020; **395**(10229): 1054-62.
36. Yongchen Z, Shen H, Wang X, et al. Different longitudinal patterns of nucleic acid and serology testing results based on disease severity of COVID-19 patients. *Emerg* 2020; **9**(1): 833-6.
37. Hu X, Xing Y, Jia J, et al. Factors associated with negative conversion of viral RNA in patients hospitalized with COVID-19. *Science of the Total Environment* 2020; **728 (no pagination)**.
38. Xu K, Chen Y, Yuan J, et al. Factors associated with prolonged viral RNA shedding in patients with COVID-19. *Clinical Infectious Diseases* 2020; **09**: 09.
39. Yan D, Liu X-y, Zhu Y-n, et al. Factors associated with prolonged viral shedding and impact of Lopinavir/Ritonavir treatment in patients with SARS-CoV-2 infection.
40. Wu Y, Guo C, Tang L, et al. Prolonged presence of SARS-CoV-2 viral RNA in faecal samples. *Lancet Gastroenterol Hepatol* 2020; **5**(5): 434-5.
41. Tian D, Wang L, Wang X, et al. Clinical research and factors associated with prolonged duration of viral shedding in patients with COVID-19. *ResearchSquare* 2020.
42. Zhou B, She J, Wang Y, Ma X. The duration of viral shedding of discharged patients with severe COVID-19. *Clinical Infectious Diseases* 2020; **17**: 17.
43. Sakurai A, Sasaki T, Kato S, et al. Natural History of Asymptomatic SARS-CoV-2 Infection. *New England Journal of Medicine* 2020.
44. Talmy T, Tsur A, Shabtay O. Duration of Viral Clearance in IDF Soldiers with Mild COVID-19. *medRxiv*.
45. Xiao AT, Tong YX, Zhang S. Profile of RT-PCR for SARS-CoV-2: a preliminary study from 56 COVID-19 patients. *Clinical Infectious Diseases* 2020; **19**: 19.

46. Shastri A, Wheat J, Agrawal S, et al. Delayed clearance of SARS-CoV2 in male compared to female patients: High ACE2 expression in testes suggests possible existence of gender-specific viral reservoirs.
47. Ling Y, Xu S-B, Lin Y-X, et al. Persistence and clearance of viral RNA in 2019 novel coronavirus disease rehabilitation patients. *Chinese Medical Journal* 2020; **133**(9).
48. Zha L, Li S, Pan L, et al. Corticosteroid treatment of patients with coronavirus disease 2019 (COVID-19). *Medical Journal of Australia* 2020; **212**(9): 416-20.
49. Liang M, Chen P, He M, et al. Corticosteroid Treatment in Critically Ill Patients with COVID-19: A Retrospective Cohort Study. *ResearchSquare* 2020.
50. Hung IFN, Lung KC, Tso EYK, et al. Triple combination of interferon beta-1b, lopinavir-ritonavir, and ribavirin in the treatment of patients admitted to hospital with COVID-19: an open-label, randomised, phase 2 trial. *The Lancet* 2020; **395**(10238): 1695-704.
51. Huang H, Guan L, Yang Y, et al. Chloroquine, arbidol (umifenovir) or lopinavir/ritonavir as the antiviral monotherapy for COVID-19 patients: a retrospective cohort study. 2020.
52. Zhou R, Li F, Chen F, et al. Viral dynamics in asymptomatic patients with COVID-19. *International Journal of Infectious Diseases* 2020; **96**: 288-90.
53. Chau NVV, Thanh Lam V, Thanh Dung N, et al. The natural history and transmission potential of asymptomatic SARS-CoV-2 infection. *Clinical Infectious Diseases* 2020.
54. Arons MM, Hatfield KM, Reddy SC, et al. Presymptomatic SARS-CoV-2 Infections and Transmission in a Skilled Nursing Facility. *New England Journal of Medicine* 2020; **382**(22): 2081-90.
55. Hu Z, Song C, Xu C, et al. Clinical characteristics of 24 asymptomatic infections with COVID-19 screened among close contacts in Nanjing, China. *Science China Life Sciences* 2020; **63**(5): 706-11.
56. Yang R, Gui X, Xiong Y. Comparison of Clinical Characteristics of Patients with Asymptomatic vs Symptomatic Coronavirus Disease 2019 in Wuhan, China. *JAMA Netw Open* 2020; **3**(5).
57. Bullard J, Dust K, Funk D, et al. Predicting infectious SARS-CoV-2 from diagnostic samples. *Clinical Infectious Diseases*.
58. La Scola B, Le Bideau M, Andreani J, et al. Viral RNA load as determined by cell culture as a management tool for discharge of SARS-CoV-2 patients from infectious disease wards. *Eur J Clin Microbiol Infect Dis* 2020: 1-3.
59. Le TQM, Takemura T, Moi ML, et al. Severe Acute Respiratory Syndrome Coronavirus 2 Shedding by Travelers, Vietnam, 2020. *Emerg Infect Dis* 2020; **26**(7): 02.
60. To KK-W, Tsang OT-Y, Yip CC-Y, et al. Consistent Detection of 2019 Novel Coronavirus in Saliva. *Clinical Infectious Diseases* 2020; (ciaa149).
61. Liu W, Tang F, Fontanet A, et al. Long-term SARS coronavirus excretion from patient cohort, China. *Emerg Infect Dis* 2004; **10**(10): 1841-3.
62. Xiao F, Sun J, Xu Y, et al. Infectious SARS-CoV-2 in Feces of Patient with Severe COVID-19. *Emerging Infectious Disease journal* 2020; **26**(8).
63. Andersson M, Arancibia - Carcamo CV, Auckland K, et al. SARS-CoV-2 RNA detected in blood samples from patients with COVID-19 is not associated with infectious virus. *medRxiv*.
64. Chan PK, To WK, Ng KC, et al. Laboratory diagnosis of SARS. *Emerg Infect Dis* 2004; **10**(5): 825-31.
65. Chen WJ, Yang JY, Lin JH, et al. Nasopharyngeal shedding of severe acute respiratory syndrome-associated coronavirus is associated with genetic polymorphisms. *Clinical Infectious Diseases* 2006; **42**(11): 1561-9.
66. Xu D, Zhang Z, Jin L, et al. Persistent shedding of viable SARS-CoV in urine and stool of SARS patients during the convalescent phase. *European Journal of Clinical Microbiology and Infectious Diseases* 2005; **24**(3): 165-71.
67. Cheng PK, Wong DA, Tong LK, et al. Viral shedding patterns of coronavirus in patients with probable severe acute respiratory syndrome. *Lancet* 2004; **363**(9422): 1699-700.
68. Kwan BC, Leung CB, Szeto CC, et al. Severe acute respiratory syndrome in dialysis patients. *J Am Soc Nephrol* 2004; **15**(7): 1883-8.

69. Leong HN, Chan KP, Khan AS, et al. Virus-specific RNA and antibody from convalescent-phase SARS patients discharged from hospital. *Emerg Infect Dis* 2004; **10**(10): 1745-50.
70. Peiris JSM, Chu CM, Cheng VCC, et al. Clinical progression and viral load in a community outbreak of coronavirus-associated SARS pneumonia: a prospective study. *The Lancet* 2003; **361**(9371): 1767-72.
71. Min CK, Cheon S, Ha NY, et al. Comparative and kinetic analysis of viral shedding and immunological responses in MERS patients representing a broad spectrum of disease severity. *Sci* 2016; **6**: 25359.
72. Shalhoub S, Farahat F, Al-Jiffri A, et al. IFN-alpha2a or IFN-beta1a in combination with ribavirin to treat Middle East respiratory syndrome coronavirus pneumonia: a retrospective study. *J Antimicrob Chemother* 2015; **70**(7): 2129-32.
73. Al Hosani FI, Pringle K, Al Mulla M, et al. Response to Emergence of Middle East Respiratory Syndrome Coronavirus, Abu Dhabi, United Arab Emirates, 2013-2014. *Emerg Infect Dis* 2016; **22**(7): 1162-8.
74. Oh MD, Park WB, Choe PG, et al. Viral load kinetics of MERS coronavirus infection. *New England Journal of Medicine* 2016; **375**(13): 1303-5.
75. Arabi YM, Al-Omari A, Mandourah Y, et al. Critically Ill Patients With the Middle East Respiratory Syndrome: A Multicenter Retrospective Cohort Study. *Crit Care Med* 2017; **45**(10): 1683-95.
76. Hong KH, Choi JP, Hong SH, et al. Predictors of mortality in Middle East respiratory syndrome (MERS). *Thorax* 2018; **73**(3): 286-9.
77. Corman VM, Albarrak AM, Omrani AS, et al. Viral Shedding and Antibody Response in 37 Patients With Middle East Respiratory Syndrome Coronavirus Infection. *Clinical Infectious Diseases* 2016; **62**(4): 477-83.
78. Muth D, Corman VM, Meyer B, et al. Infectious middle east respiratory syndrome coronavirus excretion and serotype variability based on live virus isolates from patients in Saudi Arabia. *Journal of Clinical Microbiology* 2015; **53**(9): 2951-5.
79. Wang Y, Tian H, Zhang L, et al. Reduction of secondary transmission of SARS-CoV-2 in households by face mask use, disinfection and social distancing: a cohort study in Beijing, China. *BMJ Global Health* 2020; **5**(5): e002794.
80. Böhmer MM, Buchholz U, Corman VM, et al. Investigation of a COVID-19 outbreak in Germany resulting from a single travel-associated primary case: a case series. *The Lancet Infectious Diseases*.
81. Cheng H-Y, Jian S-W, Liu D-P, et al. Contact Tracing Assessment of COVID-19 Transmission Dynamics in Taiwan and Risk at Different Exposure Periods Before and After Symptom Onset. *JAMA Internal Medicine* 2020.
82. Wang Y, Guo Q, Yan Z, et al. Factors Associated With Prolonged Viral Shedding in Patients With Avian Influenza A(H7N9) Virus Infection. *J Infect Dis* 2018; **217**(11): 1708-17.
83. Memish A. Viral shedding and antibody response in MERS. *Vox Sanguinis* 2016; **111 (Supplement 1)**: 48-9.
84. Wang W, Xu Y, Gao R, et al. Detection of SARS-CoV-2 in Different Types of Clinical Specimens. *JAMA* 2020; **323**(18): 1843-4.
85. Ip DKM, Lau LLH, Leung NHL, et al. Viral Shedding and Transmission Potential of Asymptomatic and Paucisymptomatic Influenza Virus Infections in the Community. *Clin Infect Dis* 2017; **64**(6): 736-42.
86. Walsh KA, Jordan K, Clyne B, et al. SARS-CoV-2 detection, viral load and infectivity over the course of an infection. *Journal of Infection*.
87. Kretzschmar ME, Rozhnova G, Bootsma MCJ, van Boven M, van de Wijgert JHHM, Bonten MJM. Impact of delays on effectiveness of contact tracing strategies for COVID-19: a modelling study. *The Lancet Public Health*.

88. Chang D, Mo G, Yuan X, et al. Time Kinetics of Viral Clearance and Resolution of Symptoms in Novel Coronavirus Infection. *Am J Respir Crit Care Med* 2020; **201**(9): 1150-2.
89. Chen X, Ling J, Mo P, et al. Restoration of leukomonocyte counts is associated with viral clearance in COVID-19 hospitalized patients. *medRxiv* 2020: 2020.03.03.20030437.
90. Corman VM, Rabenau HF, Adams O, et al. SARS-CoV-2 asymptomatic and symptomatic patients and risk for transfusion transmission. *Transfusion* 2020; **60**(6): 1119-22.
91. Fu S, Fu X, Song Y, et al. Virologic and clinical characteristics for prognosis of severe COVID-19: a retrospective observational study in Wuhan, China. 2020.
92. Huang L, Chen Z, Ni L, et al. Impact of Angiotensin-converting Enzyme Inhibitors and Angiotensin Receptor Blockers on Inflammatory Responses and Viral Clearance in COVID-19 Patients: A Multicenter Retrospective Cohort Study. *ResearchSquare* 2020.
93. Li N, Wang X, Lv T. Prolonged SARS-CoV-2 RNA shedding: Not a rare phenomenon. *Journal of Medical Virology*; **n/a**(n/a).
94. Liu L, Liu W, Zheng Y, et al. A preliminary study on serological assay for severe acute respiratory syndrome coronavirus 2 (SARS-CoV-2) in 238 admitted hospital patients. *Microbes and Infection* 2020; **22**(4): 206-11.
95. Lo IL, Lio CF, Cheong HH, et al. Evaluation of SARS-CoV-2 RNA shedding in clinical specimens and clinical characteristics of 10 patients with COVID-19 in Macau. *Int J Biol Sci* 2020; **16**(10): 1698-707.
96. Lou B, Li T, Zheng S, et al. Serology characteristics of SARS-CoV-2 infection since the exposure and post symptoms onset.
97. Pongpirul WA, Mott JA, Woodring JV, et al. Clinical Characteristics of Patients Hospitalized with Coronavirus Disease, Thailand - Volume 26, Number 7—July 2020 - Emerging Infectious Diseases journal - CDC.
98. Qian GQ, Chen XQ, Lv DF, et al. Duration of SARS-CoV-2 viral shedding during COVID-19 infection. *Infect Dis (Lond)* 2020: 1-2.
99. quan w, zheng q, tian j, et al. No SARS-CoV-2 in expressed prostatic secretion of patients with coronavirus disease 2019: a descriptive multicentre study in China.
100. Seah IYJ, Anderson DE, Kang AEZ, et al. Assessing Viral Shedding and Infectivity of Tears in Coronavirus Disease 2019 (COVID-19) Patients. *Ophthalmology* 2020; **24**: 24.
101. Song C, Wang Y, Li W, et al. Detection of 2019 novel coronavirus in semen and testicular biopsy specimen of COVID-19 patients.
102. Song R, Han B, Song M, et al. Clinical and epidemiological features of COVID-19 family clusters in Beijing, China. *Journal of Infection* 2020.
103. Tu Y-H, Wei Y-Y, Zhang D-W, Chen C-S, Hu X-W, Fei G. Analysis of factors affected the SARS-CoV-2 viral shedding time of COVID-19 patients in Anhui, China: a retrospective study. 2020.
104. Wang L, Gao Y-h, Lou L-L, Zhang G-J. The clinical dynamics of 18 cases of COVID-19 outside of Wuhan, China. *European Respiratory Journal* 2020.
105. Wang S, Tu J, Sheng Y. Clinical characteristics and fecal-oral transmission potential of patients with COVID-19. *medRxiv*.
106. Wu B, Lei Z-Y, Wu K-L, et al. Epidemiological and clinical features of imported and local patients with coronavirus disease 2019 (COVID-19) in Hainan, China. *ResearchSquare* 2020.
107. Xu l, Zhang X, Song W, et al. Conjunctival polymerase chain reaction-tests of 2019 novel coronavirus in patients in Shenyang,China.
108. Yang Y, Yang M, Shen C, et al. Evaluating the accuracy of different respiratory specimens in the laboratory diagnosis and monitoring the viral shedding of 2019-nCoV infections. 2020.
109. Xu D, Zhang Z, Jin L, et al. Persistent shedding of viable SARS-CoV in urine and stool of SARS patients during the convalescent phase. *Eur J Clin Microbiol Infect Dis* 2005; **24**(3): 165-71.
110. Al-Jasser FS, Nouh RM, Youssef RM. Epidemiology and predictors of survival of MERS-CoV infections in Riyadh region, 2014-2015. *J Infect Public Health* 2019; **12**(2): 171-7.

111. Alkendi F, Nair SC, Hashmey R. Descriptive Epidemiology, Clinical Characteristics and Outcomes for Middle East Respiratory Syndrome Coronavirus (MERS-CoV) Infected Patients in AlAin - Abu Dhabi Emirate. *J Infect Public Health* 2019; **12 (1)**: 137.

112. Park WB, Poon LLM, Choi SJ, et al. Replicative virus shedding in the respiratory tract of patients with Middle East respiratory syndrome coronavirus infection. *International Journal of Infectious Diseases* 2018; **72**: 8-10.

frontiers in Public Health

SYSTEMATIC REVIEW
published: 19 March 2021
doi: 10.3389/fpubh.2021.652842

Characteristics of Viral Shedding Time in SARS-CoV-2 Infections: A Systematic Review and Meta-Analysis

Danying Yan†, Xiaobao Zhang†, Can Chen, Daixi Jiang, Xiaoxiao Liu, Yuqing Zhou, Chenyang Huang, Yiyi Zhou, Zhou Guan, Cheng Ding, Lu Chen, Lei Lan, Xiaofang Fu, Jie Wu, Lanjuan Li* and Shigui Yang**

State Key Laboratory for Diagnosis and Treatment of Infectious Diseases, National Clinical Research Center for Infectious Diseases, Collaborative Innovation Center for Diagnosis and Treatment of Infectious Diseases, College of Medicine, The First Affiliated Hospital, Zhejiang University, Hangzhou, China

OPEN ACCESS

Edited by:
Walid Alali,
Kuwait University, Kuwait

Reviewed by:
Rami H. Al-Rifai,
United Arab Emirates University, United Arab Emirates
Abhilash Perisetti,
University of Arkansas for Medical Sciences, United States

***Correspondence:**
Shigui Yang
yangshigui@zju.edu.cn
Lanjuan Li
ljli@zju.edu.cn
Jie Wu
15955118479@163.com

†These authors have contributed equally to this work and share first authorship

Specialty section:
This article was submitted to Infectious Diseases - Surveillance, Prevention and Treatment, a section of the journal Frontiers in Public Health

Received: *13 January 2021*
Accepted: *22 February 2021*
Published: *19 March 2021*

Citation:
Yan D, Zhang X, Chen C, Jiang D, Liu X, Zhou Y, Huang C, Zhou Y, Guan Z, Ding C, Chen L, Lan L, Fu X, Wu J, Li L and Yang S (2021) Characteristics of Viral Shedding Time in SARS-CoV-2 Infections: A Systematic Review and Meta-Analysis. Front. Public Health 9:652842. doi: 10.3389/fpubh.2021.652842

Background: The viral shedding time (VST) of SARS-CoV-2 mainly determines its transmission and duration of infectiousness. However, it was heterogeneous in the existing studies. Here, we performed a meta-analysis to comprehensively summarize the VST of SARS-CoV-2.

Methods: We searched PubMed, Web of Science, MedRxiv, BioRxiv, CNKI, CSTJ, and Wanfang up to October 25, 2020, for studies that reported VSTs of SARS-CoV-2. Pooled estimates and 95% CIs for the VSTs were calculated using log-transformed data. The VSTs in SARS-CoV-2 infections based on different demographic and clinical characteristics, treatments and specimens were stratified by subgroup analysis.

Results: A total of 35 studies involving 3,385 participants met the inclusion criteria. The pooled mean VST was 16.8 days (95% CI: 14.8–19.4, $I^2 = 99.56\%$) in SARS-CoV-2 infections. The VST was significantly longer in symptomatic infections (19.7 days, 95% CI: 17.2–22.7, $I^2 = 99.34\%$) than in asymptomatic infections (10.9 days, 95% CI: 8.3–14.3, $I^2 = 98.89\%$) ($P < 0.05$). The VST was 23.2 days (95% CI: 19.0–28.4, $I^2 = 99.24\%$) in adults, which was significantly longer than that in children (9.9 days, 95% CI: 8.1–12.2, $I^2 = 85.74\%$) ($P < 0.05$). The VST was significantly longer in persons with chronic diseases (24.2 days, 95% CI: 19.2–30.2, $I^2 = 84.07\%$) than in those without chronic diseases (11.5 days, 95% CI: 5.3–25.0, $I^2 = 82.11\%$) ($P < 0.05$). Persons receiving corticosteroid treatment (28.3 days, 95% CI: 25.6–31.2, $I^2 = 0.00\%$) had a longer VST than those without corticosteroid treatment (16.2 days, 95% CI: 11.5–22.5, $I^2 = 92.27\%$) ($P = 0.06$). The VST was significantly longer in stool specimens (30.3 days, 95% CI: 23.1–39.2, $I^2 = 92.09\%$) than in respiratory tract specimens (17.5 days, 95% CI: 14.9–20.6, $I^2 = 99.67\%$) ($P < 0.05$).

Conclusions: A longer VST was found in symptomatic infections, infected adults, persons with chronic diseases, and stool specimens.

Keywords: viral shedding time, SARS- CoV-2, COVID-19, systematic review, meta-analysis

INTRODUCTION

Coronaviruses (CoVs), belonging to Nidovirales order, have caused three global outbreaks in the past 20 years. The first epidemic was Severe Acute Respiratory Syndrome (SARS) caused by SARS-CoV-1 in 2003, the second outbreak was Middle East Respiratory Syndrome (MERS) caused by MERS-CoV in 2012, and the third and most recent pandemic was Coronavirus Disease 2019 (COVID-19) caused by SARS-CoV-2 (1, 2). As of February 4, 2021, more than 104 million cases of COVID-19 have been reported with over 2.2 million deaths globally (3). Pulmonary clinical manifestations are the most common clinical presentations of COVID-19, such as fever, cough, shortness of breath, sputum production, respiratory failure and even acute respiratory distress syndrome (ARDS). Diarrhea, loss of smell or taste, and other extra-pulmonary clinical manifestations can also be found in some patients (4–7).

Persons infected with SARS-CoV-2 with long viral shedding times (VSTs) have drawn considerable concern, which put greater challenges and difficulties on epidemic prevention and control (8–11). The VST is an important parameter for judging hospital discharge, discontinuation of quarantine and the effect of antiviral treatment for infectious diseases, which mainly determines disease transmission and the duration of infectiousness (12). However, the characteristics of the VST in SARS-CoV-2 infections have not been well-clarified. Although there have been many studies on the VSTs of SARS-CoV-2, the results across studies so far have been heterogeneous (13, 14). A meta-analysis performed by Muge Cevik found that the mean VST of SARS-CoV-2 in the upper respiratory tract, lower respiratory tract, stool and serum was 17.0, 14.6, 17.2, and 16.6 days, respectively (15). However, a comprehensive summary of VSTs in SARS-CoV-2 infections with different demographic and clinical features is still lacking. Therefore, we performed a meta-analysis to estimate the mean VST in SARS-CoV-2 infections and explore the characteristics of VSTs in SARS-CoV-2 infections based on different demographic features, clinical characteristics, treatments and specimens.

MATERIALS AND METHODS

Our meta-analysis was strictly conducted in accordance with the Preferred Reporting Items for Systematic Reviews and Meta-Analyses Protocols (PRISMA-P) guidelines (16).

The Definition of the VST

The definition of the VST varied among the studies, so a unified definition was made. We defined the VST as the time from illness onset to viral shedding cessation. Illness onset was defined as the first appearance of the symptoms for symptomatic infections and the first positive RT-PCR results for asymptomatic infections. Viral shedding cessation referred to the occurrence of the last positive RT-PCR results or negative RT-PCR results.

Search Strategy and Selection Criteria

We searched PubMed, Web of Science, MedRxiv, BioRxiv, the China National Knowledge Infrastructure Database (CNKI), the China Science and Technology Journal Database (CSTJ), and the Wanfang Database up to October 25, 2020, for studies that reported VSTs of SARS-CoV-2. The details of the search strategy are shown in **Supplementary Table 1**.

In this systematic review with no study design limit, studies meeting the following inclusion criteria were eligible: (i) SARS-CoV-2 infections were based on positive RT-PCR results; (ii) the VSTs of SARS-CoV-2 infections including sample size, mean and standard deviation (SD) could be obtained directly from the original studies or by calculation; and (iii) the definition of the VST in the original studies was consistent with our definition.

We excluded (i) duplicated data; (ii) case reports and case series with <5 participants due to reporting bias; and (iii) studies without original data (e.g., modeling studies and reviews). Studies presenting VSTs with medians and interquartile ranges (IQRs) or ranges were excluded to reduce the errors caused by data conversion.

Screening, Data Extraction, and Quality Assessment

After removing duplicates, two reviewers (DY and XZ) independently performed the initial screening of titles and abstracts to exclude studies that clearly contained no data for VST of SARS-CoV-2. All retained full-text articles were scrutinized against the eligibility criteria by two independent reviewers (DY and XZ). Nine investigators (DY, XZ, CC, DJ, XL, YZ, CH, YZ, and ZG) participated in the data extraction. And data extraction from each study was performed by three independent investigators. Disagreements and uncertainties were consulted by SY to reach a consensus. The following data were extracted: basic information of the studies (first author, publication time, journal name, sample size), VSTs in SARS-CoV-2 infections based on sex, age (adult and child), infection status (symptomatic infection and asymptomatic infection), disease severity (severe infection and non-severe infection), treatments (corticosteroid treatment and antiviral therapy) and specimens (respiratory tract specimens (RTS), upper respiratory tract specimens (URTS), lower respiratory tract specimens (LRTS), stool and serum). The cutoff point for classifying adults and children was 18 years old. Asymptomatic infections referred to the absence of any clinical symptoms throughout the disease course. Non-severe infections included mild and moderate infections, and severe infections included severe and critical infections. Antiviral drugs included interferon, lopinavir/ritonavir, abidor, ribavirin, chloroquine and hydroxychloroquine. URTS included nasopharyngeal, oropharyngeal and oronasopharyngeal swabs, and LRTS included sputum and bronchoalveolar lavage fluid.

The overall VST of the total participants was extracted to estimate the overall pooled VST. If studies did not report the overall VST of the total participants, the stratified VSTs were extracted to estimate the overall pooled VST. If a study included more than one independent study population, each population was extracted as a separate dataset in the meta-analysis. When the same study reported the VSTs of multiple specimens, the VSTs of the URTS were extracted to estimate the overall pooled VST, and the VSTs of other specimens were

displayed in the subgroup analysis. In subgroup analysis, only studies having clear population characteristics were included in the corresponding subgroup, and studies having no clear information or mixed population group were included in the unclassified group.

The scale recommended by the Agency for Healthcare Research and Quality was used to assess the quality of the included studies (17). The scale consists of 11 items, and 1 point is given to each item when the conditions are met. It mainly focuses on information source, inclusion and exclusion criteria, study period, selection of participants, evaluation of subjective outcomes/components, quality assurance, possible confounding variables, handling of missing data, participants' response rates and completeness of data collection. According to the total score, the studies were divided into low-(0–3), medium-(4–7) and high-quality (8–11) groups. EndNote (version X9) was used to manage the articles and citations.

Statistical Analysis

We first extracted the individual VSTs from the published articles and found that the distribution type of the VST was approximately in accordance with the log-normal distribution by using P-P plots (**Supplementary Figure 1**). Then, we used the method developed by McAloon C (18) to transform the original VST data to make the data obey a normal distribution. We used random-effects model to perform the meta-analysis due to the high heterogeneity. Finally, we used the method developed by McAloon C (18) to back-transform the point estimates and their 95% confidence intervals (CIs). The *I*-squared (I^2) statistic was used to evaluate the heterogeneity among the studies. Meta-regression was used to quantify the sources of heterogeneity and to explore the level of significance between subgroup comparisons. We did not assess publication bias because usual appraisal methods are uninformative when studies in the meta-analysis do not include a test of significance. The data cleaning and analysis were performed using the Microsoft Excel 2016 and R version 3.2.3.

RESULTS

A total of 17,284 records were retrieved through a database search. The titles and abstracts of 11,911 records were screened after deleting duplicates, and then 526 records were selected for full-text review. Finally, 35 full texts met the inclusion criteria (**Figure 1**). This study included 35 observational studies and involved 3,385 individuals infected with SARS-CoV-2, of which 2,955 were symptomatic infections and 338 were asymptomatic infections (**Table 1**). According to the scale, 32 studies were of high quality, 3 studies were of medium quality and none were of low quality (**Table 1** and **Supplementary Table 2**).

VSTs in SARS-CoV-2 Infections and Subgroup Results Based on Clinical Characteristics

The initial pooled estimate of the log-transformed VST in SARS-CoV-2 infections was 2.82 (95% CI: 2.69–2.96) (**Figure 2**). The pooled mean VST was 16.8 days (95% CI: 14.8–19.4) in SARS-CoV-2 infections. The mean VST of symptomatic infections was 19.7 days (95% CI: 17.2–22.7), which was significantly longer than that of asymptomatic infections (10.9 days, 95% CI: 8.3–14.3) ($P < 0.05$). The mean VST was 24.3 days (95% CI: 18.9–31.1) in severe patients and 22.8 days (95% CI: 16.4–32.0) in non-severe patients (**Figure 3**).

VSTs in SARS-CoV-2 Infections Subgrouped by Demographic Features

The mean VST was 19.4 days (95% CI: 9.5–39.4) in females and 11.9 days (95% CI: 8.4–16.9) in males. The VST was significantly shorter in the infected children (9.9 days, 95% CI: 8.1–12.2) than in the infected adults (23.2 days, 95% CI: 19.0–28.4) ($P < 0.05$). The VST of persons with chronic diseases was 24.2 days (95% CI: 19.2–30.2), which was significantly longer than that of persons without chronic diseases (11.5 days, 95% CI: 5.3–25.0) ($P < 0.05$) (**Figure 3**).

VSTs in SARS-CoV-2 Infections Subgrouped by Treatments

In persons receiving corticosteroid treatment, the VST was 28.3 days (95% CI: 25.6–31.2), which was longer than that in those without corticosteroid treatment (16.2 days, 95% CI: 11.5–22.5). However, there was no statistically significant difference between them ($P = 0.06$). The VST was 17.6 days (95% CI: 13.4–22.2) in persons receiving antiviral therapy, 21.2 days (95% CI: 15.3–29.2) in persons receiving mono-antiviral therapy and 20.3 days (95% CI: 13.7–30.3) in persons receiving multi-antiviral therapy (**Figure 3**). Only one study reported the VSTs of 5 patients without antiviral therapy, and the result was 11.2 ± 5.2 days (33).

VSTs in SARS-CoV-2 Infections Subgrouped by Different Specimens

Most studies (63%) reported the VSTs in the URTS. Among the different specimens, the mean VST was 17.5 days (95% CI: 14.9–20.6) in the RTS and 17.5 days (95% CI: 14.6–21.0) in the URTS. Compared with the RTS, a longer VST was found in the stool specimens (30.3 days, 95% CI: 23.1–39.2) ($P < 0.05$) (**Figure 4**). No included study reported VSTs in LRTS or serum specimens.

Meta-Regression for Heterogeneity

The univariate meta-regression model indicated that the mean age ($R^2 = 35.28\%$, $P < 0.05$) and the proportion of the asymptomatic cases ($R^2 = 22.64\%$, $P < 0.05$) could partly explain the overall heterogeneity. By introducing these two variables into the multivariate meta-regression model, nearly half of

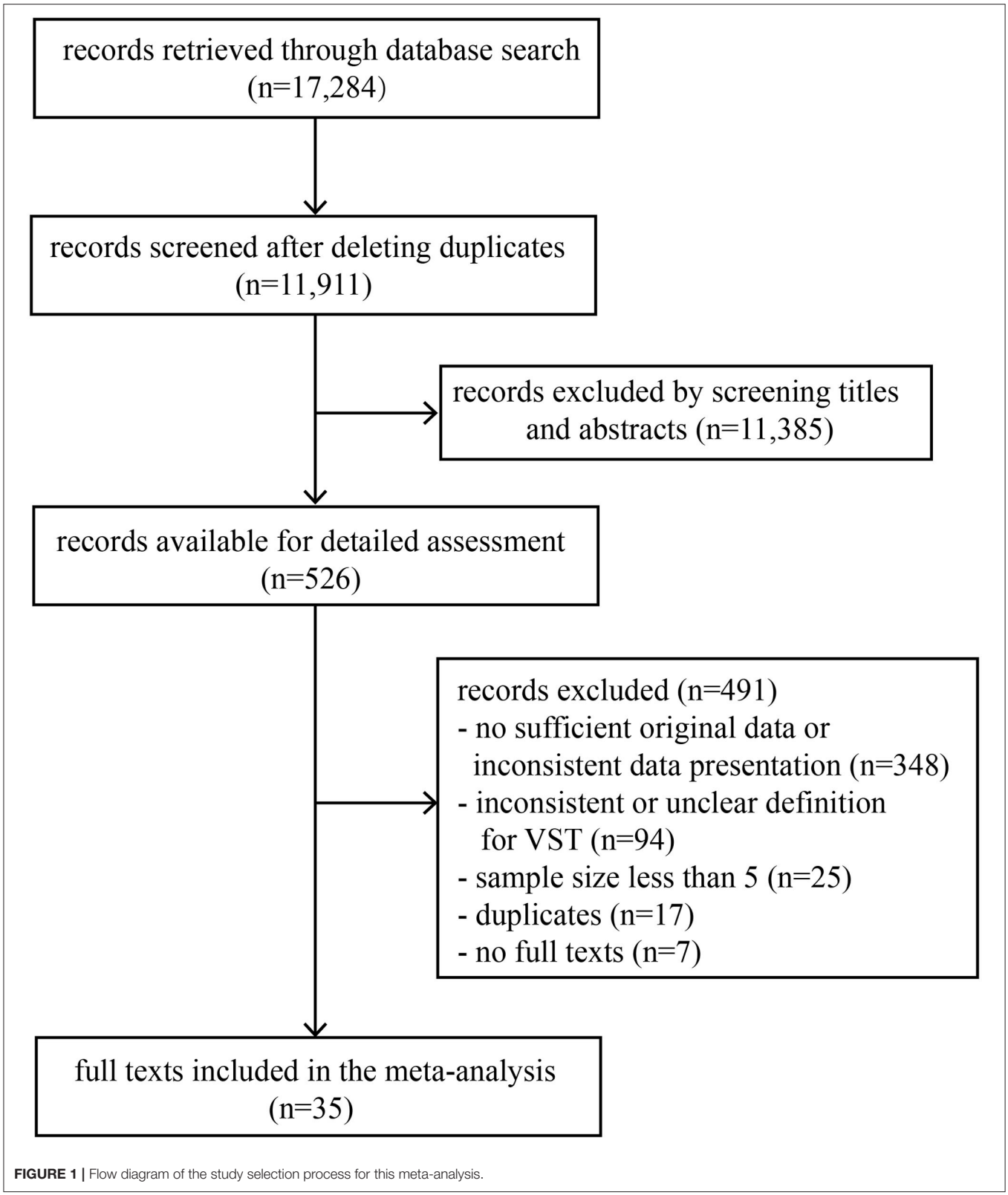

FIGURE 1 | Flow diagram of the study selection process for this meta-analysis.

TABLE 1 | Characteristics of included studies.

References	Country	Study design	Sample size, n	Age, years*	Female, n (%)	Infection status	Asymptomatic case#, n (%)	Specimen types	Study quality
Jiehao et al. (19)	China	Case series	10	6.5	6 (60)	sym	0 (0)	URTS	8 (High)
Xiong et al. (20)	China	Cohort study	51	/	21 (41)	asym	51 (100)	URTS	8 (High)
Yang et al. (21)	China	Case series	5	49	2 (40)	sym, asym	2 (40)	URTS	8 (High)
Noh et al. (22)	Korea	Cohort study	53	/	/	asym	53 (100)	/	8 (High)
Zheng et al. (23)	China	Cohort study	1,320	50	741 (56)	sym	0 (0)	URTS	8 (High)
Lee et al. (24)	Korea	Cohort study	89	22	55 (62)	asym	89 (100)	RTS	8 (High)
Song et al. (25)	China	Case series	16	8.5	6 (38)	sym, asym	8 (50)	URTS	8 (High)
Jun et al. (26)	China	Cross-sectional study	242	/	/	sym	0 (0)	URTS	8 (High)
Zhu et al. (27)	China	Case series	20	/	/	sym	0 (0)	URTS	8 (High)
Han et al. (28)	China	Cohort study	206	62.5	115 (56)	sym	0 (0)	URTS	8 (High)
Yan et al. (29)	China	Cross-sectional study	24	/	/	asym	24 (100)	RTS	8 (High)
Gong et al. (30)	China	Cohort study	34	/	12 (35)	sym	0 (0)	URTS	8 (High)
Warabi et al. (31)	Japan	Cross-sectional study	8	14	6 (75)	sym	0 (0)	URTS	8 (High)
Pan et al. (32)	China	Cross-sectional study	26	29.5	10 (38)	asym	26 (100)	RTS	7 (Medium)
Hua et al. (33)	China	Cross-sectional study	43	/	/	/	/	URTS	8 (High)
Cano et al. (34)	Switzerland	Cohort study	251	53	103 (41)	sym	0 (0)	URTS	7 (Medium)
Wu et al. (35)	China	Cross-sectional study	74	/	/	sym	0 (0)	URTS, stool	8 (High)
Otsubo et al. (36)	/	Case series	5	74	2 (40)	sym	0 (0)	URTS	7 (Medium)
Tan et al. (37)	China	Case series	12	34.5	3 (25)	asym	12 (100)	URTS	8 (High)
Xiao et al. (38)	China	Cohort study	63	/	/	sym, asym	19 (30)	/	8 (High)
Yao et al. (39)	China	Case series	5	47	3 (60)	sym, asym	1 (20)	URTS	8 (High)
Liu et al. (40)	China	Cohort study	53	8	19 (36)	asym	53 (100)	URTS	8 (High)
Shi et al. (41)	China	Cross-sectional study	33	41	14 (42)	sym	0 (0)	URTS	8 (High)
Li et al. (42)	China	Cohort study	46	45.6	25 (54)	sym	0 (0)	/	8 (High)
Jiang et al. (43)	China	Cross-sectional study	24	37	10 (42)	sym	0 (0)	/	8 (High)
Gong et al. (44)	China	Cross-sectional study	179	57.4	90 (50)	sym	0 (0)	URTS	8 (High)
Zhao et al. (45)	China	Cohort study	63	/	32 (51)	sym	0 (0)	/	8 (High)
Zhang et al. (46)	China	Cross-sectional study	30	/	/	sym	0 (0)	RTS, stool	8 (High)
Xu et al. (47)	China	Cohort study	59	49.3	31 (53)	sym	0 (0)	URTS	8 (High)
Xie et al. (48)	China	Cross-sectional study	49	49.4	24 (49)	/	/	/	8 (High)
Sun et al. (49)	China	Cross-sectional study	46	/	/	sym	0 (0)	RTS	8 (High)
Ren et al. (50)	China	Cross-sectional study	89	/	/	sym	0 (0)	RTS	8 (High)
Ran et al. (51)	China	Cross-sectional study	28	59.4	9 (32)	sym	0 (0)	RTS	8 (High)
Liu et al. (53)	China	Cross-sectional study	41	68	21 (51)	sym	0 (0)	URTS	8 (High)
Li et al. (54)	China	Cohort study	88	46	34 (39)	sym	0 (0)	URTS	8 (High)

sym, symptomatic infection; asym, asymptomatic infection; RTS, respiratory tract specimen; URTS, upper respiratory tract specimen.
**: Median or mean; #: Asymptomatic cases with VST of SARS-CoV-2; /: Unreported or unclassified or incalculable.*

the heterogeneity could be explained (R^2= 44.18%, $P < 0.05$) (**Supplementary Table 3**).

DISCUSSION

We performed a meta-analysis to clarify the characteristics of VSTs in SARS-CoV-2 infections, which was important for determining hospital discharge, discontinuation of quarantine and the effect of antiviral treatment for COVID-19. Compared with the meta-analysis conducted by Muge Cevik (15), our study not only estimated the VSTs in different specimens but also summarized the VSTs in SARS-CoV-2 infections based on different demographic features, clinical characteristics and treatments.

Previous studies have shown that the basic reproduction number (R0) of SARS-CoV-2 is between 2 and 6.7, which indicates that SARS-CoV-2 is more infectious than SARS-CoV-1 and MERS-CoV (55–57). In our study, we found that the mean VST of SARS-CoV-2 was 16.8 days (95% CI: 14.8–19.4), which was between that of SARS-CoV-1 (21.0 days) and MERS-CoV (13.2 days) (58, 59). In addition to the VST, the viral load released is also important to evaluate the transmissibility. Some studies

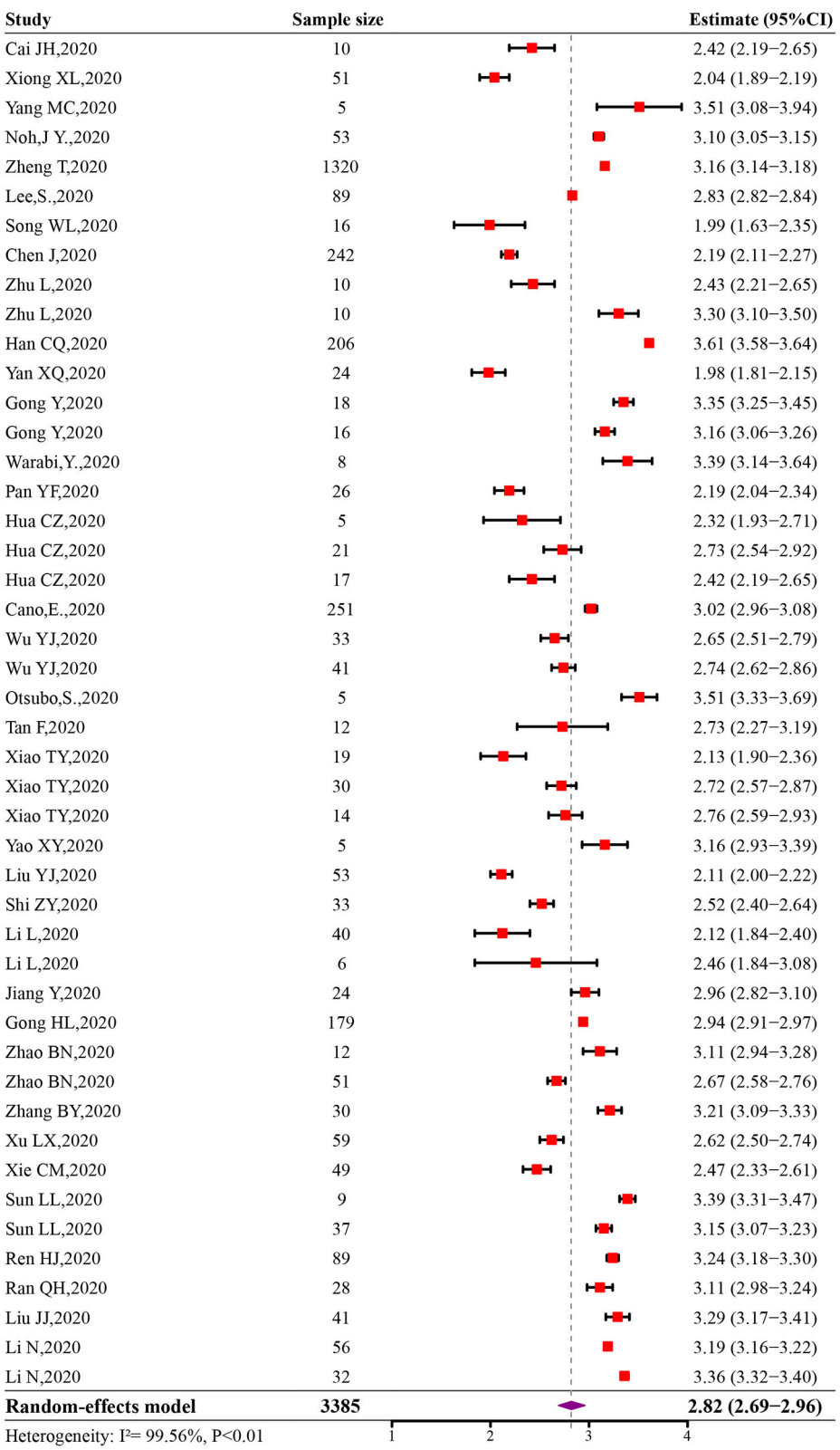

FIGURE 2 | Forest plot of meta-analysis of log-transformed VST in SARS-CoV-2 infections.

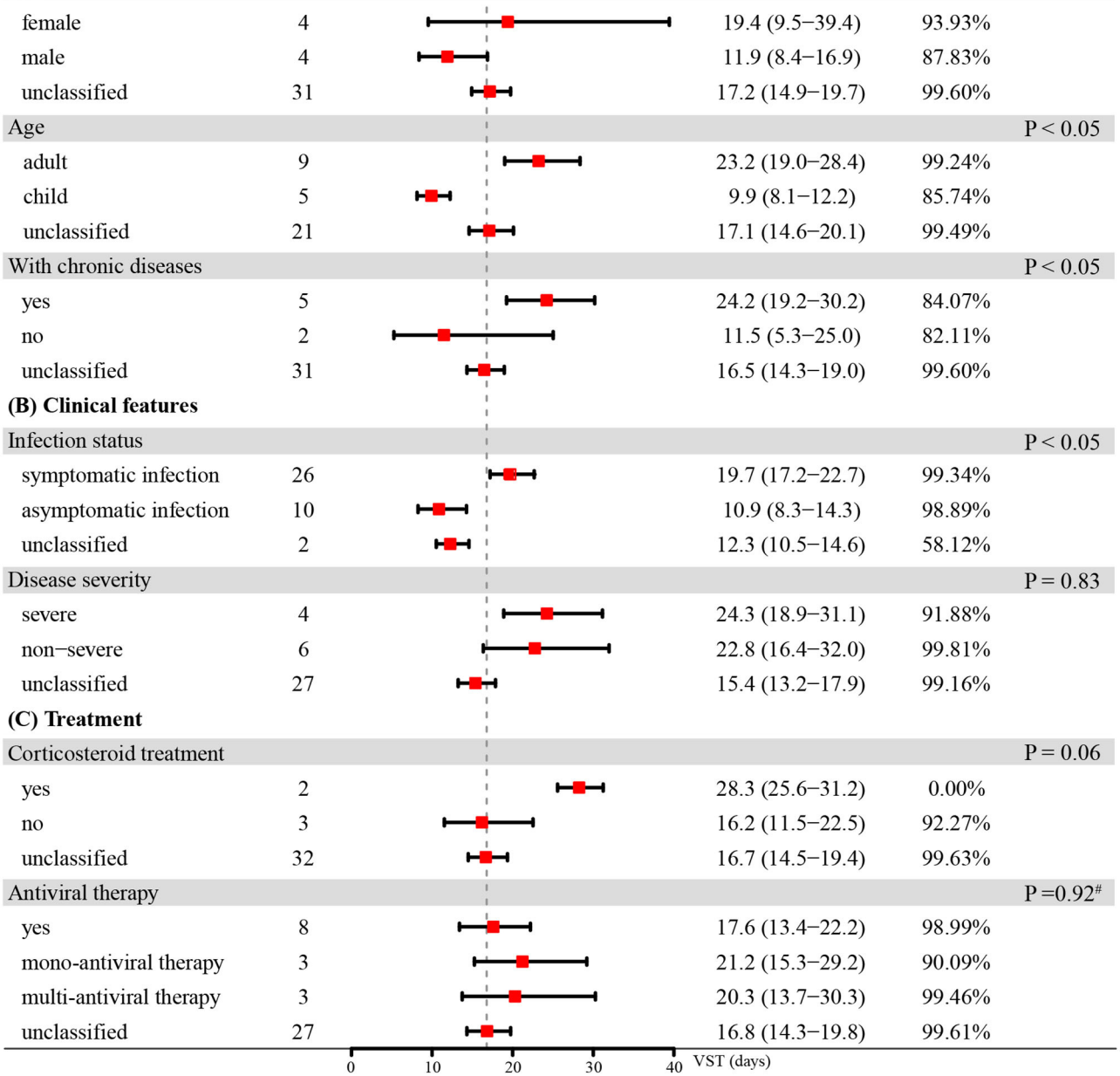

FIGURE 3 | The VST in SARS-CoV-2 infections based on different demographic features, clinical features and treatments. * Unclassified groups were not included in the *P*-values calculation for the subgroup comparisons. #*P*-value for comparison between group with antiviral mono-therapy and group with antiviral muti-therapy.

have found that the viral load of SARS-CoV-2 is highest during the 1st week after symptom onset and subsequently declines with time (60–62). Based on the above analysis, from the perspective of epidemic prevention and control, strict precautions should be taken throughout the disease course, especially within 1 week after the onset of the disease.

The duration of viral shedding is mainly related to the host immune status (63). Persons with chronic diseases always have relatively low immunity, which might lead to longer viral shedding. In our study, we found that the VST of symptomatic infections was longer than that of asymptomatic infections. One reason is that virus clearance in asymptomatic individuals is

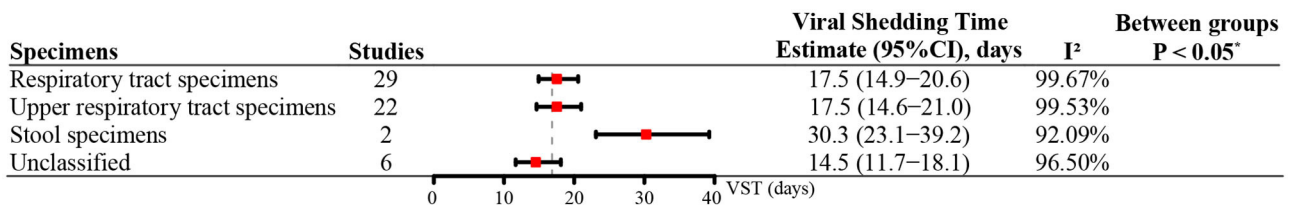

FIGURE 4 | The VST in SARS-CoV-2 infections based on different specimens. **P*-value for comparison between respiratory tract specimens and stool specimens.

indeed faster than that in symptomatic cases (38, 52). Another reason was that the VST for asymptomatic infections was calculated from the first positive PCR results and depended mainly on close contact tracking investigations. These individuals might have begun viral shedding before the first positive PCR results, and were ignored due to the absence of clinical features. A higher proportion of asymptomatic infections and milder clinical symptoms were found in infected children compared with infected adults (64, 65), which might explain the shorter VST of children.

The VST is an important parameter for evaluating the effect of antiviral treatment for infectious diseases. Until now, there have been no specific antiviral drugs for COVID-19, and inhibiting the cytokine storm has been an important treatment for patients with severe COVID-19. Corticosteroids are used because of their rapid, powerful anti-inflammatory effects. In our study, we found that the patients who received corticosteroid treatment had longer VSTs, although no statistically significant difference was found. This phenomenon was also found in severe SARS and MERS, where high-dose corticosteroids could cause prolonged viral clearance, secondary infection and long-term complications (66). Although corticosteroids can inhibit lung inflammation and alleviate possible immune-mediated pulmonary damage, it can also inhibit the systemic immune response dominated by T cell response, resulting in the delayed virus clearance (67). This finding alerted us that high-dose corticosteroids might prolong VSTs in SARS-CoV-2 infections and that appropriate doses of corticosteroids should be used after weighing the advantages and disadvantages according to the patients' condition.

The VST is also an important parameter for determining hospital discharge and discontinuation of quarantine. Two consecutive negative PCR results of RTS are one of the current criteria for hospital discharge or discontinuation of quarantine in China (68). The overexpression of ACE-2 in the gastrointestinal (GI) epithelial cells suggested the replication and shedding of SARS-CoV-2 in GI tract (69). Similar to SARS-CoV-1 (59), the VST of SARS-CoV-2 in stool specimens was longer than that in RTS. One study suggested that the VST in stool specimens could be prolonged by 5 weeks after SARS-CoV-2 had turned negative in RTS (35). Given that, the negative PCR results in RTS might not guarantee that patients no longer shed virus. Recently, several incidents of cold chain food polluted by SARS-CoV-2 have caused widespread concern by indicating that the virus could indeed infect individuals by polluting the environment. Considering the potential risk of oral-fecal transmission (70) and the long VST in stool specimens, more comprehensive protective measures should be taken for high-risk groups of oral-fecal transmission, such as GI endoscopy staff (2, 71), and stool or anal swabs collection and testing staff.

Our results might provide scientific support for the formulation of antiviral treatment and criteria for hospital discharge and discontinuation of quarantine for COVID-19, and help identify which patients need more attention and more effective preventive measures. Based on the mean VST of SARS-CoV-2 infections, hospitals could estimate the number of individuals with COVID-19 who can be admitted in a period of time, and reasonably allocate medical resources, such as the number of beds and medical staff.

This study has several limitations. The mean age, disease severity, treatment regimens, underlying diseases and infection status of individuals infected with SARS-CoV-2 varied in the included studies, which might cause high statistical heterogeneity. In the multivariate meta-regression model, nearly half of the heterogeneity could be explained by mean age and the proportion of the asymptomatic cases ($R^2 = 44.18\%$, $P < 0.05$). In some subgroup analyses, the number of included studies was small and most were case series with limited sample sizes, which might make the effect size of some outcomes insufficient. For example, the pooled mean VST in the stool specimens was based on estimates obtained in only two studies. More studies on the VST of SARS-CoV-2 are needed to provide further evidence. It would be better to incorporate as many studies as possible to obtain sufficient subgroup data and to ensure the homogeneity of the studies. Furthermore, the day of symptom onset for symptomatic infections depended on subjective memories and the day of the first positive RT-PCR results for asymptomatic infections relied mainly on close contact tracking investigations. If the individuals' recall was incorrect or close contact tracking investigations were not timely, these would cause the obtained VSTs to deviate from the real values.

CONCLUSIONS

This study provided a comprehensive overview of VSTs in SARS-CoV-2 infections, which was important for determining hospital discharge, discontinuation of quarantine and the effect of antiviral treatment for COVID-19. The pooled mean VST was 16.8 days (95% CI: 14.8–19.4) in SARS-CoV-2 infections. Due to the high infectivity of SARS-CoV-2, strict precautions should be taken to reduce the risk of disease transmission,

especially for adults, persons with chronic diseases, symptomatic infections and persons with positive RT-PCR results in stool specimens, in whom longer VSTs were found. Given that high-dose corticosteroids could alleviate possible immune-mediated pulmonary damage but might prolong VSTs in SARS-CoV-2 infections, corticosteroids should be used with caution after analyzing the risk of prolonged VST with reducing the disease severity.

DATA AVAILABILITY STATEMENT

The original contributions presented in the study are included in the article/**Supplementary Material**, further inquiries can be directed to the corresponding author/s.

AUTHOR CONTRIBUTIONS

SY, LJL, and JW designed the study and revised the manuscript. DY and XZ independently performed the literature identification and uncertainties were consulted by SY to reach a consensus. DY, XZ, CC, DJ, XL, YZ, CH, YZ, and ZG extracted data. CD, LC, LL, and XF rechecked the data. DY carried out the data analysis. DY and XZ interpreted data and wrote the manuscript. All authors have read and approved the final version of the manuscript for submission.

FUNDING

This study was supported by grants from the National Natural Science Foundation of China (Grant Nos: 81672005, U1611264, and 81001271), the Mega-Project of National Science and Technology for the 12th and 13th Five-Year Plan of China (Grant Nos: 2018ZX10715-014-002 and 2014ZX10004008).

SUPPLEMENTARY MATERIAL

The Supplementary Material for this article can be found online at: https://www.frontiersin.org/articles/10.3389/fpubh.2021.652842/full#supplementary-material

REFERENCES

1. Mann R, Perisetti A, Gajendran M, Gandhi Z, Umapathy C, Goyal H. Clinical characteristics, diagnosis, and treatment of major coronavirus outbreaks. *Front Med.* (2020) 7:766. doi: 10.3389/fmed.2020.581521
2. Perisetti A, Gajendran M, Boregowda U, Bansal P, Goyal H. COVID-19 and gastrointestinal endoscopies: current insights and emergent strategies. *Dig Endosc.* (2020) 32:715–22. doi: 10.1111/den.13693
3. World Coronavirus Death. *Coronavirus Death Toll and Trends –Worldometer*. (2020). Available online at: https://www.worldometers.info/coronavirus (accessed February 4, 2021).
4. Perisetti A, Gajendran M, Mann R, Elhanafi S, Goyal H. COVID-19 extrapulmonary illness - special gastrointestinal and hepatic considerations. *Dis Mon.* (2020) 66:101064. doi: 10.1016/j.disamonth.2020.101064
5. Johnson KD, Harris C, Cain JK, Hummer C, Goyal H, Perisetti A. Pulmonary and extra-pulmonary clinical manifestations of COVID-19. *Front Med.* (2020) 7:526. doi: 10.3389/fmed.2020.00526
6. Aziz M, Goyal H, Haghbin H, Lee-Smith WM, Gajendran M, Perisetti A. The association of "loss of smell" to COVID-19: a systematic review and meta-analysis. *Am J Med Sci.* (2020) 361:216–25. doi: 10.1016/j.amjms.2020.09.017
7. Goyal H, Sachdeva S, Perisetti A, Mann R, Inamdar S, Tharian B. Hyperlipasemia and potential pancreatic injury patterns in COVID-19: a marker of severity or innocent bystander? *Gastroenterology.* (2020) 160:946–8.e2. doi: 10.1053/j.gastro.2020.10.037
8. Tan L, Kang X, Zhang B, Zheng S, Liu B, Yu T, et al. A special case of COVID-19 with long duration of viral shedding for 49 days. *medRxiv.* (2020). doi: 10.1101/2020.03.22.20040071
9. Yang JR, Deng DT, Wu N, Yang B, Li HJ, Pan XB. Persistent viral RNA positivity during the recovery period of a patient with SARS-CoV-2 infection. *J Med Virol.* (2020) 92:1681–3. doi: 10.1002/jmv.25940
10. Li Q, Zheng XS, Shen XR, Si HR, Wang X, Wang Q, et al. Prolonged shedding of severe acute respiratory syndrome coronavirus 2 in patients with COVID-19. *Emerg Microbes Infect.* (2020) 9:2571–7. doi: 10.1080/22221751.2020.1852058
11. Xing YH, Ni W, Wu Q, Li WJ, Li GJ, Wang WD, et al. Prolonged viral shedding in feces of pediatric patients with coronavirus disease 2019. *J Microbiol Immunol Infect.* (2020) 53:473–80. doi: 10.1016/j.jmii.2020.03.021
12. de Sousa R, Reusken C, Koopmans M. MERS coronavirus: data gaps for laboratory preparedness. *J Clin Virol.* (2014) 59:4–11. doi: 10.1016/j.jcv.2013.10.030
13. Shi D, Wu W, Wang Q, Xu K, Xie J, Wu J, et al. Clinical characteristics and factors associated with long-term viral excretion in patients with severe acute respiratory syndrome coronavirus 2 infection: a single-center 28-day study. *J Infect Dis.* (2020) 222:910–8. doi: 10.1093/infdis/jiaa388
14. Shen Y, Zheng F, Sun D, Ling Y, Chen J, Li F, et al. Epidemiology and clinical course of COVID-19 in Shanghai, China. *Emerg Microbes Infect.* (2020) 9:1537–45. doi: 10.1080/22221751.2020.1787103
15. Cevik M, Tate M, Lloyd O, Maraolo AE, Schafers J, Ho A. SARS-CoV-2, SARS-CoV, and MERS-CoV viral load dynamics, duration of viral shedding, and infectiousness: a systematic review and meta-analysis. *Lancet Microbe.* (2020) 2:e13–22. doi: 10.1016/S2666-5247(20)30172-5
16. Hutton B, Salanti G, Caldwell DM, Chaimani A, Schmid CH, Cameron C, et al. The PRISMA extension statement for reporting of systematic reviews incorporating network meta-analyses of health care interventions: checklist and explanations. *Ann Intern Med.* (2015) 162:777–84. doi: 10.7326/m14-2385
17. Meyers D. Introduction from the agency for healthcare research and quality. *J Am Board Fam Med.* (2012) 25(Suppl 1): S1. doi: 10.3122/jabfm.2012.02.120023
18. McAloon C, Collins Á, Hunt K, Barber A, Byrne AW, Butler F, et al. Incubation period of COVID-19: a rapid systematic review and meta-analysis of observational research. *BMJ Open.* (2020) 10:e039652. doi: 10.1136/bmjopen-2020-039652
19. Jiehao C, Jin X, Daojiong L, Zhi Y, Lei X, Zhenghai Q, et al. A case series of children with 2019 novel coronavirus infection: clinical and epidemiological features. *Clin infect Dis.* (2020) 71:1547–51. doi: 10.1093/cid/ciaa198
20. Xiong X, Chua GT, Chi S, Kwan MYW, Sang Wong WH, Zhou A, et al. A comparison between Chinese children infected with coronavirus disease-2019 and with severe acute respiratory syndrome 2003. *J Pediatr.* (2020) 224:30–6. doi: 10.1016/j.jpeds.2020.06.041
21. Yang MC, Hung PP, Wu YK, Peng MY, Chao YC, Su WL. A three-generation family cluster with COVID-19 infection: should quarantine be prolonged? *Public Health.* (2020) 185:31–3. doi: 10.1016/j.puhe.2020.05.043
22. Noh JY, Yoon JG, Seong H, Choi WS, Sohn JW, Cheong HJ, et al. Asymptomatic infection and atypical manifestations of COVID-19: Comparison of viral shedding duration. *J Infect.* (2020) 81:816–46. doi: 10.1016/j.jinf.2020.05.035
23. Zheng T, Yang C, Wang H-Y, Chen X, Yu L, Wu Z-L, et al. Clinical characteristics and outcomes of COVID-19 patients with gastrointestinal symptoms admitted to Jianghan Fangcang Shelter Hospital in Wuhan, China. *J Med Virol.* (2020) 92:2735–41. doi: 10.1002/jmv.26146

24. Lee S, Kim T, Lee E, Lee C, Kim H, Rhee H, et al. Clinical course and molecular viral shedding among asymptomatic and symptomatic patients with SARS-CoV-2 infection in a community treatment center in the Republic of Korea. *JAMA Inter Med.* (2020) 180:1–6. doi: 10.1001/jamainternmed.2020.3862
25. Song W, Li J, Zou N, Guan W, Pan J, Xu W. Clinical features of pediatric patients with coronavirus disease (COVID-19). *J Clin Virol.* (2020) 127:104377. doi: 10.1016/j.jcv.2020.104377
26. Jun C, Tangkai Q, Li L, Yun L, Zhiping Q, Tao L, et al. Clinical progression of patients with COVID-19 in Shanghai, China. *J Infect.* (2020) 80:e1–6. doi: 10.1016/j.jinf.2020.03.004
27. Zhu L, Gong N, Liu B, Lu X, Chen D, Chen S, et al. Coronavirus disease 2019 pneumonia in immunosuppressed renal transplant recipients: a summary of 10 confirmed cases in Wuhan, China. *Euro Urol.* (2020) 77:748–54. doi: 10.1016/j.eururo.2020.03.039
28. Han C, Duan C, Zhang S, Spiegel B, Shi H, Wang W, et al. Digestive symptoms in COVID-19 patients with mild disease severity: clinical presentation, stool viral RNA testing, and outcomes. *Am J Gastroenterol.* (2020) 115:916–23. doi: 10.14309/ajg.0000000000000664
29. Yan X, Han X, Fan Y, Fang Z, Long D, Zhu Y. Duration of SARS-CoV-2 viral RNA in asymptomatic carriers. *Crit Care.* (2020) 24:245. doi: 10.1186/s13054-020-02952-0
30. Gong Y, Guan L, Jin Z, Chen S, Xiang G, Gao B. Effects of methylprednisolone use on viral genomic nucleic acid negative conversion and CT imaging lesion absorption in COVID-19 patients under 50 years old. *J Med Virol.* (2020) 92:2551–5. doi: 10.1002/jmv.26052
31. Warabi Y, Tobisawa S, Kawazoe T, Murayama A, Norioka R, Morishima R, et al. Effects of oral care on prolonged viral shedding in coronavirus disease 2019 (COVID-19). *Special Care Dentistr.* (2020) 40:470–4. doi: 10.1111/scd.12498
32. Pan Y, Yu X, Du X, Li Q, Li X, Qin T, et al. Epidemiological and clinical characteristics of 26 asymptomatic severe acute respiratory syndrome coronavirus 2 carriers. *J Infect Dis.* (2020) 221:1940–7. doi: 10.1093/infdis/jiaa205
33. Hua CZ, Miao ZP, Zheng JS, Huang Q, Sun QF, Lu HP, et al. Epidemiological features and viral shedding in children with SARS-CoV-2 infection. *J Med Virol.* (2020) 92:2804–12. doi: 10.1002/jmv.26180
34. Cano E, Corsini Campioli C, O'Horo JC. Nasopharyngeal SARS-CoV-2 viral RNA shedding in patients with diabetes mellitus. *Endocrine.* (2020) 71:26–7. doi: 10.1007/s12020-020-02516-w
35. Wu Y, Guo C, Tang L, Hong Z, Zhou J, Dong X, et al. Prolonged presence of SARS-CoV-2 viral RNA in faecal samples. *Lancet Gastroenterol Hepatol.* (2020) 5:434–5. doi: 10.1016/s2468-1253(20)30083-2
36. Otsubo S, Aoyama Y, Kinoshita K, Goto T, Otsubo Y, Kamano D, et al. Prolonged shedding of SARS-CoV-2 in COVID-19 infected hemodialysis patients. *Therap Apher Dial.* (2020). doi: 10.1111/1744-9987.13566
37. Tan F, Wang K, Liu J, Liu D, Luo J, Zhou R. Viral transmission and clinical features in asymptomatic carriers of SARS-CoV-2 in Wuhan, China. *Front Med.* (2020) 7:547. doi: 10.3389/fmed.2020.00547
38. Xiao T, Wang Y, Yuan J, Ye H, Wei L, Liao X, et al. Early viral clearance and antibody kinetics of COVID-19 among asymptomatic carriers. *medRxiv.* (2020) 2020.04.28.20083139. doi: 10.1101/2020.04.28.20083139
39. Yao X, Zhao X, Wang M, Xu W, Bai H, Ai X. Familial clustering infection caused by asymptomatic COVID-19 (in Chinese). *Int J Respi.* (2020) 40:982–7. doi: 10.3760/cma.j.cn131368-20200318-00175
40. Liu YJ, Chen P, Liu ZS, Li Y, Du H, Xu JL. Clinical features of asymptomatic or subclinical COVID-19 in children (in Chinese). *Zhongguo Dang dai er ke za zhi.* (2020) 22:578–82. doi: 10.7499/j.issn.1008-8830.2004088
41. Shi Z, He Y, Yang M, Duan M, Wang Y, Lai M, et al. Influencing factors of negative conversion time of viral nucleic acid of nasopharyngeal swabs in patients with novel coronavirus infected pneumonia (in Chinese). *Pract J Clin Med.* (2020) 17:45–8. Available online at: http://www.wanfangdata.com.cn/details/detail.do?_type=perio&id=syyylczz202002015
42. Li l, Yang H, Gou C, Wang X, Luo X, Zhang J, et al. Traditional Chinese medicine characteristics of 46 patients with COVID-19 (in Chinese). *J Capital Med Univ.* (2020) 41:155–60. doi: 10.3969/j.issn.1006-7795.2020.02.002
43. Jiang Y, Wang H, Si G, Deng L, Ou C, Rong X. Clinical ananlysis of corona virus disease 2019: a report of 24 cases (in Chinese). *J Chongqing Med Univ.* (2020) 45:968–70. doi: 10.13406/j.cnki.cyxb.002453
44. Gong H, Huang H, Zhou X, Luo S, Zhang Z, Zhang S, et al. Related factors of the conversion time of virus nucleic acid turning negative in patients with coronavirus disease 2019 and its effect on prognosis (in Chinese). *Herald Med.* (2020) 39:811–4. doi: 10.3870/j.issn.1004-0781.2020.06.015
45. Zhao B, Liu D, Liu Y, Lan L, Du Q, Chen H, et al. Differences in laboratory indicators and prognosis between COVID-19 patients with or without diabetes mellitus (in Chinese). *Sichuan Med J.* (2020) 41:913–7. doi: 10.16252/j.cnki.issn1004-0501-2020.09.005
46. Zhang B, Zhang Z, Li Z, Chi Q, Zheng J, Dai X. Retrospective analysis of viral nucleic acid test results of 116 fecal samples from COVID-19 patients (in Chinese). *Jinagsu Med J.* (2020) 46:571–2. doi: 10.19460/j.cnki.0253-3685.2020.06.009
47. Xu L, Peng P, Li S, Wu P, Han J, Mo X. Clinical characteristics of 59 cases of COVID-19 in Guangzhou (in Chinese). *China Trop Med.* (2020) 20:871–4. doi: 10.13604/j.cnki.46-1064/r.2020.09.17
48. Xie C, Qin P, Zeng X, Deng H, Cheng S, Xie Y. Dynamic changes of IgM and IgG in confirmed COVID-19 cases: detection results analysis (in Chinese). *Chin J Publ Heal.* (2020) 36:1396–8. doi: 10.11847/zgggws1130146
49. Sun L, Li X, Li S, Niu C, Pan S, Wang Q, et al. Nucleic acid detection analysis of 71 cases of COVID-19 with biological samples of diferent disease course(in Chinese). *China Trop Med.* (2020) 20:763–6. doi: 10.13604/j.cnki.46-1064/r.2020.08.16
50. Ren H, Lei H, Sun G, Li H, Bai J, Tang L. Clinical characteristics of 2019 novel coronavirus pneumonia in a mobile cabin hospital in Wuhan: analysis of 94 cases (in Chinese). *Chinese J Hygiene Rescue.* (2020) 6:209–13. doi: 10.3877/cma.j.issn.2095-9133.2020.04.003
51. Ran Q, Chen H, Zhang L, Zhong Y. Analysis of Factors influencing viral shedding time in severe and critical COVID-19 patients (in Chinese). *Adv Clin Med.* (2020) 10:1717–24. doi: 10.12677/acm.2020.108258
52. Lu Y, Li Y, Deng W, Liu M, He Y, Huang L, et al. Symptomatic infection is associated with prolonged duration of viral shedding in mild coronavirus disease 2019: a retrospective study of 110 children in Wuhan. *Pediatr Infect Dis J.* (2020) 39:e95–9. doi: 10.1097/inf.0000000000002729
53. Liu J, Liu X, Yang M, Xiao X, Cen C. Influencing factors for positive duration of viral nucleic acid in patients with severe coronavirus disease 2019 (in Chinese). *Acad J Second Military Med Univ.* (2020) 41:966–9. doi: 10.16781/j.0258-879x.2020.09.0966
54. Li N, Xie T, Wei X, Yi S, Cao Y, Jiang S, et al. Chloroquine phosphate accelerates the conversion of nucleic acid to negative in 88 common COVID?19 patients (in Chinese). *J Pract Med.* (2020) 36:2759–62. doi: 10.3969/j.issn.1006-5725.2020.20.003
55. Tang B, Wang X, Li Q, Bragazzi NL, Tang S, Xiao Y, et al. Estimation of the transmission risk of the 2019-nCoV and its implication for public health interventions. *J Clin Med.* (2020) 9:462. doi: 10.3390/jcm9020462
56. Wu JT, Leung K, Leung GM. Nowcasting and forecasting the potential domestic and international spread of the 2019-nCoV outbreak originating in Wuhan, China: a modelling study. *Lancet.* (2020) 395:689–97. doi: 10.1016/s0140-6736(20)30260-9
57. Zhao S, Lin Q, Ran J, Musa SS, Yang G, Wang W, et al. Preliminary estimation of the basic reproduction number of novel coronavirus (2019-nCoV) in China, from 2019 to 2020: a data-driven analysis in the early phase of the outbreak. *Int J Infect Dis.* (2020) 92:214–7. doi: 10.1016/j.ijid.2020.01.050
58. Al-Jasser FS, Nouh RM, Youssef RM. Epidemiology and predictors of survival of MERS-CoV infections in Riyadh region, 2014-2015. *J Infect Public Health.* (2019) 12:171–7. doi: 10.1016/j.jiph.2018.09.008
59. Liu W, Tang F, Fontanet A, Zhan L, Zhao QM, Zhang PH, et al. Long-term SARS coronavirus excretion from patient cohort, China. *Emerg Infect Dis.* (2004) 10:1841–3. doi: 10.3201/eid1010.040297
60. He X, Lau EHY, Wu P, Deng X, Wang J, Hao X, et al. Temporal dynamics in viral shedding and transmissibility of COVID-19. *Nat Med.* (2020) 26:672–5. doi: 10.1038/s41591-020-0869-5
61. To KK, Tsang OT, Leung WS, Tam AR, Wu TC, Lung DC, et al. Temporal profiles of viral load in posterior oropharyngeal saliva

samples and serum antibody responses during infection by SARS-CoV-2: an observational cohort study. *Lancet Infect Dis.* (2020) 20:565–74. doi: 10.1016/s1473-3099(20)30196-1
62. Wölfel R, Corman VM, Guggemos W, Seilmaier M, Zange S, Müller MA, et al. Virological assessment of hospitalized patients with COVID-2019. *Nature.* (2020) 581:465–9. doi: 10.1038/s41586-020-2196-x
63. Hao S, Lian J, Lu Y, Jia H, Hu J, Yu G, et al. Decreased B cells on admission associated with prolonged Viral RNA shedding from the respiratory tract in coronavirus disease 2019: a case-control study. *J Infect Dis.* (2020) 222:367–71. doi: 10.1093/infdis/jiaa311
64. Wu Z, McGoogan JM. Characteristics of and important lessons from the coronavirus disease 2019 (COVID-19) outbreak in China: summary of a report of 72,314 cases from the chinese center for disease control and prevention. *JAMA*. (2020) 323:1239–42. doi: 10.1001/jama.2020.2648
65. Lu X, Zhang L, Du H, Zhang J, Li YY, Qu J, et al. SARS-CoV-2 infection in children. *N Engl J Med.* (2020) 382:1663–5. doi: 10.1056/NEJMc2005073
66. Russell CD, Millar JE, Baillie JK. Clinical evidence does not support corticosteroid treatment for 2019-nCoV lung injury. *Lancet*. (2020) 395:473–5. doi: 10.1016/s0140-6736(20)30317-2
67. Lee N, Allen Chan KC, Hui DS, Ng EK, Wu A, Chiu RW, et al. Effects of early corticosteroid treatment on plasma SARS-associated Coronavirus RNA concentrations in adult patients. *J Clin Virol.* (2004) 31:304–9. doi: 10.1016/j.jcv.2004.07.006
68. National Health Commission of the People's Republic of China. *Diagnosis and Treatment for COVID-19 (Trial Version 8)*. (2020). Available online at: http://www.nhc.gov.cn (accessed November 16, 2020).
69. Wan Y, Shang J, Graham R, Baric RS, Li F. Receptor recognition by the novel coronavirus from Wuhan: an analysis based on decade-long structural studies of SARS Coronavirus. *J Virol.* (2020) 94:e00127-20. doi: 10.1128/jvi.00127-20
70. Islam MS, Rahman KM, Sun Y, Qureshi MO, Abdi I, Chughtai AA, et al. Current knowledge of COVID-19 and infection prevention and control strategies in healthcare settings: a global analysis. *Infect Control Hosp Epidemiol.* (2020) 41:1196–206. doi: 10.1017/ice.2020.237
71. Perisetti A, Goyal H, Sharma N. Gastrointestinal endoscopy in the Era of COVID-19. *Front Med.* (2020) 7:587602. doi: 10.3389/fmed.2020.587602

Conflict of Interest: The authors declare that the research was conducted in the absence of any commercial or financial relationships that could be construed as a potential conflict of interest.

PLOS BIOLOGY

RESEARCH ARTICLE

Viral dynamics of acute SARS-CoV-2 infection and applications to diagnostic and public health strategies

Stephen M. Kissler[1☯], Joseph R. Fauver[2☯], Christina Mack[3,4☯], Scott W. Olesen[1], Caroline Tai[3], Kristin Y. Shiue[3,4], Chaney C. Kalinich[2], Sarah Jednak[5], Isabel M. Ott[2], Chantal B. F. Vogels[2], Jay Wohlgemuth[6], James Weisberger[7], John DiFiori[8,9], Deverick J. Anderson[10], Jimmie Mancell[11], David D. Ho[12], Nathan D. Grubaugh[2‡], Yonatan H. Grad[1‡*]

1 Department of Immunology and Infectious Diseases, Harvard T.H. Chan School of Public Health, Boston, Massachusetts, United States of America, **2** Department of Epidemiology of Microbial Diseases, Yale School of Public Health, New Haven, Connecticut, United States of America, **3** Real World Solutions, IQVIA, Durham, North Carolina, United States of America, **4** Department of Epidemiology, University of North Carolina at Chapel Hill, Chapel Hill, North Carolina, United States of America, **5** Department of Health Management and Policy, University of Michigan School of Public Health, Ann Arbor, Michigan, United States of America, **6** Quest Diagnostics, San Juan Capistrano, California, United States of America, **7** Bioreference Laboratories, Elmwood Park, New Jersey, United States of America, **8** Hospital for Special Surgery, New York, New York, United States of America, **9** National Basketball Association, New York, New York, United States of America, **10** Duke Center for Antimicrobial Stewardship and Infection Prevention, Durham, North Carolina, United States of America, **11** Department of Medicine, University of Tennessee Health Science Center, Memphis, Tennessee, United States of America, **12** Aaron Diamond AIDS Research Center, Columbia University Vagelos College of Physicians and Surgeons, New York, New York, United States of America

☯ These authors contributed equally to this work.
‡ These authors are joint senior authors on this work.
* ygrad@hsph.harvard.edu

Citation: Kissler SM, Fauver JR, Mack C, Olesen SW, Tai C, Shiue KY, et al. (2021) Viral dynamics of acute SARS-CoV-2 infection and applications to diagnostic and public health strategies. PLoS Biol 19(7): e3001333. https://doi.org/10.1371/journal.pbio.3001333

Academic Editor: Steven Riley, Imperial College London, UNITED KINGDOM

Received: January 14, 2021

Accepted: June 21, 2021

Published: July 12, 2021

Data Availability Statement: Data are available at https://github.com/gradlab/CtTrajectories.

Funding: This study was funded by the NWO Rubicon 019.181EN.004 (CBFV), a clinical research agreement with the NBA and NBPA (NDG), the Huffman Family Donor Advised Fund (NDG), Fast Grant funding support from the Emergent Ventures at the Mercatus Center, George Mason University (NDG), and the Morris-Singer Fund for the Center for Communicable Disease Dynamics at the Harvard T.H. Chan School of Public Health (YHG).

Abstract

SARS-CoV-2 infections are characterized by viral proliferation and clearance phases and can be followed by low-level persistent viral RNA shedding. The dynamics of viral RNA concentration, particularly in the early stages of infection, can inform clinical measures and interventions such as test-based screening. We used prospective longitudinal quantitative reverse transcription PCR testing to measure the viral RNA trajectories for 68 individuals during the resumption of the 2019–2020 National Basketball Association season. For 46 individuals with acute infections, we inferred the peak viral concentration and the duration of the viral proliferation and clearance phases. According to our mathematical model, we found that viral RNA concentrations peaked an average of 3.3 days (95% credible interval [CI] 2.5, 4.2) after first possible detectability at a cycle threshold value of 22.3 (95% CI 20.5, 23.9). The viral clearance phase lasted longer for symptomatic individuals (10.9 days [95% CI 7.9, 14.4]) than for asymptomatic individuals (7.8 days [95% CI 6.1, 9.7]). A second test within 2 days after an initial positive PCR test substantially improves certainty about a patient's infection stage. The effective sensitivity of a test intended to identify infectious individuals declines substantially with test turnaround time. These findings indicate that SARS-CoV-2 viral concentrations peak rapidly regardless of symptoms. Sequential tests can help

The funders had no role in study design, data collection and analysis, decision to publish, or preparation of the manuscript.

Competing interests: I have read the journal's policy and the authors of this manuscript have the following competing interests: JW is an employee of Quest Diagnostics. JW is an employee of Bioreference Laboratories. NDG has a consulting agreement for Tempus and receives financial support from Tempus to develop SARS-CoV-2 diagnostic tests. SMK, SWO, and YHG have a consulting agreement with the NBA.

Abbreviations: CI, credible interval; Ct, cycle threshold; NBA, National Basketball Association; RT-qPCR, quantitative reverse transcription polymerase chain reaction.

reveal a patient's progress through infection stages. Frequent, rapid-turnaround testing is needed to effectively screen individuals before they become infectious.

Introduction

A critical strategy to curb the spread of SARS-CoV-2 is to rapidly identify and isolate infectious individuals. Because symptoms are an unreliable indicator of infectiousness and infections are frequently asymptomatic [1], testing is key to determining whether a person is infected and may be contagious. Real-time quantitative reverse transcription polymerase chain reaction (RT-qPCR) tests are the gold standard for detecting SARS-CoV-2 infection. Normally, these tests yield a binary positive/negative diagnosis based on detection of viral RNA. However, they can also quantify the viral titer via the cycle threshold (Ct). The Ct is the number of thermal cycles needed to amplify sampled viral RNA to a detectable level: the higher the sampled viral RNA concentration, the lower the Ct. This inverse correlation between Ct and viral concentration makes RT-qPCR tests far more valuable than a binary diagnostic, as they can be used to reveal a person's progress through key stages of infection [2], with the potential to assist clinical and public health decision-making. However, the dynamics of the Ct during the earliest stages of infection, when contagiousness is rapidly increasing, have been unclear, because diagnostic testing is usually performed after the onset of symptoms, when viral RNA concentration has peaked and already begun to decline, and is performed only once [3,4]. Without a clear picture of the course of SARS-CoV-2 viral concentrations across the full duration of acute infection, it has been impossible to specify key elements of testing algorithms such as the frequency of rapid at-home testing [5] that would be needed to reliably screen infectious individuals before they transmit infection. Here, we fill this gap by analyzing the prospective longitudinal SARS-CoV-2 RT-qPCR testing performed for players, staff, and vendors during the resumption of the 2019–2020 National Basketball Association (NBA) season.

Methods

Data collection

The study period began in teams' local cities from June 23 through July 9, 2020, and testing continued for all teams as they transitioned to Orlando, Florida, through September 7, 2020. A total of 68 individuals (90% male) were tested at least 5 times during the study period and recorded at least 1 positive test with Ct value < 40. Most consecutive tests (85%) were recorded within 1 day of each other, and fewer than 3% of the intervals between consecutive tests exceeded 4 days (S1 Fig). Many individuals were being tested daily as part of Orlando campus monitoring. Due to a lack of new infections among players and team staff after clearing quarantine in Orlando, all players and team staff included in the results predate the Orlando phase of the restarted season. A diagnosis of "acute" or "persistent" infection was abstracted from physician records. "Acute" denoted a likely new infection. "Persistent" indicated the presence of virus in a clinically recovered individual, likely due to infection that developed prior to the onset of the study. There were 46 acute infections; the remaining 22 individuals were assumed to be persistently shedding SARS-CoV-2 RNA due to a known infection that occurred prior to the study period [6]. This persistent RNA shedding can last for weeks after an acute infection and likely represents noninfectious viral RNA [7]. Of the individuals included in the study, 27 of the 46 with acute infections and 40 of the 68 overall were staff and vendors. The Ct values for all tests for the 68 individuals included in the analysis, with their designations of acute or

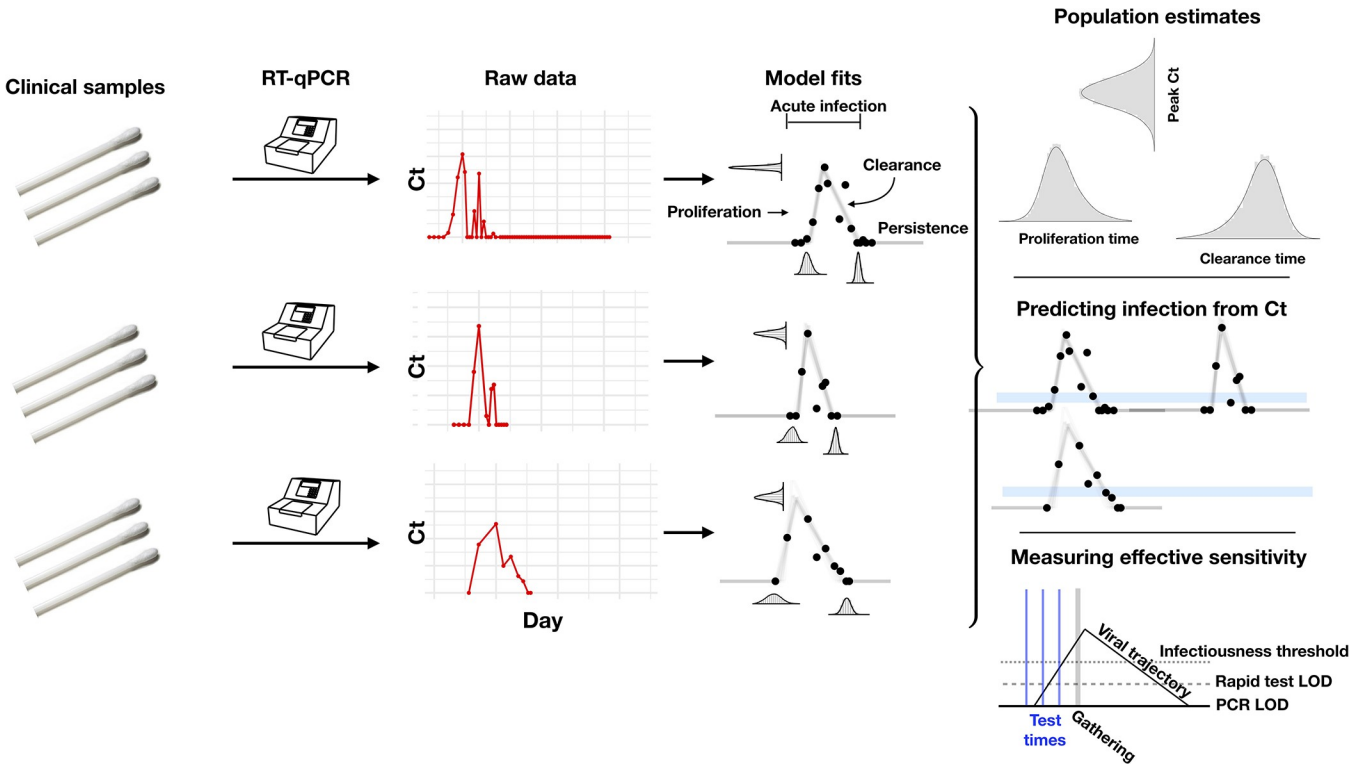

Fig 1. Illustration of the analysis pipeline. Combined anterior nares and oropharyngeal swabs were tested using a RT-qPCR assay to generate longitudinal Ct values ("Raw data"; red points) for each person. Using a statistical model (see S6 Fig for a schematic of the model), we estimated Ct trajectories consistent with the data, represented by the thin lines under the "Model fits" heading. These produced posterior probability distributions for the peak Ct value, the duration of the proliferation phase (first potential detectability of infection to peak Ct), and the duration of the clearance phase (peak Ct to resolution of acute infection) for each person. We estimated population means for these quantities (under the heading "Population estimates"). The model fits also allowed us to determine how frequently a given Ct value or pair of Ct values within a 5-unit window (blue bars, under the heading "Predicting infection from Ct") was associated with the proliferation phase, the clearance phase, or a persistent infection. Finally, the model fits allowed us to measure the "effective sensitivity" of a test for predicting future infectiousness. The schematic illustration titled "Measuring effective sensitivity" depicts the relationship between testing lags and the ability to detect infectious individuals at a gathering. The illustrated viral trajectory surpasses the infectiousness threshold (dotted line) at the time of the gathering (vertical grey bar), so unless this individual is screened by a pre-gathering test, he or she would attend the event while infectious. One day prior to the gathering, the individual's infection could be detected by either a rapid test or a PCR test. Two days prior to the event, the individual's infection could be detected by a PCR test but not by a rapid test. Three days prior to the event, neither test would detect the individual's infection. Ct, cycle threshold; LOD, limit of detection; RT-qPCR, quantitative reverse transcription polymerase chain reaction.

https://doi.org/10.1371/journal.pbio.3001333.g001

persistent infection, are depicted in S2–S5 Figs. A schematic diagram of the data collection and analysis pipeline is given in Fig 1.

Ethics

Residual de-identified viral transport media from anterior nares and oropharyngeal swabs collected from NBA players, staff, and vendors were obtained from Quest Diagnostics or BioReference Laboratories. In accordance with the guidelines of the Yale Human Investigation Committee, this work with de-identified samples was approved for research not involving human subjects by the Yale Institutional Review Board (HIC protocol #2000028599). This project was designated exempt by the Harvard Institutional Review Board (IRB20-1407).

Statistical analysis

Due to imperfect sampling, persistent viral shedding, and test uncertainty near the limit of detection, a straightforward analysis of the data would be insufficient to reveal the duration

and peak magnitude of the viral trajectory. Imperfect sampling would bias estimates of the peak viral concentration towards lower concentrations/higher Ct values since the moment of peak viral concentration is unlikely to be captured. Persistent shedding and test uncertainty would bias estimates of the trajectory duration towards longer durations of infection. To address these problems, we used a Bayesian statistical model to infer the peak Ct value and the durations of the proliferation and clearance stages for the 46 acute infections (Fig 1; S1 Text). We assumed that the viral concentration trajectories consisted of a proliferation phase, with exponential growth in viral RNA concentration, followed by a clearance phase, characterized by exponential decay in viral RNA concentration [8]. Since Ct values are roughly proportional to the negative logarithm of viral concentration [2], this corresponds to a linear decrease in Ct followed by a linear increase. We therefore constructed a piecewise linear regression model to estimate the peak Ct value, the time from infection onset to peak (i.e., the duration of the proliferation stage), and the time from peak to infection resolution (i.e., the duration of the clearance stage). This allowed us to separate the viral trajectories into the 3 distinct phases: proliferation (from the onset of detectability to the peak viral concentration, or t_o to t_p in S6 Fig), clearance (from the peak viral concentration to the resolution of acute infection, or t_p to t_r in S6 Fig), and persistence (lasting indefinitely after the resolution of acute infection, or after t_r in S6 Fig; see also Fig 1). Note that for the 46 individuals with acute infections, the persistence phase is identified using the viral trajectory model, whereas for the 22 other infections, the entire series of observations was classified as "persistent" due to clinical evidence of a probable infection prior to the start of the study period. We estimated the parameters of the regression model by fitting to the available data using a Hamiltonian Monte Carlo algorithm [9] yielding simulated draws from the Bayesian posterior distribution for each parameter. Full details on the fitting procedure are given in S1 Text. Code is available at https://github.com/gradlab/CtTrajectories [10].

Inferring stage of infection

Next, we determined whether individual or paired Ct values can reveal whether an individual is in the proliferation, clearance, or persistent stage of infection. To assess the predictive value of a single Ct value, we extracted all observed Ct values within a 5-unit window (e.g., between 30.0 and 34.9 Ct) and measured how frequently these values sat within the proliferation stage, the clearance stage, or the persistent stage. We measured these frequencies across 10,000 posterior parameter draws to account for the fact that Ct values near stage transitions (e.g., near the end of the clearance stage) could be assigned to different infection stages depending on the parameter values (see Fig 1, bottom right). We did this for 23 windows with midpoint spanning from Ct = 37.5 to Ct = 15.5 in increments of 1 Ct.

To calculate the probability that a Ct value sitting within a 5-unit window corresponded to an acute infection (i.e., either the proliferation or the clearance stage), we summed the proliferation and clearance frequencies for all samples within that window and divided by the total number of samples in the window. We similarly calculated the probability that a Ct sitting within the 5-unit window corresponded to just the proliferation phase.

To assess the information gained by conducting a second test within 2 days of an initial positive test, we restricted our attention to all samples that had a subsequent sample taken within 2 days. We repeated the above calculations for (a) consecutive tests with decreasing Ct and (b) consecutive tests with increasing Ct. That is, we measured the frequency with which a given Ct value sitting within a 5-unit window, followed by a second test with either a lower or a higher Ct, sat within with the proliferation, clearance, or persistence stages.

Measuring the effective sensitivity of screening tests

The sensitivity of a test is defined as the probability that the test correctly identifies an individual who is positive for some criterion of interest. For clinical diagnostic SARS-CoV-2 tests, the criterion of interest is current infection with SARS-CoV-2. Alternatively, a common goal is to predict infectiousness at some point in the future, as in the context of test-based screening prior to a social gathering. The "effective sensitivity" of a test in this context (i.e., its ability to predict future infectiousness) may differ substantially from its clinical sensitivity (i.e., its ability to detect current infection). A test's effective sensitivity depends on its inherent characteristics, such as its limit of detection and sampling error rate, as well as the viral dynamics of infected individuals.

To illustrate this, we estimated the effective sensitivity of (a) a test with a limit of detection of 40 Ct and a 1% sampling error probability (akin to RT-qPCR) and (b) a test with a limit of detection of 35 Ct and a 5% sampling error probability (akin to some rapid antigen tests). We measured the frequency with which such tests would successfully identify an individual who would be infectious at the time of a gathering when the test was administered between 0 and 3 days prior to the gathering, given viral trajectories informed by the longitudinal testing data (see schematic in Fig 1). To accomplish this, we drew 1,000 individual-level viral concentration trajectories from the fitted model, restricting to trajectories with peak viral concentration above a given infectiousness threshold (any samples with peak viral concentration below the infectiousness threshold would never be infectious and so would not factor into the sensitivity calculation). For the main analysis, we assumed that the infectiousness threshold was at 30 Ct [11]. In a supplemental analysis, we also assessed infectiousness thresholds of 35 and 20 Ct. We drew onset-of-detectability times (i.e., the onset of the proliferation stage) according to a random uniform distribution so that each person would have a Ct value exceeding the infectiousness threshold at the time of the gathering. Then, we calculated the fraction of trajectories that would be successfully identified using a test with (a) a limit of detection of 40 Ct and (b) a limit of detection of 35 Ct, administered between 0 and 3 days prior to the gathering. Full details are given in S1 Text and S7A Fig.

Next, we shifted attention from the individual to the gathering. We estimated the number of individuals who would be expected to arrive at a 1,000-person gathering while infectious given each testing strategy (40-Ct limit of detection with 1% false negative rate; 35-Ct limit of detection with 5% false negative rate) assuming a 2% prevalence of PCR-detectable infection in the population. To do so, we again drew 1,000 individual-level viral concentration trajectories from the fitted model and drew onset-of-detectability times according to a random uniform distribution from the range of possible times that would allow for the person to have detectable virus ($Ct < 40$) during the gathering. We counted the number of people who would have been infectious at the gathering (a) in the absence of testing and (b) given a test administered between 0 and 3 days prior to the gathering. As before, we assumed that the infectiousness threshold corresponded to a Ct value of 30 for the main analysis and considered infectiousness thresholds of 35 Ct and 20 Ct in a supplemental analysis. Full details are given in S1 Text and S7B Fig. To facilitate the exploration of different scenarios, we have generated an online tool (https://stephenkissler.shinyapps.io/shiny/) where users can input test and population characteristics and calculate the effective sensitivity and expected number of infectious individuals at a gathering.

Results

Of the 46 individuals with acute infections, 13 reported symptoms at the time of diagnosis; the timing of the onset of symptoms was not recorded. The median number of positive tests for

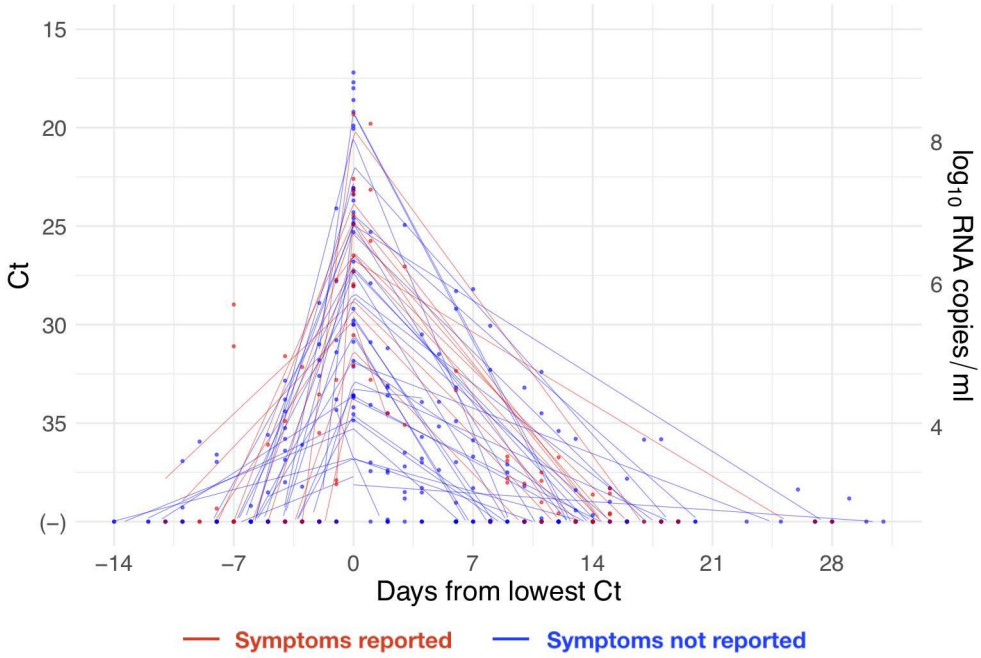

Fig 2. Reported cycle threshold (Ct) values with individual-level piecewise linear fits. Ct values (points) for the 46 acute infections aligned by the date when the minimum Ct was recorded for each individual. Lines depict the best-fit piecewise linear regression lines for each individual with breakpoint at day 0. Red points/lines represent individuals who reported symptoms, and blue points/lines represent individuals who did not report symptoms. Five positive tests were omitted that occurred >20 days prior to the individual's minimum Ct value, all of which had Ct > 35. The vertical axis on the right-hand side gives the conversion from Ct values to RNA concentration. Underlying data are available at https://github.com/gradlab/CtTrajectories/tree/main/figure_data/Fig2 [10].

https://doi.org/10.1371/journal.pbio.3001333.g002

the 46 individuals was 3 (IQR 2, 5). The minimum recorded Ct value across the 46 individuals had mean 26.4 (IQR 23.2, 30.4). The recorded Ct values for the acute infections with individual-level piecewise linear regressions are depicted in Fig 2.

Based on the viral trajectory model, the mean peak Ct value for symptomatic individuals was 22.3 (95% credible interval [CI] 19.3, 25.3), the mean duration of the proliferation phase was 3.4 days (95% CI 2.0, 4.8), and the mean duration of clearance was 10.9 days (95% CI 7.9, 14.4) (Fig 3). This compares with 22.3 Ct (95% CI 20.0, 24.4), 3.5 days (95% CI 2.5, 4.5), and 7.8 days (95% CI 6.1, 9.7), respectively, for individuals who did not report symptoms at the time of diagnosis (Fig 3). This yielded a slightly longer overall duration of acute infection for individuals who reported symptoms (14.3 days [95% CI 11.0, 17.7]) versus those who did not (11.2 days [95% CI 9.4, 13.4]). For all individuals, regardless of symptoms, the mean peak Ct value, proliferation duration, clearance duration, and duration of acute shedding were 22.3 Ct (95% CI 20.5, 23.9), 3.3 days (95% CI 2.5, 4.2), 8.5 days (95% CI 6.9, 10.1), and 11.7 days (95% CI 10.1, 13.6) (S8 Fig). A full list of the model-inferred viral trajectory parameters is reported in Table 1. There was a substantial amount of individual-level variation in the peak Ct value and the proliferation and clearance stage durations (S9–S14 Figs).

Using the full dataset of 68 individuals, we estimated the frequency with which a given Ct value was associated with an acute infection (i.e., the proliferation or clearance phase, but not the persistence phase) and, if so, the probability that it was associated with the proliferation stage alone. The probability of an acute infection increased rapidly with decreasing Ct (increasing viral load), with Ct < 30 virtually guaranteeing an acute infection in this dataset (Fig 4A). However, a single Ct value provided little information about whether an acute infection was in

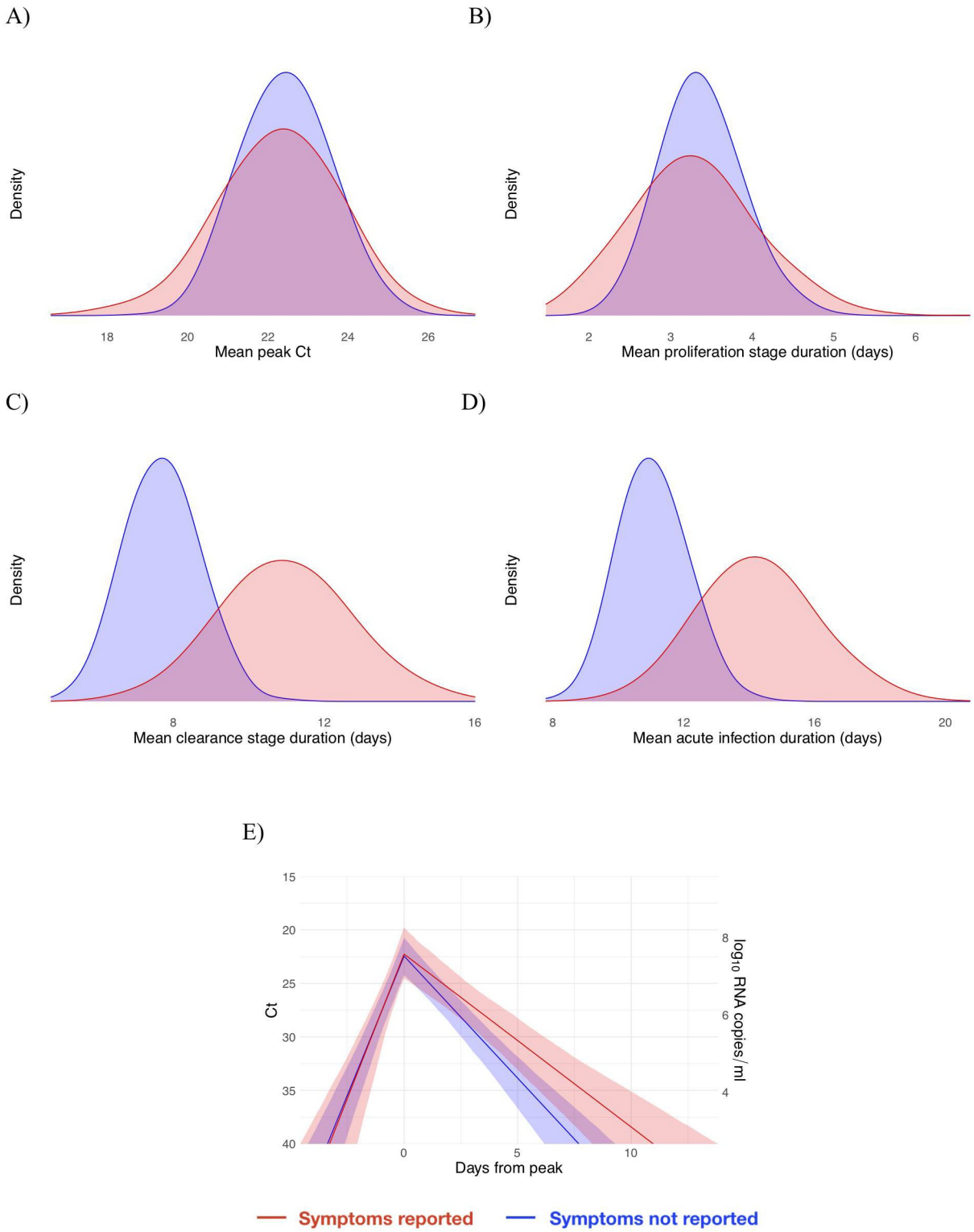

Fig 3. Peak cycle threshold (Ct) value and infection stage duration distributions according to symptoms reported at time of diagnosis. Posterior distributions obtained from 2,000 simulated draws from the posterior distributions for mean peak Ct value (A), mean duration of the proliferation stage (first potential infection detectability to peak Ct) (B), mean duration of the clearance stage (peak Ct to resolution of acute RNA shedding) (C), and total duration of acute shedding (D) across the 46 individuals with an acute infection. The distributions are separated according to whether the person reported symptoms (red, 13 individuals) or did not report symptoms (blue, 33 individuals). The mean Ct trajectory corresponding to the mean values for peak Ct, proliferation duration, and clearance duration for symptomatic versus asymptomatic

individuals is depicted in (E) (solid lines), where shading depicts the 90% credible intervals. Underlying data are available at https://github.com/gradlab/CtTrajectories/tree/main/output/params_df_split.csv [10].

https://doi.org/10.1371/journal.pbio.3001333.g003

the proliferation or the clearance stage (Fig 4B). This is unsurprising since the viral trajectory must pass through any given value during both the proliferation and the clearance stage. With roughly uniform sampling over time, a given Ct value is more likely to correspond to the clearance stage simply because the clearance stage is longer.

We assessed whether a second test within 2 days of the first could improve these predictions. A positive test followed by a second test with lower Ct (higher viral RNA concentration) was slightly more likely to be associated with an active infection than a positive test alone (Fig 4C), and was much more likely to be associated with the proliferation phase than with the clearance phase (Fig 4D).

We next estimated how the effective sensitivity of a pre-event screening test declines with increasing time to the event. For a test with a limit of detection of 40 Ct and a 1% chance of sampling error, the effective sensitivity declines from 99% when the test coincides with the start of the event to 76% when the test is administered 2 days prior to the event (Fig 5A), assuming a threshold of infectiousness at 30 Ct [11]. This 2-day-ahead sensitivity is slightly lower than the effective sensitivity of a test with a limit of detection at 35 Ct and a 5% sampling error administered 1 day before the event (82%), demonstrating that limitations in testing technology can be compensated for by reducing turnaround time. Using these effective sensitivities, we estimated the number of infectious individuals who would be expected to arrive at a gathering with 1,000 people given a pre-gathering screening test and a 2% prevalence of infectiousness in the population. Just as the effective sensitivity declines with time to the gathering, the predicted number of infectious individuals rises with time to the gathering (Fig 5B) since longer delays between the screening test and the gathering make it more likely that an individual's infection will be undetectable at the time of testing but the individual will be infectious at the time of the event. Changing the infectiousness threshold modulates the magnitude of the decline in effective sensitivity associated with longer testing delays; however, the overall pattern is consistent (S18 Fig).

Discussion

We provide to our knowledge the first comprehensive data on the early-infection RT-qPCR Ct dynamics associated with SARS-CoV-2 infection. We found that viral titers peak quickly,

Table 1. Viral dynamic parameters, overall and separated by reported symptoms.

Parameter	Mean (95% CI)		
	Symptoms*	No symptoms*	Overall
Peak Ct	22.2 (19.1, 25)	22.4 (20.2, 24.5)	22.4 (20.7, 24)
Peak viral concentration (log RNA copies/ml/day)	7.6 (6.8, 8.4)	7.5 (7, 8.1)	7.5 (7.1, 8)
Proliferation duration (days)	3.3 (1.9, 5.1)	3.4 (2.5, 4.5)	3.2 (2.4, 4.2)
Proliferation rate (Ct/day)	5.6 (3.4, 9.3)	5.2 (3.8, 7.1)	5.6 (4.2, 7.3)
Proliferation rate (log RNA copies/ml/day)	1.6 (0.9, 2.6)	1.5 (1.0, 2.0)	1.5 (1.2, 2)
Clearance duration (days)	10.9 (7.8, 14.2)	7.8 (6.1, 9.7)	8.5 (6.8, 10.2)
Clearance rate (Ct/day)	1.7 (1.2, 2.4)	2.3 (1.7, 3)	2.1 (1.7, 2.6)
Clearance rate (log RNA copies/ml/day)	0.5 (0.3, 0.7)	0.6 (0.5, 0.8)	0.6 (0.5, 0.7)
Infection duration (days)	14.3 (11, 17.8)	11.2 (9.4, 13.3)	11.7 (9.9, 13.5)

CI, credible interval; Ct, cycle threshold. Population sizes for each category are as follows: symptoms, $N = 13$; no symptoms, $N = 33$; overall, $N = 46$.

*Symptom reporting was imperfect as follow-up during the course of the disease was not systematic for all individuals.

https://doi.org/10.1371/journal.pbio.3001333.t001

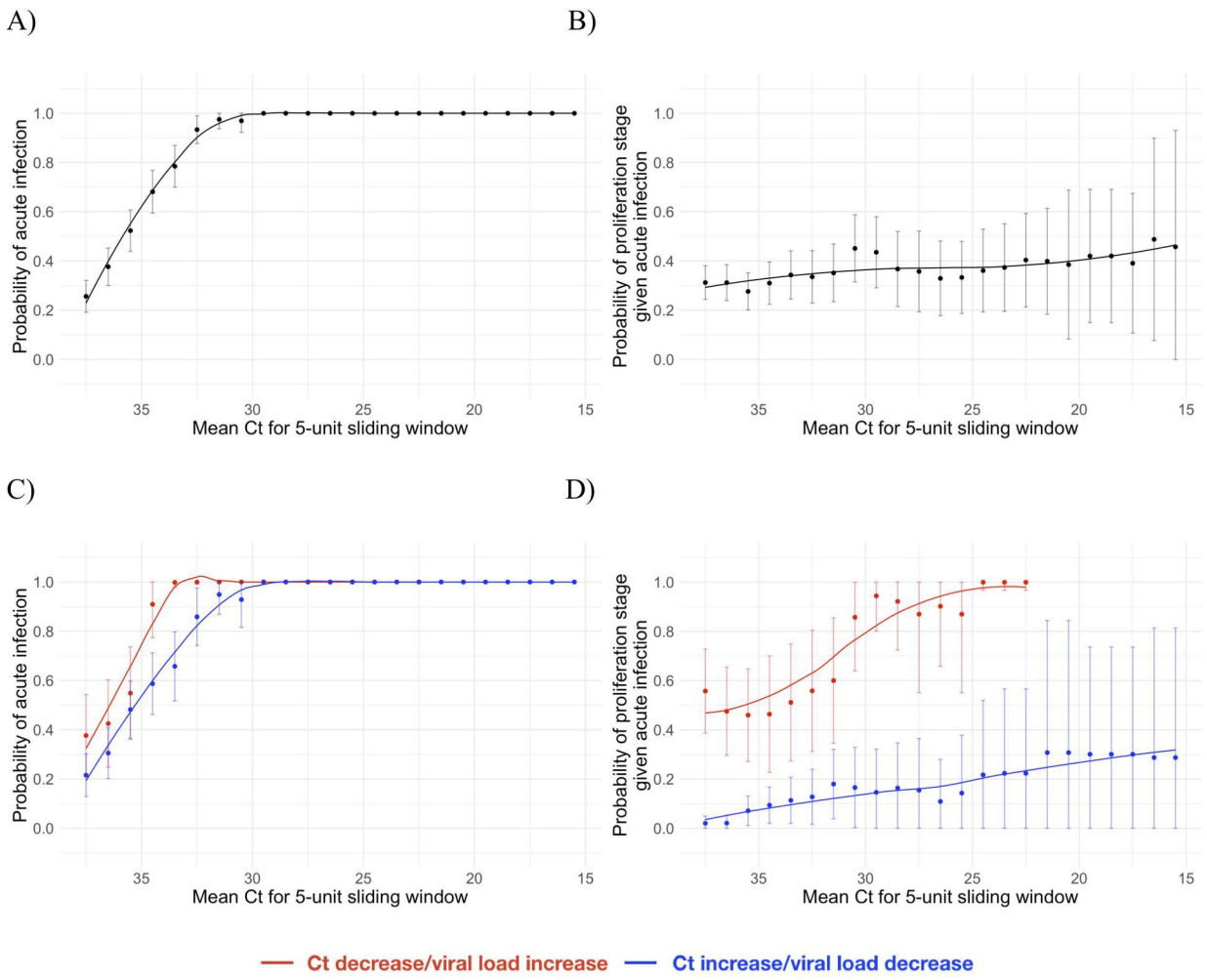

Fig 4. Relationship between single/paired cycle threshold (Ct) values and infection stage. Probability that a given Ct value lying within a 5-unit window (horizontal axis) corresponds to an acute infection (A and C) or to the proliferation phase of infection assuming an acute infection (B and D). (A) and (B) depict the predictive probabilities for a single Ct value, while (C) and (D) depict the predictive probabilities for a positive test paired with a subsequent test with either lower (red) or higher (blue) Ct. The curves are locally estimated scatterplot smoothing (LOESS) curves to better visualize the patterns. Error bars represent the 90% Wald confidence interval. Underlying data are available at https://github.com/gradlab/CtTrajectories/tree/main/figure_data/Fig4 [10].

https://doi.org/10.1371/journal.pbio.3001333.g004

normally within 3 days of the first possible RT-qPCR detection, regardless of symptoms. Our findings highlight that repeated PCR tests can be used to infer the stage of a patient's infection. While a single test can inform on whether a patient is in the acute or persistent viral RNA shedding stage, a subsequent test can help identify whether viral RNA concentrations are increasing or decreasing, thus informing clinical care. For example, patients near the beginning of their infection may need to be isolated for different amounts of time than patients near the end of their infection. For patients at risk for complications, closer monitoring and more proactive treatment may be preferred for patients near the start of infection than for those who are already nearing its resolution. We also show that the effective sensitivity of pre-event screening tests declines rapidly with test turnaround time due to the rapid progression from detectability to peak viral titers. Due to the transmission risk posed by large gatherings [12], the trade-off between test speed and sensitivity must be weighed carefully. Our data offer to our knowledge the first direct measurements capable of informing such decisions.

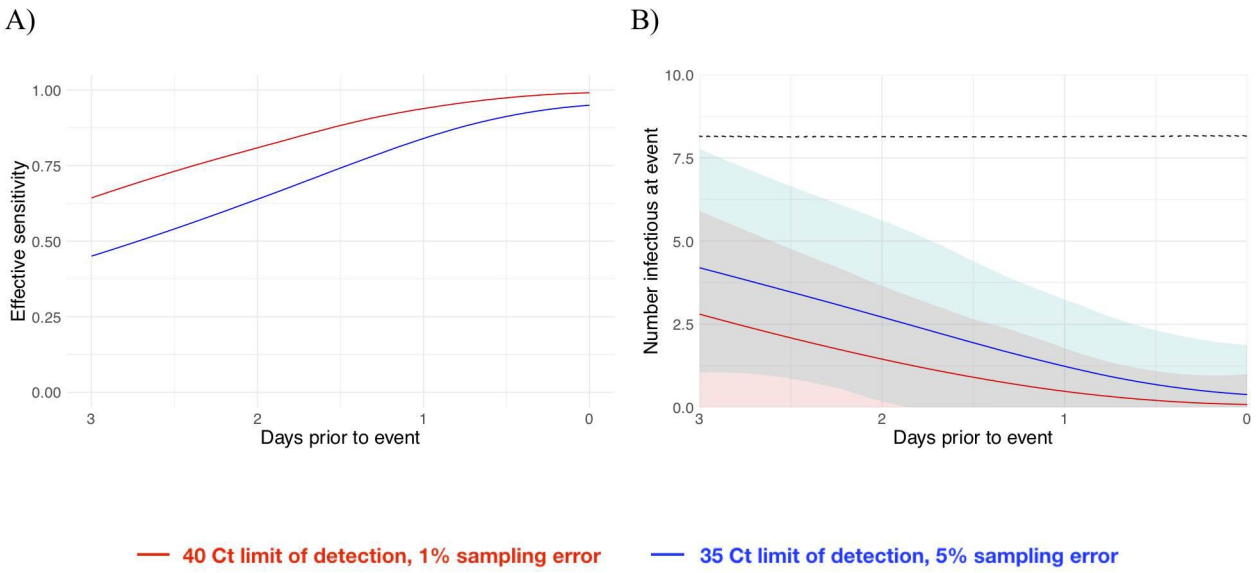

Fig 5. Effective sensitivity and expected number of infectious attendees at an event, for tests with varying sensitivity. (A) Effective sensitivity for a test with limit of detection of 40 Ct and 1% sampling error probability (red) and limit of detection of 35 Ct and 5% sampling error probability (blue). (B) Number of infectious individuals expected to attend an event of size 1,000 assuming a population prevalence of 2% infectious individuals for a test with limit of detection of 40 Ct and 1% sampling error probability (red) and limit of detection of 35 Ct and 5% sampling error probability (blue). Shaded bands represent 90% prediction intervals generated from the quantiles of 1,000 simulated events and capture uncertainty both in the number of infectious individuals who would arrive at the event in the absence of testing and in the probability that the test successfully identifies infectious individuals. The dashed line depicts the expected number of infectious individuals who would attend the gathering in the absence of testing. Underlying data are available at https://github.com/gradlab/CtTrajectories/tree/main/figure_data/Fig5 [10].

https://doi.org/10.1371/journal.pbio.3001333.g005

Our findings on the duration of SARS-CoV-2 viral RNA shedding expand on and agree with previous studies [13–15] and with observations that peak Ct does not differ substantially between symptomatic and asymptomatic individuals [3]. While previous studies have largely relied on serial sampling of admitted hospital patients, our study used prospective sampling of ambulatory infected individuals to characterize complete viral dynamics for the presymptomatic stage and for individuals who did not report symptoms. This allowed us to assess differences between the viral RNA proliferation and clearance stages for individuals with and without reported symptoms. The similarity in the early-infection viral RNA dynamics for symptomatic and asymptomatic individuals underscores the need for SARS-CoV-2 screening regardless of symptoms. The progression from a negative test to a peak Ct value 2–4 days later aligns with modeling assumptions made in various studies [5,16] to evaluate the potential effectiveness of frequent rapid testing programs, strengthening the empirical bases for their findings. Taken together, the dynamics of viral RNA shedding substantiate the need for frequent population-level SARS-CoV-2 screening and a greater availability of diagnostic tests.

The statistical model we developed to infer the viral trajectory parameters is phenomenological: It assumes an exponential increase in viral RNA concentration followed by an exponential decay but does not explicitly encode a biological mechanism leading to these exponential rates and the transition between them. Similar phenomenological models have been used to study the viral dynamics of HIV [17]. More biologically explicit mechanistic models have been used to study SARS-CoV-2 [18,19], but these remain in the early stages of development due to the limited amount of data available to inform such models. Since our primary interest is in the public health implications of SARS-CoV-2 viral trajectories with different magnitudes and durations, a phenomenological model is suitable and has the advantage of being straightforward to implement. The data presented here could be used to parameterize

detailed mechanistic models as well, from which further biological insights about SARS-CoV-2 might be gained.

Our findings are limited for several reasons. The sample size is small, especially with respect to symptomatic acutely infected individuals. The cohort does not constitute a representative sample from the population, as it was a predominantly male, healthy, young population inclusive of professional athletes. Viral trajectories may differ for individuals who have been vaccinated or who have been infected with different SARS-CoV-2 variants, which we were unable to assess due to the time frame of our study. Some of the trajectories were sparsely sampled, limiting the precision of our posterior estimates. Symptom reporting was imperfect, particularly after initial evaluation, as follow-up during the course of the disease was not systematic for all individuals. As with all predictive tests, the probabilities that link Ct values with infection stages (Fig 4) pertain to the population from which they were calibrated and do not necessarily generalize to other populations for which the prevalence of infection and testing protocols may differ. Still, we anticipate that the central patterns will hold across populations: first, that low Ct values (<30) strongly predict acute infection and, second, that a follow-up test collected within 2 days of an initial positive test can substantially help to discern whether a patients are closer to the beginning or the end of their infection. Our study did not test for the presence of infectious virus, though previous studies have documented a close inverse correlation between Ct values and culturable virus [11]. Our assessment of pre-event testing assumed that individuals become infectious immediately upon passing a threshold and that this threshold is the same for the proliferation and for the clearance phase. In reality, the threshold for infectiousness is unlikely to be at a fixed viral concentration for all individuals and may be at a higher Ct/lower viral concentration during the proliferation stage than during the clearance stage. Further studies that measure culturable virus during the various stages of infection and that infer infectiousness based on contact tracing combined with prospective longitudinal testing will help to clarify the relationship between viral concentration and infectiousness.

To manage the spread of SARS-CoV-2, we must develop novel technologies and find new ways to extract more value from the tools that are already available. Our results suggest that integrating the quantitative viral RNA trajectory into algorithms for clinical management could offer benefits. The ability to chart patients' progress through their infection underpins our ability to provide appropriate clinical care and to institute effective measures to reduce the risk of onward transmission. Marginally more sophisticated diagnostic and screening algorithms may greatly enhance our ability to manage the spread of SARS-CoV-2 using tests that are already available.

Supporting information

S1 Fig. Distribution of intervals between consecutive tests. Histogram of the proportion of consecutive tests that are within n days of one another up to $n = 12$ days. Only 12 of 2,343 intervals (0.05%) exceeded 12 days. Underlying data are available at https://github.com/gradlab/CtTrajectories/tree/main/figure_data/FigS1.
(PDF)

S2 Fig. Observed Ct values from the study participants (1/4). Points depict observed Ct values, which are connected with lines to better visualize patterns. Individuals with presumed acute infections are in red. All others are in black. Underlying data are available at https://github.com/gradlab/CtTrajectories/tree/main/data.
(PDF)

S3 Fig. Observed Ct values from the study participants (2/4). Points depict observed Ct values, which are connected with lines to better visualize patterns. Individuals with presumed acute infections are in red. All others are in black. Underlying data are available at https://github.com/gradlab/CtTrajectories/tree/main/data.
(PDF)

S4 Fig. Observed Ct values from the study participants (3/4). Points depict observed Ct values, which are connected with lines to better visualize patterns. Individuals with presumed acute infections are in red. All others are in black. Underlying data are available at https://github.com/gradlab/CtTrajectories/tree/main/data.
(PDF)

S5 Fig. Observed Ct values from the study participants (4/4). Points depict observed Ct values, which are connected with lines to better visualize patterns. Individuals with presumed acute infections are in red. All others are in black. Underlying data are available at https://github.com/gradlab/CtTrajectories/tree/main/data.
(PDF)

S6 Fig. A theoretical Ct trajectory. E[Ct] is the expected Ct value on a given day. The Ct begins at the limit of detection, then declines from the time of infection (t_o) to the peak at χ cycles below the limit of detection at time t_p. The Ct then rises again to the limit of detection after t_r days. The model incorporating these parameter values used to generate this piecewise curve is given in the equation for E[Ct(t)] in S1 Text (Supplemental Methods, under the heading "Model fitting").
(PDF)

S7 Fig. Schematics illustrating calculations for effective sensitivity for the expected number of infectious attendees at a gathering, given a pre-gathering test. (A) To calculate the effective sensitivity of a test intended to screen infectious individuals before a gathering, we first drew 1,000 viral trajectories as defined by the peak Ct, proliferation time, and clearance time from the fitted model (step 1, with 3 draws illustrated in red, green, and blue). We restricted to only individuals with viral concentrations above the infectiousness threshold (here the threshold is at Ct = 30, requiring us to omit the fourth entry). Then, we assigned detectability onset times—i.e., the times at which the trajectories could first be detected by PCR with limit of detection at 40 Ct—according to a standard uniform distribution, ensuring that the trajectories surpassed the infectiousness threshold at some point during the gathering (step 2). The onset times are depicted as colored dots. Finally, for a test administered some span of time prior to the event, we calculated the fraction of these infections the test would detect—this is the effective sensitivity (step 3). For a test administered at the time marked by the vertical black bar, the green trajectory would be detected by both PCR and a rapid test, the red trajectory would be detected by PCR but not a rapid test, and the blue trajectory would not be detected by either test. (B) To calculate the number of people who would arrive at a gathering while infectious, we performed a similar procedure. First, given a gathering size N and prevalence of PCR-detectable individuals p, we drew η trajectories from the fitted model where $\eta \sim \text{Binomial}(N, p)$. Three such draws are depicted in step 1; note that, here, the only requirement was that the individuals were detectable (not necessarily infectious) at the time of the gathering, and so the previously omitted value could now be chosen. Then, as before, detectability onset times (colored dots) were drawn from a uniform distribution ensuring that the individuals were PCR-detectable at the time of the gathering (2). Finally, in step 3, the number of infectious individuals who would attend the gathering in the absence of a pre-gathering test were counted (in this case just the blue trajectory) as well as the number of

individuals who would attend the event given a pre-gathering test. Here, the blue trajectory would be detected by a PCR test but not a rapid test at the test time depicted by the vertical black bar. The purple trajectory would be detected by both a rapid test and a PCR test, yet it would not have been infectious at the gathering (in fact, this trajectory never surpasses the infectiousness threshold depicted here). The green trajectory would not be detected by either test but also would not have arrived at the gathering while infectious since it has a relatively late onset time. Repeating this procedure for many simulated gatherings gives an estimate of the expected number of infectious people who would arrive at a gathering given a pre-gathering testing protocol.
(PDF)

S8 Fig. Mean peak Ct value and distributions of the proliferation stage, clearance stage, and acute infection duration for individuals with acute infections. Posterior distributions obtained from 10,000 posterior draws from the distributions for peak Ct value (A), duration of the proliferation stage (infection detection to peak Ct) (B), duration of the clearance stage (peak Ct to resolution of acute RNA shedding) (C), and total duration of acute shedding (D) across the 46 individuals with a verified infection. The mean Ct trajectory corresponding to the mean values for peak Ct, proliferation duration, and clearance duration is depicted in (E) (solid lines), where shading depicts the 90% credible interval. Underlying data are available at https://github.com/gradlab/CtTrajectories/tree/main/output/params_df_combined.csv.
(PDF)

S9 Fig. Posterior peak Ct value distributions for the 46 individuals with acute infections. Underlying data are available at https://github.com/gradlab/CtTrajectories/tree/main/output/params_df_split.csv.
(PDF)

S10 Fig. Posterior distributions for the duration of the proliferation stage for 46 individuals with acute infections. Underlying data are available at https://github.com/gradlab/CtTrajectories/tree/main/output/params_df_split.csv.
(PDF)

S11 Fig. Posterior distributions for the clearance stage duration for 46 individuals with acute infections. Underlying data are available at https://github.com/gradlab/CtTrajectories/tree/main/output/params_df_split.csv.
(PDF)

S12 Fig. Best-fit Ct trajectories for the 46 individuals with acute infections. Thin grey lines depict 500 sampled trajectories. Points represent the observed data, with symptomatic individuals represented in red and asymptomatic individuals in blue. Underlying data are available at https://github.com/gradlab/CtTrajectories/tree/main/output/params_df_split.csv (lines) and https://github.com/gradlab/CtTrajectories/tree/main/data (points).
(PDF)

S13 Fig. Individual-level peak Ct value and distribution of the proliferation stage, clearance stage, and acute infection duration. Histograms (grey bars) of 10,000 posterior draws from the distributions for peak Ct value (A), time from onset to peak (B), time from peak to recovery (C), and total duration of infection (D) across the 46 individuals with an acute infection. Grey curves are kernel density estimators to more clearly exhibit the shape of the histogram. Black curves represent the best-fit normal (A) or gamma (B–D) distributions to the histograms. The duration of infection is the sum of the time from onset to peak and the time from peak to recovery. The best-fit normal distribution to the posterior peak Ct value

distribution had mean 22.3 and standard deviation 4.2. The best-fit gamma distribution to the proliferation stage duration had shape parameter 2.3 and inverse scale parameter 0.7. The best-fit gamma distribution to the clearance stage duration had shape parameter 2.4 and inverse scale parameter 0.3. The best-fit gamma distribution to the total duration of infection had shape parameter 4.3 and inverse scale parameter 0.4. Alternatively, the proliferation, clearance, and total duration of infection distributions can be summarized as log-normal distributions. The best-fit log-normal distribution to the proliferation stage duration had location parameter $\mu = 0.93$ and scale parameter $\sigma = 0.82$. The best-fit log-normal distribution to the clearance stage duration had location parameter $\mu = 1.9$ and scale parameter $\sigma = 0.83$. The best-fit log-normal distribution to the total duration of infection had location parameter $\mu = 2.3$ and scale parameter $\sigma = 0.53$. Underlying data are available at https://github.com/gradlab/CtTrajectories/tree/main/output/params_df_split.csv.
(PDF)

S14 Fig. Peak viral concentration and overall posterior viral concentration trajectories in terms of genome equivalents per milliliter. Posterior peak viral concentration distribution for symptomatic (red) and asymptomatic (blue) individuals (A) and for all individuals combined (B). Underlying data are available at https://github.com/gradlab/CtTrajectories/tree/main/output/params_df_split.csv (A) and https://github.com/gradlab/CtTrajectories/tree/main/output/params_df_combined.csv (B).
(PDF)

S15 Fig. Ct values from the Yale and Florida labs. Points depict the Ct values for SARS-CoV-2 nasal swab samples that were tested in both the Florida and Yale labs. Ct values from Florida represent Target 1 (ORF1ab) on the Roche cobas system, and Ct values from Yale represent N1 in the Yale multiplex assay. The solid black line depicts the best-fit linear regression (intercept = −6.25, slope = 1.34, $R^2 = 0.86$). The dashed black line marks the 1–1 line where the points would be expected to fall if the 2 labs produced identical results. Underlying data are available at https://github.com/gradlab/CtTrajectories/tree/main/figure_data/FigS15.
(PDF)

S16 Fig. Residuals from the Yale/Florida Ct regression. Points depict the residual after removing the best-fit linear trend in the relationship between the Yale and Florida Ct values. Underlying data are available at https://github.com/gradlab/CtTrajectories/tree/main/figure_data/FigS16.
(PDF)

S17 Fig. Quantile–quantile plot of the residuals from the Yale/Florida Ct regression. The residuals were standardized (by subtracting the mean of all residuals from each residual and then dividing each residual by the standard deviation of all residuals) before being compared with the theoretical quantiles of a normal distribution with mean 0 and standard deviation 1. The points depict the empirical quantiles of the data points, and the line depicts where the points would be expected to fall if they were drawn from a standard normal distribution. Underlying data are available at https://github.com/gradlab/CtTrajectories/tree/main/figure_data/FigS17.
(PDF)

S18 Fig. Effective sensitivity and expected number of infectious attendees at a gathering, given a pre-gathering test and varying infectiousness thresholds. (A and C) Effective sensitivity and (B and D) number of infectious individuals expected to attend a gathering of size 1,000 assuming a population prevalence of 2% infectious individuals and a test with limit of

detection of 40 Ct and 1% sampling error probability (red) and a test with limit of detection of 35 Ct and 5% sampling error probability (blue) administered between 0 and 3 days before the gathering. For (A) and (B) individuals are assumed to be infectious when their Ct value is below 35. For (C) and (D) individuals are assumed to be infectious when their Ct value is below 20. Shaded bands represent 90% prediction intervals generated from the quantiles of 1,000 simulated events and capture uncertainty both in the number of infectious individuals who would arrive at the event in the absence of testing and in the probability that the test successfully identifies infectious individuals. The dashed lines in (B) and (D) depict the expected number of infectious individuals who would attend the gathering in the absence of testing. Setting the infectiousness threshold at higher viral concentration (20 Ct versus 35 Ct) makes it less likely that an individual will become infectious at all during the course of their acute infection, leading to the lower expected number of infectious individuals at the gathering in (D) versus (B). Underlying data are available at https://github.com/gradlab/CtTrajectories/tree/main/figure_data/FigS18.
(PDF)

S19 Fig. Illustration of why effective sensitivity declines more sharply with testing delays for high versus low infectiousness thresholds. For a given viral trajectory conditioned on infectiousness during a gathering, there is a wider range of possible proliferation onset times when the infectiousness threshold is low (blue) versus when the infectiousness threshold is high (red). Additionally, the range of possible onset times for the low infectiousness threshold versus the high infectiousness threshold is skewed to the left since the clearance time is longer than the proliferation time. Because of this, a low infectiousness threshold makes it easier for a pre-gathering test to pick up a trajectory that would be infectious at the time of the gathering. Conversely, a high infectiousness threshold shortens the window of possible onset times that guarantee infectiousness during the gathering, making it more difficult for a pre-gathering test to detect the trajectory. This is reflected in the steeper decline in the effective sensitivity for a high infectiousness threshold (Ct = 20) than for a low infectiousness threshold (Ct = 35) (see S18A and S18C Fig).
(PDF)

S1 Table. Standard curve relationship between genome equivalents and Ct values. Synthetic T7 RNA transcripts corresponding to a 1,363-base-pair segment of the SARS-CoV-2 nucleocapsid gene were serially diluted from 10^6 to 10^0 and evaluated in duplicate with RT-qPCR. The best-fit linear regression of the average Ct on the log10-transformed standard values had slope −3.60971 and intercept 40.93733 ($R^2 = 0.99$).
(PDF)

S2 Table. Viral dynamic parameters for sensitivity analysis 1, omitting person 3047.
(PDF)

S3 Table. Viral dynamic parameters for sensitivity analysis 2, assuming 95% PCR sensitivity or a 5% probability of false negative.
(PDF)

S4 Table. Viral dynamic parameters for sensitivity analysis 3, removing the upper bounds for the proliferation and clearance times.
(PDF)

S5 Table. Viral dynamic parameters for sensitivity analysis 4, using "low" priors for the proliferation and clearance times (mean 3.5 and 7.5 days, respectively).
(PDF)

S6 Table. Viral dynamic parameters for sensitivity analysis 5, using "high" priors for the proliferation and clearance times (mean 10.5 days and 22.5 days, respectively).
(PDF)

S1 Text. Supplemental methods.
(PDF)

Acknowledgments

We thank the NBA, the National Basketball Players Association (NBPA), and all of the study participants who are committed to applying what they learned from sports towards enhancing public health. In particular, we thank D. Weiss of the NBA for his continuous support and leadership. We are appreciative of the discussions from the COVID-19 Sports and Society Working Group. We also thank D. Larremore for comments on the manuscript, J. Hay and R. Niehus for suggestions on the statistical approach, and P. Jack and S. Taylor for laboratory support.

Author Contributions

Conceptualization: Stephen M. Kissler, Joseph R. Fauver, Christina Mack, Scott W. Olesen, Caroline Tai, John DiFiori, Nathan D. Grubaugh, Yonatan H. Grad.

Data curation: Joseph R. Fauver, Christina Mack, Caroline Tai, Kristin Y. Shiue, Chaney C. Kalinich, Sarah Jednak, Isabel M. Ott, Jay Wohlgemuth, James Weisberger, John DiFiori, Deverick J. Anderson, Jimmie Mancell, David D. Ho, Nathan D. Grubaugh.

Formal analysis: Stephen M. Kissler, Joseph R. Fauver, Scott W. Olesen, Nathan D. Grubaugh.

Funding acquisition: Nathan D. Grubaugh, Yonatan H. Grad.

Investigation: Stephen M. Kissler, Joseph R. Fauver, Christina Mack, Caroline Tai, Chaney C. Kalinich, Sarah Jednak, Nathan D. Grubaugh, Yonatan H. Grad.

Methodology: Stephen M. Kissler, Joseph R. Fauver, Scott W. Olesen, Caroline Tai, Kristin Y. Shiue, Isabel M. Ott, Chantal B. F. Vogels, Jay Wohlgemuth, James Weisberger, John DiFiori, Deverick J. Anderson, Jimmie Mancell, David D. Ho, Nathan D. Grubaugh, Yonatan H. Grad.

Project administration: Nathan D. Grubaugh, Yonatan H. Grad.

Resources: Nathan D. Grubaugh, Yonatan H. Grad.

Software: Stephen M. Kissler, Scott W. Olesen.

Supervision: Nathan D. Grubaugh, Yonatan H. Grad.

Validation: Stephen M. Kissler.

Visualization: Scott W. Olesen.

Writing – original draft: Stephen M. Kissler, Joseph R. Fauver, Christina Mack, Caroline Tai, John DiFiori, Nathan D. Grubaugh, Yonatan H. Grad.

Writing – review & editing: Stephen M. Kissler, Joseph R. Fauver, Christina Mack, Caroline Tai, Kristin Y. Shiue, Chaney C. Kalinich, Sarah Jednak, Isabel M. Ott, Chantal B. F. Vogels, Jay Wohlgemuth, James Weisberger, John DiFiori, Deverick J. Anderson, Jimmie Mancell, David D. Ho, Nathan D. Grubaugh, Yonatan H. Grad.

References

1. Furukawa NW, Brooks JT, Sobel J. Evidence supporting transmission of severe acute respiratory syndrome coronavirus 2 while presymptomatic or asymptomatic. Emerg Infect Dis. 2020; 26(7):e201595. https://doi.org/10.3201/eid2607.201595 PMID: 32364890
2. Tom MR, Mina MJ. To interpret the SARS-CoV-2 test, consider the cycle threshold value. Clin Infect Dis. 2020; 71(16):2252–4. https://doi.org/10.1093/cid/ciaa619 PMID: 32435816
3. Walsh KA, Jordan K, Clyne B, Rohde D, Drummond L, Byrne P, et al. SARS-CoV-2 detection, viral load and infectivity over the course of an infection. J Infect. 2020; 81(3):357–71. https://doi.org/10.1016/j.jinf.2020.06.067 PMID: 32615199
4. Wyllie AL, Fournier J, Casanovas-Massana A, Campbell M, Tokuyama M, Vijayakumar P, et al. Saliva or nasopharyngeal swab specimens for detection of SARS-CoV-2. N Engl J Med. 2020; 383(13):1283–6. https://doi.org/10.1056/NEJMc2016359 PMID: 32857487
5. Larremore DB, Wilder B, Lester E, Shehata S, Burke JM, Hay JA, et al. Test sensitivity is secondary to frequency and turnaround time for COVID-19 surveillance. Sci Adv. 2021; 7(1):eabd5393. https://doi.org/10.1126/sciadv.abd5393 PMID: 33219112
6. Mack CD, DiFiori J, Tai CG, Shiue KY, Grad YH, Anderson DJ, et al. SARS-CoV-2 transmission risk among National Basketball Association players, staff, and vendors exposed to individuals with positive test results after COVID-19 recovery during the 2020 regular and postseason. JAMA Intern Med. 2021 Apr 22. https://doi.org/10.1001/jamainternmed.2021.2114 PMID: 33885715
7. Xiao AT, Tong YX, Zhang S. Profile of RT-PCR for SARS-CoV-2: a preliminary study from 56 COVID-19 patients. Clin Infect Dis. 2020; 71(16):2249–51. https://doi.org/10.1093/cid/ciaa460 PMID: 32306036
8. Cleary B, Hay JA, Blumenstiel B, Harden M, Cipicchio M, Bezney J, et al. Using viral load and epidemic dynamics to optimize pooled testing in resource-constrained settings. Science Translational Medicine. 2021 apr 14. https://doi.org/10.1126/scitranslmed.abf1568 PMID: 32511487
9. Carpenter B, Gelman A, Hoffman MD, Lee D, Goodrich B, Betancourt M, et al. Stan: a probabilistic programming language. J Stat Softw. 2017; 76(1). https://doi.org/10.18637/jss.v076.i01
10. Kissler S. gradlab/CtTrajectories. Zenodo. 2021 Jun 17. https://doi.org/10.5281/zenodo.4977246
11. Singanayagam A, Patel M, Charlett A, Lopez Bernal J, Saliba V, Ellis J, et al. Duration of infectiousness and correlation with RT-PCR cycle threshold values in cases of COVID-19, England, January to May 2020. Euro Surveill. 2020; 25(32):2001483. https://doi.org/10.2807/1560-7917.ES.2020.25.32.2001483 PMID: 32794447
12. Cevik M, Marcus J, Buckee C, Smith T. SARS-CoV-2 transmission dynamics should inform policy. SSRN Electron J. 2020 Sep 21. https://doi.org/10.1093/cid/ciaa1442 PMID: 32964919
13. Cevik M, Tate M, Lloyd O, Enrico Maraolo A, Schafers J, Ho A. SARS-CoV-2, SARS-CoV, and MERS-CoV viral load dynamics, duration of viral shedding, and infectiousness: a systematic review and meta-analysis. The Lancet Microbe. 2020 19 Nov. https://doi.org/10.1016/S2666-5247(20)30172-5 PMID: 33521734
14. Houlihan C, Vora N, Byrne T, Lewer D, Heaney J, Moore DA, et al. SARS-CoV-2 virus and antibodies in front-line Health Care Workers in an acute hospital in London: preliminary results from a longitudinal study. medRxiv. 2020 Jun 9. https://doi.org/10.1101/2020.06.08.20120584
15. Lee S, Kim T, Lee E, Lee C, Kim H, Rhee H, et al. Clinical course and molecular viral shedding among asymptomatic and symptomatic patients with SARS-CoV-2 infection in a community treatment center in the Republic of Korea. JAMA Intern Med. 2020; 180(11):1447–52. https://doi.org/10.1001/jamainternmed.2020.3862 PMID: 32780793
16. Paltiel AD, Zheng A, Walensky RP. Assessment of SARS-CoV-2 screening strategies to permit the safe reopening of college campuses in the United States. JAMA Netw Open. 2020; 3(7):e2016818. https://doi.org/10.1001/jamanetworkopen.2020.16818 PMID: 32735339
17. Huang Y, Dagne GA, Zhou S, Wang Z. Piecewise mixed-effects models with skew distributions for evaluating viral load changes: a Bayesian approach. Stat Methods Med Res. 2015; 24(6):730–46. https://doi.org/10.1177/0962280211426184 PMID: 22045781
18. Ke R, Zitzmann C, Ribeiro RM, Perelson AS. Kinetics of SARS-CoV-2 infection in the human upper and lower respiratory tracts and their relationship with infectiousness. medRxiv. 2020 Sep 27. https://doi.org/10.1101/2020.09.25.20201772
19. Goyal A, Reeves DB, Cardozo-Ojeda EF, Schiffer JT, Mayer BT. Viral load and contact heterogeneity predict SARS-CoV-2 transmission and super-spreading events. eLife. 2021 Feb 23. https://doi.org/10.7554/eLife.63537 PMID: 33620317

RESEARCH ARTICLE SUMMARY

CORONAVIRUS

Estimating infectiousness throughout SARS-CoV-2 infection course

Terry C. Jones[1,2,3]†, Guido Biele[4,5]†, Barbara Mühlemann[1,2], Talitha Veith[1,2], Julia Schneider[1,2], Jörn Beheim-Schwarzbach[1], Tobias Bleicker[1], Julia Tesch,[1] Marie Luisa Schmidt[1], Leif Erik Sander[6], Florian Kurth[6,7], Peter Menzel[8], Rolf Schwarzer[8], Marta Zuchowski[8], Jörg Hofmann[8], Andi Krumbholz[9,10], Angela Stein[8], Anke Edelmann[8], Victor Max Corman[1,2], Christian Drosten[1,2]*

INTRODUCTION: Although post facto studies have revealed the importance of severe acute respiratory syndrome coronavirus 2 (SARS-CoV-2) transmission from presymptomatic, asymptomatic, and mildly symptomatic (PAMS) cases, the virological basis of their infectiousness remains largely unquantified. The reasons for the rapid spread of variant lineages of concern, such as B.1.1.7, have yet to be fully determined.

RATIONALE: Viral load (viral RNA concentration) in patient samples and the rate of isolation success of virus from clinical specimens in cell culture are the clinical parameters most directly relevant to infectiousness and hence to transmission. To increase our understanding of the infectiousness of SARS-CoV-2, especially in PAMS cases and those infected with the B.1.1.7 variant, we analyzed viral load data from 25,381 German cases, including 9519 hospitalized patients, 6110 PAMS cases from walk-in test centers, 1533 B.1.1.7 variant infections, and the viral load time series of 4434 (mainly hospitalized) patients. Viral load results were then combined with estimated cell culture isolation probabilities, producing a clinical proxy estimate of infectiousness.

RESULTS: PAMS subjects had, at the first positive test, viral loads and estimated infectiousness only slightly less than hospitalized patients. Similarly, children were found to have mean viral loads only slightly lower (0.5 $\log_{10}$ units or less) than those of adults and ~78% of the adult peak cell culture isolation probability. Eight percent of first-positive viral loads were 10^9 copies per swab or higher, across a wide age range (mean 37.6 years, standard deviation 13.4 years), representing a likely highly infectious minority, one-third of whom were PAMS. Relative to non-B.1.1.7 cases, patients with the B.1.1.7 variant had viral loads that were higher by a factor of 10 and estimated cell culture infectivity that was higher by a factor of 2.6. Similar ranges of viral loads from B.1.1.7 and B.1.177 samples were shown to be capable of causing infection in Caco-2 cell culture. A time-course analysis estimates that a peak viral load of $10^{8.1}$ copies per swab is reached 4.3 days after onset of shedding and shows that, across the course of infection, hospitalized patients have slightly higher viral loads than nonhospitalized cases, who in turn have viral loads slightly higher than PAMS cases. Higher viral loads are observed in first-positive tests of PAMS subjects, likely as a result of systematic earlier testing. Mean culture isolation probability declines to 0.5 at 5 days after peak viral load and to 0.3 at 10 days after peak viral load. We estimate a rate of viral load decline of 0.17 $\log_{10}$ units per day, which, combined with reported estimates of incubation time and time to loss of successful cell culture isolation, suggests that viral load peaks 1 to 3 days before onset of symptoms (in symptomatic cases).

CONCLUSION: PAMS subjects who test positive at walk-in test centers can be expected to be approximately as infectious as hospitalized patients. The level of expected infectious viral shedding of PAMS people is of high importance because they are circulating in the community at the time of detection of infection. Although viral load and cell culture infectivity cannot be translated directly to transmission probability, it is likely that the rapid spread of the B.1.1.7 variant is partly attributable to higher viral load in these cases. Easily measured virological parameters can be used, for example, to estimate transmission risk from different groups (by age, gender, clinical status, etc.), to quantify variance, to show differences in virus variants, to highlight and quantify overdispersion, and to inform quarantine, containment, and elimination strategies. ■

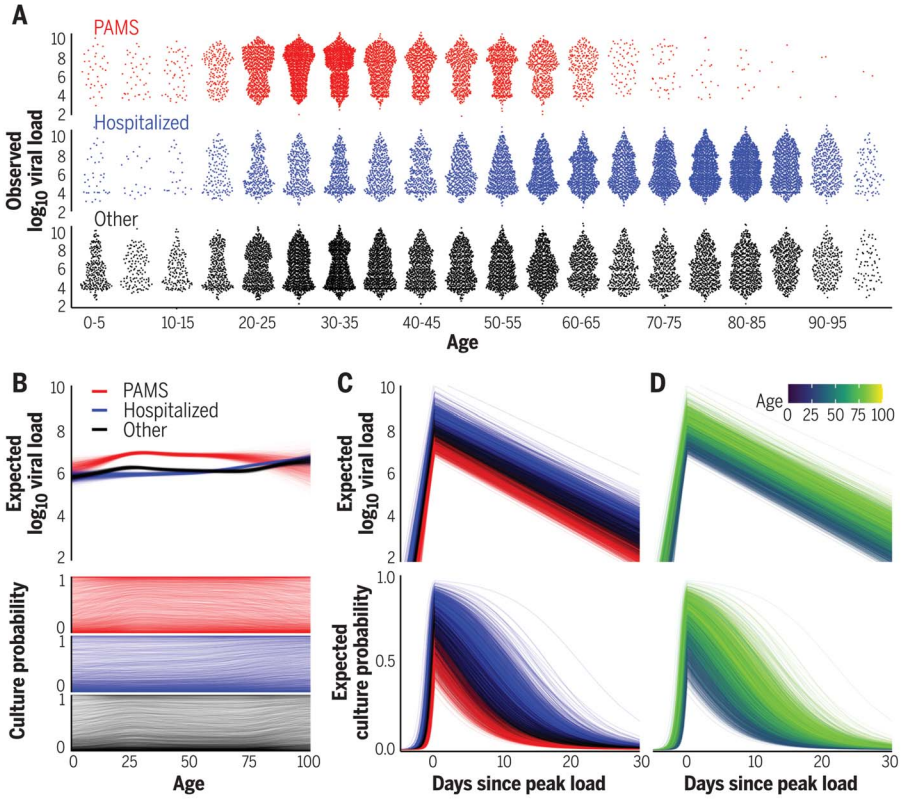

Viral load and cell culture infectivity in 25,381 SARS-CoV-2 infections. (**A**) Viral loads in presymptomatic, asymptomatic, and mildly symptomatic cases (PAMS; red), hospitalized patients (blue), and other subjects (black). (**B**) Expected first-positive viral load and cell culture isolation probability, colored as in (A). (**C**) Temporal estimation with lines representing patients, colored as in (A). (**D**) As in (C), but colored by age.

The list of author affiliations is available in the full article online.
*Corresponding author. Email: christian.drosten@charite.de
†These authors contributed equally to this work.

Cite this article as T. C. Jones *et al.*, *Science* **373**, eabi5273 (2021). DOI: 10.1126/science.abi5273

READ THE FULL ARTICLE AT
https://doi.org/10.1126/science.abi5273

RESEARCH ARTICLE

CORONAVIRUS

Estimating infectiousness throughout SARS-CoV-2 infection course

Terry C. Jones[1,2,3]†, Guido Biele[4,5]†, Barbara Mühlemann[1,2], Talitha Veith[1,2], Julia Schneider[1,2], Jörn Beheim-Schwarzbach[1], Tobias Bleicker[1], Julia Tesch[1], Marie Luisa Schmidt[1], Leif Erik Sander[6], Florian Kurth[6,7], Peter Menzel[8], Rolf Schwarzer[8], Marta Zuchowski[8], Jörg Hofmann[8], Andi Krumbholz[9,10], Angela Stein[8], Anke Edelmann[8], Victor Max Corman[1,2], Christian Drosten[1,2]*

Two elementary parameters for quantifying viral infection and shedding are viral load and whether samples yield a replicating virus isolate in cell culture. We examined 25,381 cases of severe acute respiratory syndrome coronavirus 2 (SARS-CoV-2) in Germany, including 6110 from test centers attended by presymptomatic, asymptomatic, and mildly symptomatic (PAMS) subjects, 9519 who were hospitalized, and 1533 B.1.1.7 lineage infections. The viral load of the youngest subjects was lower than that of the older subjects by 0.5 (or fewer) $\log_{10}$ units, and they displayed an estimated ~78% of the peak cell culture replication probability; in part this was due to smaller swab sizes and unlikely to be clinically relevant. Viral loads above 10^9 copies per swab were found in 8% of subjects, one-third of whom were PAMS, with a mean age of 37.6 years. We estimate 4.3 days from onset of shedding to peak viral load ($10^{8.1}$ RNA copies per swab) and peak cell culture isolation probability (0.75). B.1.1.7 subjects had mean $\log_{10}$ viral load 1.05 higher than that of non-B.1.1.7 subjects, and the estimated cell culture replication probability of B.1.1.7 subjects was higher by a factor of 2.6.

Respiratory disease transmission is highly context-dependent and difficult to quantify or predict at the individual level. This is especially the case when transmission from presymptomatic, asymptomatic, and mildly symptomatic (PAMS) subjects is frequent, as with severe acute respiratory syndrome coronavirus 2 (SARS-CoV-2) (*1*–*8*). Transmission is therefore typically inferred from population-level information and summarized as a single overall average, known as the basic reproductive number, R_0. Although R_0 is an essential and critical parameter for understanding and managing population-level disease dynamics, it is a resultant, downstream characterization of transmission. With regard to SARS-CoV-2, many finer-grained upstream questions regarding infectiousness remain unresolved or unaddressed. Three categories of uncertainty are (i) differences in infectiousness among individuals or groups such as PAMS subjects, according to age, gender, vaccination status, etc.; (ii) timing and degree of peak infectiousness, timing of loss of infectiousness, rates of infectiousness increase and decrease, and how these relate to onset of symptoms (when present); and (iii) differences in infectiousness due to inherent properties of virus variants.

These interrelated issues can all be addressed through the combined study of two clinical virological parameters: the viral load (viral RNA concentration) in patient samples, and virus isolation success in cell culture trials. Viral load and cell culture infectivity cannot be translated directly to in vivo infectiousness, and the impact of social context and behavior on transmission is very high; nonetheless, these quantifiable parameters can generally be expected to be those most closely associated with transmission likelihood. A strong relationship between SARS-CoV-2 viral load and transmission has been reported (*9*), comparing favorably with the situation with influenza virus, where the association is less clear (*10*, *11*).

The emergence of more transmissible SARS-CoV-2 variants, such as the B.1.1.7 lineage (UK Variant of Concern 202012/01), emphasizes the importance of correlates of shedding and transmission. The scarcity of viral load data in people with recent variants, and in PAMS subjects of all ages (*12*), is a blind spot of key importance because many outbreaks have clearly been triggered and fueled by these subjects (*2*, *13*–*17*). Viral load data from PAMS cases are rarely available, greatly reducing the number of studies with information from both symptomatic and PAMS subjects and that span the course of infections (*12*, *18*). Making matters worse, it is not possible to place positive reverse transcription polymerase chain reaction (RT-PCR) results from asymptomatic subjects in time relative to a nonexistent day of symptom onset, so these cases cannot be included in studies focused on incubation period. Additionally, viral load time courses relative to the day of symptom onset rely on patient recall, a suboptimal measure that is subject to human error and that overlooks infections from presymptomatic or asymptomatic contacts (*12*). An alternative and more fundamental parameter, the day of peak viral load, can be estimated from dated viral load time-series data, drawn from the entire period of viral load rise and fall and the full range of symptomatic statuses.

To better understand SARS-CoV-2 infectiousness, we analyzed viral load, cell culture isolation, and genome sequencing data from a diagnostic laboratory in Berlin (Charité–Universitätsmedizin Berlin Institute of Virology and Labor Berlin). We first address a set of questions regarding infectiousness at the moment of disease detection, especially in PAMS subjects whose infections were detected at walk-in community test centers. Because these people are circulating in the general community before their infections are detected, and are healthy enough to present themselves at such centers, their prevalence and shedding are of key importance to the understanding and prevention of transmission. In addition to PAMS subjects, we consider the infectiousness suggested by first-positive tests from hospitalized patients, including differences according to age, virus variant, and gender. A further set of temporal questions are then addressed by studying how infectiousness changes during the infection course. Using viral load measurements from patients with at least three RT-PCR tests, we estimate the onset of infectious viral shedding, peak viral load, and the rates of viral load increase and decline. Knowledge of these parameters enables fundamental comparisons between groups of subjects and between virus strains, and highlights the misleading impression created by viral loads from first-positive RT-PCR tests if the time of testing in the infection course is not considered.

Study composition

We examined 936,423 SARS-CoV-2 routine diagnostic RT-PCR results from 415,935 subjects aged 0 to 100 years from 24 February 2020 to 2 April 2021. Samples were collected at test centers and medical practices mostly in and around Berlin, Germany, and analyzed with LightCycler 480 and cobas 6800/8800 systems from Roche. Of all tested subjects, 25,381 (6.1%)

[1]Institute of Virology, Charité–Universitätsmedizin Berlin, corporate member of Freie Universität Berlin, Humboldt-Universität zu Berlin, and Berlin Institute of Health, 10117 Berlin, Germany. [2]German Centre for Infection Research (DZIF), partner site Charité, 10117 Berlin, Germany. [3]Centre for Pathogen Evolution, Department of Zoology, University of Cambridge, Cambridge CB2 3EJ, U.K. [4]Norwegian Institute of Public Health, 0473 Oslo, Norway. [5]University of Oslo, 0315 Oslo, Norway. [6]Department of Infectious Diseases and Respiratory Medicine, Charité–Universitätsmedizin Berlin, corporate member of Freie Universität Berlin and Humboldt-Universität zu Berlin, 10117 Berlin, Germany. [7]Department of Tropical Medicine, Bernhard Nocht Institute for Tropical Medicine, and Department of Medicine I, University Medical Centre Hamburg-Eppendorf, 20359 Hamburg, Germany. [8]Labor Berlin–Charité Vivantes GmbH, Sylter Straße 2, 13353 Berlin, Germany. [9]Institute for Infection Medicine, Christian-Albrechts-Universität zu Kiel and University Medical Center Schleswig-Holstein, Campus Kiel, 24105 Kiel, Germany. [10]Labor Dr. Krause und Kollegen MVZ GmbH, 24106 Kiel, Germany.
*Corresponding author. Email: christian.drosten@charite.de
†These authors contributed equally to this work.

Table 1. Age stratification of first-positive RT-PCR tests and viral load for 25,381 positive cases.
N, number of subjects with a positive test result; Pos. %, percentage of positive subjects; Load (SD), mean $\log_{10}$(viral load) and standard deviation; ≥3 tests, number of subjects with at least three RT-PCR test results, as used in the viral load time course analysis. Age ranges (in years) are open-closed intervals.

	All cases				PAMS cases			Hospitalized cases		
Age	*N*	Pos. %	Load (SD)	≥3 tests	*N*	Pos. %	Load (SD)	*N*	Pos. %	Load (SD)
0–5	330	1.8	5.9 (1.84)	16	36	5.1	6.6 (1.87)	32	0.9	5.6 (2.22)
5–10	185	1.8	6.0 (1.73)	12	39	6.2	6.1 (1.83)	18	1.4	5.8 (1.97)
10–15	227	2.2	6.0 (1.76)	8	51	6.9	6.4 (1.92)	22	1.4	6.0 (2.02)
15–20	643	3.0	6.3 (1.87)	39	192	5.1	6.7 (1.77)	121	2.5	6.1 (1.95)
20–25	1637	3.2	6.5 (1.89)	110	696	4.0	6.9 (1.86)	246	2.7	5.9 (1.92)
25–35	4452	3.0	6.6 (1.90)	320	1988	3.9	7.0 (1.83)	614	2.2	6.0 (1.88)
35–45	3393	2.7	6.4 (1.84)	323	1277	3.5	6.9 (1.79)	576	2.0	6.0 (1.90)
45–55	3341	3.1	6.4 (1.81)	401	1012	3.4	6.9 (1.83)	733	2.3	5.9 (1.77)
55–65	3322	2.7	6.3 (1.78)	623	674	3.0	6.8 (1.82)	1039	2.1	5.9 (1.80)
>65	7851	3.0	6.4 (1.79)	2492	145	5.8	6.8 (1.87)	3434	2.3	6.2 (1.86)

had at least one positive RT-PCR test (Table 1). Positive subjects had a mean age of 51.7 years with high standard deviation (SD) of 22.7 years, and a mean of 4.5 RT-PCR tests (SD 5.7), of which 1.7 (SD 1.4) were positive. Of the positive subjects, 4344 had tests on at least 3 days (with at least two tests positive) and were included in a time-series analysis.

We divided the 25,381 positive subjects into three groups (Fig. 1). The Hospitalized group (9519 subjects, 37.5%) included all those who tested positive in an in-patient hospitalized context at any point in their infection. The PAMS group (6110 subjects, 24.1%) included people whose first positive sample was obtained in any of 24 Berlin COVID-19 walk-in community test centers, provided they were not in the Hospitalized category. The Other group (9752 subjects, 38.4%) included everyone not in the first two categories (table S1). As Fig. 1 shows, there were relatively low numbers of young subjects in all three groups, and very few elderly PAMS subjects. The validity of the PAMS classification is supported by the fact that of the overall 6159 infections detected at walk-in test centers, only 49 subjects (0.8%) were later hospitalized. Subjects testing positive at these centers are almost certainly receiving their first positive test because they are instructed to immediately self-isolate, and our data confirm that such subjects are rarely retested: Only 4.6% of people with at least three test results had their first test at a walk-in test center. Of the 9519 subjects who were ever hospitalized, 6835 were already in hospital at the time of their first positive test. PAMS subjects had a mean age of 38.0 years (SD 13.7), typically younger than Other subjects (mean 49.1 years, SD 23.5), with Hospitalized the oldest group (mean 63.2 years, SD 20.7). Typing RT-PCR indicated that 1533 subjects were infected with a strain belonging to the B.1.1.7 lineage, as confirmed by full genomes from next-generation sequencing (see materials and methods).

First-positive viral load

Across all subjects, the mean viral load [given as $\log_{10}$(RNA copies per swab)] in the first positive-testing sample was 6.39 (SD 1.83). The PAMS subjects had viral loads higher than those of the Hospitalized subjects for ages up to 70 years, as exemplified by a 6.9 mean for PAMS compared to a 6.0 mean in Hospitalized adult subjects of 20 to 65 years. Crude comparisons of viral loads in age groups showed no substantial difference in first-positive viral load between groups of people older than 20 years (Table 1). Children and adolescents had mean first-positive viral load differences ranging between −0.49 (−0.69, −0.29) and −0.16 (−0.31, −0.01) relative to adults aged 20 to 65 (Table 2). Here and below, parameter differences between age groups show the younger value minus the older, so a negative difference indicates a lower value in the younger group. Ranges given in parentheses are 90% credible intervals.

We used a Bayesian thin-plate spline regression to estimate the relationship among age, clinical status, and viral load from the first positive RT-PCR of each subject, adjusting for gender, type of test center, and PCR system used. The Bayesian model well represents the observed data (Fig. 1B, Table 2, and fig. S1). The raw data and the Bayesian estimation (Fig. 2A) suggest consideration of subjects in three age categories: young (ages 0 to 20 years, grouped into 5-year brackets), adult (20 to 65 years), and elderly (over 65 years). We estimated an average first-positive viral load of 6.40 (6.37, 6.42) for adults and a similar mean of 6.35 (6.32, 6.39) for the elderly (Fig. 2A). Younger age groups had lower mean viral loads than adults, with the difference falling steadily from −0.50 (−0.62, −0.37) for the very youngest (0 to 5 years) to −0.18 (−0.23, −0.12) for older adolescents (15 to 20 years) (Table 2). Young age groups of PAMS subjects had lower estimated viral loads than older PAMS subjects, with differences ranging from −0.18 (−0.29, −0.07) to −0.63 (−0.96, −0.32). Among Hospitalized subjects these differences were smaller, ranging from −0.18 (−0.45, 0.07) to −0.11 (−0.22, 0.01) (Table 2 and Fig. 2B). Viral loads of subjects younger than 65 years were ~0.75 higher for PAMS subjects than for Hospitalized subjects (Fig. 2A), likely because of a systematic difference in RT-PCR test timing, discussed below.

Associating viral load with cell culture infectivity

We estimated the association between viral load and successful cell culture isolation probability (hereafter "culture probability") by combining the viral load estimated from the Bayesian regression with cell culture isolation data from our own laboratory (*19*) and from Perera *et al.* (*20*) (Fig. 2C). Across all ages, the average estimated culture probability at the time of first positive RT-PCR was 0.35 (0.01, 0.94). The mean culture probability for PAMS cases, 0.44 (0.01, 0.98), was higher than for Hospitalized cases, 0.32 (0.00, 0.92) (Fig. 2D). Comparing PAMS cases, we found differences, in particular for children aged 0 to 5 compared to adults aged 20 to 65, with average culture probabilities of 0.329 (0.003, 0.950) and 0.441 (0.008, 0.981) respectively, and a difference of −0.112 (−0.279, −0.003). Age group differences in Hospitalized cases ranged from −0.028 (−0.104, 0.009) to −0.018 (−0.055, 0) (Table 2).

First-positive viral loads are weakly bimodally distributed (Figs. 1A and 2A), which is not reflected in age-specific means. The resultant distribution includes a majority of subjects with relatively low culture probability and a minority with very high culture probability (Fig. 2E and fig. S2). The highly infectious subset includes 2228 of 25,381 positive subjects (8.78%) with a first-positive viral load of at least 9.0, corresponding to an estimated culture probability of ~0.92 to 1.0. Of these 2228 subjects, 804 (36.09%) were PAMS at the time of testing, with a mean (median) age of 37.6 (34.0) and SD of 13.4 years. PAMS subjects are overrepresented in this highly infectious group among people aged 20 to 80 years, and Hospitalized subjects are overrepresented in people aged 80 to 100 years (fig. S3).

Estimating B.1.1.7 infectiousness at first-positive test

The 1533 subjects infected with a B.1.1.7 virus in our dataset had an observed mean first-positive viral load of 7.38 (SD 1.54), which is 1.05 higher (0.97, 1.13) than non-B.1.1.7 subjects in the full dataset. To increase specificity, we compared 1453 B.1.1.7 cases with

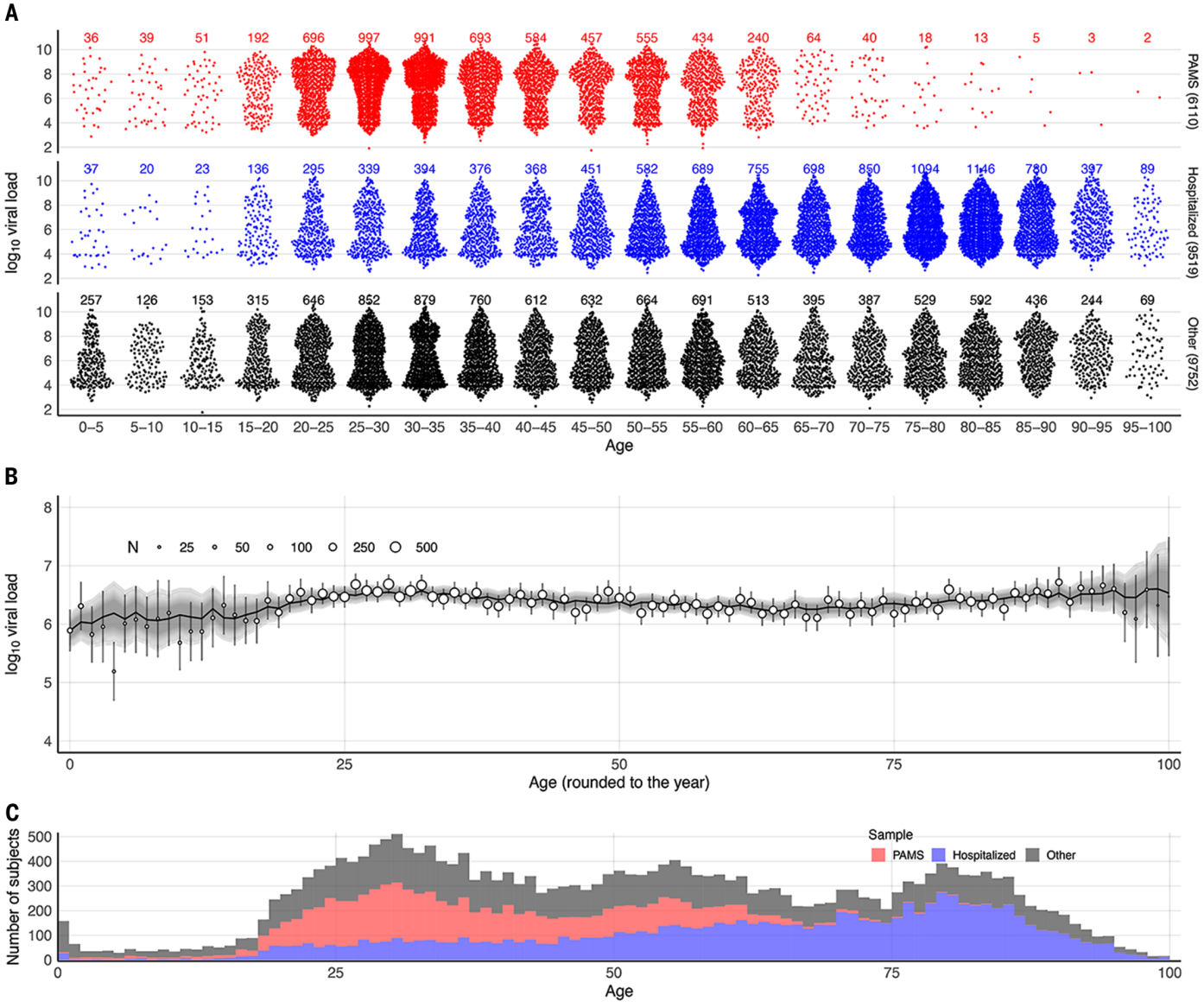

Fig. 1. Distribution of age and first-positive viral load in PAMS, Hospitalized, and Other subjects. (**A**) Distribution of observed first-positive viral loads for 25,381 subjects according to clinical status (6110 PAMS, 9519 Hospitalized, 9752 Other) and age group. (**B**) Age–viral load association. Observed viral loads are shown as circles (circle size indicates subject count) with vertical lines denoting confidence intervals; model-predicted viral loads are shown as a black, roughly horizontal line, with gray shading denoting credible intervals. (**C**) Stacked age histograms according to subject clinical status. Because inclusion in the study required a positive RT-PCR test result, and because testing is in many cases symptom-dependent, the study may have a proportion of PAMS cases that differs from the proportion in the general population.

977 non-B.1.1.7 cases using viral loads only from centers with B.1.1.7 and non-B.1.1.7 cases, and only from the same day or 1 day before or after the B.1.1.7 sample was taken. This analysis adjusted for clinical status, gender, RT-PCR system, and subject age, and also modeled random test center effects. The results show that B.1.1.7 cases are associated with a 1.0 (0.9, 1.1) higher viral load (Fig. 3 and table S2). This results in a mean estimated B.1.1.7 subject culture probability of 0.50 (0.03, 0.97), considerably higher than the overall figure of 0.31 (0.00, 0.94) for the non-B.1.1.7 subjects in the comparison, corresponding to a median factor of 2.6 (50% credible interval: 1.4, 5.1) higher culture probability for samples from B.1.1.7 cases. To investigate whether there might be a difference in cell culture infectivity due to a factor other than viral load, we isolated virus from 105 samples (22 B.1.1.7, 83 B.1.177) in Caco-2 cells from a collection of 223 samples with matched viral loads. Although no statistical difference was seen in the distribution of viral loads that resulted in successful isolation (fig. S4), uncertainty attributable to the routine diagnostic laboratory context—including uncontrolled preanalytical parameters such as transportation time and temperature, together with the small isolation-positive sample sizes—are insufficient to support a conclusion that the distributions do not differ (see materials and methods).

Estimating infectiousness over time

To investigate viral load over the course of the infection, we estimated the slopes of a model of linear increase and then decline of $\log_{10}$ viral load using a Bayesian hierarchical model. The analysis used the time series of the 4344 subjects who had RT-PCR results on at least 3 days (with at least two tests being positive). The number of subjects with multiple test

Table 2. Pairwise age comparisons of first-positive RT-PCR viral load and estimated culture probability calculated from spline regression or raw data. Only the spline-based regression adjusts for effects of the test center and RT-PCR system. Differences are mean differences, with 90% credible intervals or confidence intervals from null-hypothesis significance testing given in parentheses. *P* values are from Mann-Whitney *U* tests (*96*).

		Spline-based regression (adjusted)		Raw data (unadjusted)	
Sample	**Comparison**	**Culture probability difference**	**log_{10}(load difference)**	**log_{10}(load difference)**	***P***
All	0–5 vs. 20–65	−0.067 (−0.167, −0.002)	−0.50 (−0.62, −0.37)	−0.49 (−0.69, −0.29)	<0.001
All	5–10 vs. 20–65	−0.054 (−0.132, −0.002)	−0.40 (−0.50, −0.30)	−0.38 (−0.64, −0.13)	0.004
All	10–15 vs. 20–65	−0.045 (−0.111, −0.002)	−0.30 (−0.39, −0.22)	−0.42 (−0.65, −0.18)	<0.001
All	15–20 vs. 20–65	−0.033 (−0.076, −0.001)	−0.18 (−0.23, −0.12)	−0.16 (−0.31, −0.01)	0.033
PAMS	0–5 vs. 20–65	−0.067 (−0.167, −0.002)	−0.50 (−0.62, −0.37)	−0.49 (−0.69, −0.29)	<0.001
PAMS	5–10 vs. 20–65	−0.112 (−0.279, −0.003)	−0.63 (−0.96, −0.32)	−0.37 (−1.00, 0.26)	0.213
PAMS	10–15 vs. 20–65	−0.092 (−0.228, −0.003)	−0.51 (−0.77, −0.26)	−0.86 (−1.46, −0.26)	0.004
PAMS	15–20 vs. 20–65	−0.064 (−0.162, −0.002)	−0.35 (−0.54, −0.17)	−0.56 (−1.10, −0.02)	0.034
Hospitalized	0–5 vs. 20–65	−0.033 (−0.087, −0.001)	−0.18 (−0.29, −0.07)	−0.26 (−0.52, −0.01)	0.046
Hospitalized	5–10 vs. 20–65	−0.028 (−0.104, 0.009)	−0.18 (−0.45, 0.07)	−0.36 (−1.10, 0.37)	0.115
Hospitalized	10–15 vs. 20–65	−0.025 (−0.084, 0.003)	−0.16 (−0.36, 0.03)	−0.48 (−1.38, 0.43)	0.172
Hospitalized	15–20 vs. 20–65	−0.022 (−0.071, 0.001)	−0.14 (−0.29, 0.02)	−0.11 (−0.97, 0.74)	0.625
Other	0–5 vs. 20–65	−0.018 (−0.055, 0.000)	−0.11 (−0.22, 0.01)	0.00 (−0.33, 0.33)	0.845
Other	5–10 vs. 20–65	−0.058 (−0.148, −0.001)	−0.36 (−0.51, −0.20)	−0.33 (−0.55, −0.10)	0.004
Other	10–15 vs. 20–65	−0.044 (−0.110, −0.001)	−0.27 (−0.39, −0.15)	−0.10 (−0.40, 0.20)	0.586
Other	15–20 vs. 20–65	−0.026 (−0.072, −0.001)	−0.16 (−0.27, −0.06)	−0.31 (−0.58, −0.04)	0.045

results skews heavily toward older subjects, with very few below the age of 20 meeting the criterion (Fig. 4A). We estimated time from onset of shedding to peak viral load of 4.31 (4.04, 4.60) days, mean peak viral load of 8.1 (8.0, 8.3), and mean decreasing viral load slope of −0.168 (−0.171, −0.165) per day (fig. S5). Figure S6 shows that while Hospitalized patients are estimated to be uniformly highly infectious at peak viral load, the infectiousness of PAMS subjects at peak load is more variable.

The temporal placement of the full 18,136 RT-PCR results from these 4344 subjects (80% of whom were hospitalized with COVID-19 at some point in their infections) is shown in fig. S7. Per-subject trajectories can differ considerably from that described by the mean parameters (Fig. 4B and fig. S8). Across all subjects, PAMS cases were on average detected 5.1 (4.5, 5.7) days after peak load, 2.4 (1.7, 3.0) days before non-PAMS cases, which were on average detected 7.4 (7.2, 7.6) days after peak load. We estimate that 962 (914, 1010) of the 4344 subjects [22.14% (21.04, 23.25)] had a first positive test before the time of their peak viral load, with a mean of 1.4 (1.3, 1.5) days before reaching peak viral load. Among the infections detected after peak viral load, the timing of the first positive RT-PCR test is estimated at 9.8 (9.6, 10.0) days after peak viral load, with SD of 6.9 (6.8, 7.0) days, reflecting a broad time range of infection detection. Estimated peak viral loads were higher in Hospitalized subjects than in Other subjects, and higher in Other subjects than in PAMS subjects, with differences of 0.68 (0.83, 0.52) and 0.96 (0.33, 1.53) respectively (fig. S9 and table S3). No differences according to gender were seen. Viral load time courses were similar across age groups, although younger subjects had lower peak viral load than adults aged 45 to 55 (Fig. 5, A and C, fig. S10, and table S4). Model parameters suggest a slightly longer time to peak, a higher peak, and a more rapid decline in viral load when the analysis is restricted to subjects with successively higher numbers of RT-PCR results (fig. S11 and table S5), with an increasing percentage of hospitalized subjects. Differences in model parameters according to the number of tests in subjects may reflect increased parameter accuracy due to additional data, although other factors associated with being tested more frequently may be responsible. The Bayesian estimation of the model agrees well with a separate second implementation based on simulated annealing (fig. S12, table S5, and supplementary text).

We estimate that the rise from near-zero to peak culture probability takes 1.8 (1.3, 2.6) days, with a mean peak culture probability of 0.74 (0.61, 0.85). Mean culture probability then declines to 0.52 (0.40, 0.64) at 5 days and to 0.29 (0.19, 0.40) at 10 days after peak viral load. Subject-level time courses can deviate substantially from these mean estimates (Fig. 4C). Peak culture probabilities for age groups range from a low of 0.54 (0.39, 0.71) for 0- to 5-year-olds to 0.80 (0.67, 0.90) for subjects more than 65 years old. The least infectious youngest children have 78% (61, 94) of the peak culture probability of adults aged 45 to 55 (Fig. 5, B and D, and table S4). An insufficient amount of data precludes a reliable B.1.1.7 viral load time-series analysis at this point.

Discussion

Limitations

Our analysis attempted to account for the effects of gender, PCR system, and test center type. Although we could not incorporate inter-run variability or the variability in the sample preanalytic (such as type of swab or initial sample volume) in our conversion of RT-PCR cycle threshold values to log_{10}(viral load) values, these variabilities apply to all age groups and do not affect the interpretation of data for the purpose of our study. If the proportion of subjects with a certain clinical status differs between age groups in the study sample, this could lead to over- or underestimation of differences in viral load between age groups. However, as our study compares viral load between age groups stratified by clinical status, it appears unlikely that differential testing biases our results.

Interpreting first-positive viral loads

Viral loads and their differences are not easy to interpret without knowledge of when in the disease course the samples were taken, and of the correspondence between viral load and shedding. The higher first-positive viral loads in PAMS subjects than in Hospitalized subjects are likely due to time of detection. This is suggested in the first place by the estimated difference of 2.4 (1.7, 3.0) days in test timing, which would produce a viral load difference of ~0.4 using the −0.168 daily viral load decline gradient from the (mainly hospitalized) time-series subjects. Additionally, from the time series of PAMS, Other, and Hospitalized subjects, we can estimate that throughout the infection

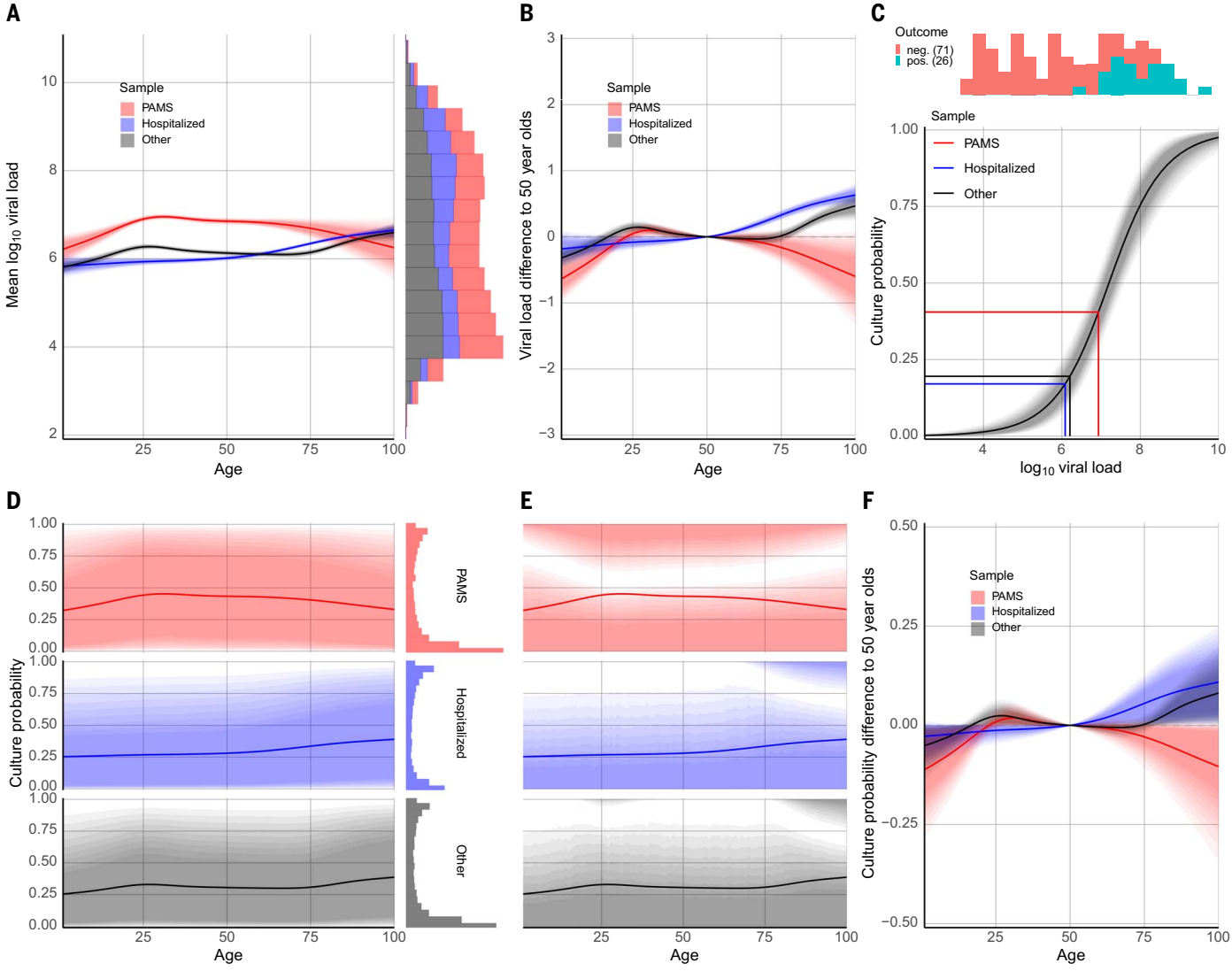

Fig. 2. Estimated viral load and culture probability at time of first positive RT-PCR test. Shaded regions denote 90% credible intervals in all panels. To indicate change within each 90% region, shading decreases in intensity from a narrow 50% credibility interval level to the full 90%. (**A**) Estimated mean viral load in first-positive RT-PCR tests according to age and status. The stacked histogram (right) shows the observed viral load distribution. Because the shaded region shows the 90% credible interval for the mean, it does not include the higher values shown in the histogram on the right. (**B**) Differences in estimated first-positive viral load according to age and status. Each colored line is specific to a particular subset of subjects (PAMS, Hospitalized, Other). Each line shows how viral load differs by age for subjects of the corresponding status from that of 50-year-old (rounded age) subjects of the same status. The comparison against 50-year-olds avoids comparing any subset of the subjects against a value (such as the overall mean) that is computed in part on the basis of that subset, thereby partially comparing data to the same data. The mean first-positive viral loads for 50-year-old PAMS and Hospitalized subjects are 7.2 and 6.2, respectively, allowing relative *y*-axis differences to be translated to approximate viral loads. (**C**) Estimation of the association between viral load and cell culture isolation success rate based on data from our own laboratory (*19*) and Perera *et al*. (*20*). Viral load differences in the $\log_{10}$ range ~6 to ~9 have a large impact on culture probability, whereas the impact is negligible for differences outside that range. The vertical lines indicate the observed mean first-positive viral loads for different subject groups; the horizontal lines show the corresponding expected probabilities of a positive culture. (**D**) Estimated culture probability at time of first-positive RT-PCR according to age and status, obtained by combining the results in (A) and (C). Culture probability is calculated from posterior predictions [i.e., the posterior means shown in (A) plus error variance]. The histogram at right shows that mean culture probabilities calculated from observed viral loads are not well matched by credible intervals, which do not include the most probable estimated culture probabilities. (**E**) Culture probability with highest–posterior density regions, which do include the most probable estimated culture probabilities and match the histograms in (D) well. The *y* axis is the same as in (D). (**F**) Differences of estimated expected culture probability at time of first-positive RT-PCR for age groups, with plot elements as described for (B).

course, the Hospitalized group has higher viral loads than the Other group, whose viral loads are in turn higher than those of the PAMS group (fig. S9 and table S3). This relationship holds across age groups (fig. S13) and also in a fine-grained split of test centers by clinical severity (fig. S14). Similarly, the lower first-positive viral loads in elderly PAMS subjects may be due to these subjects being less likely to be tested as early because they are more likely to be house-bound, less likely to be employed, less mobile, more cautious (therefore disinclined to get tested with only mild symptoms), etc. The impact on infectiousness of differences in viral load must be informed by

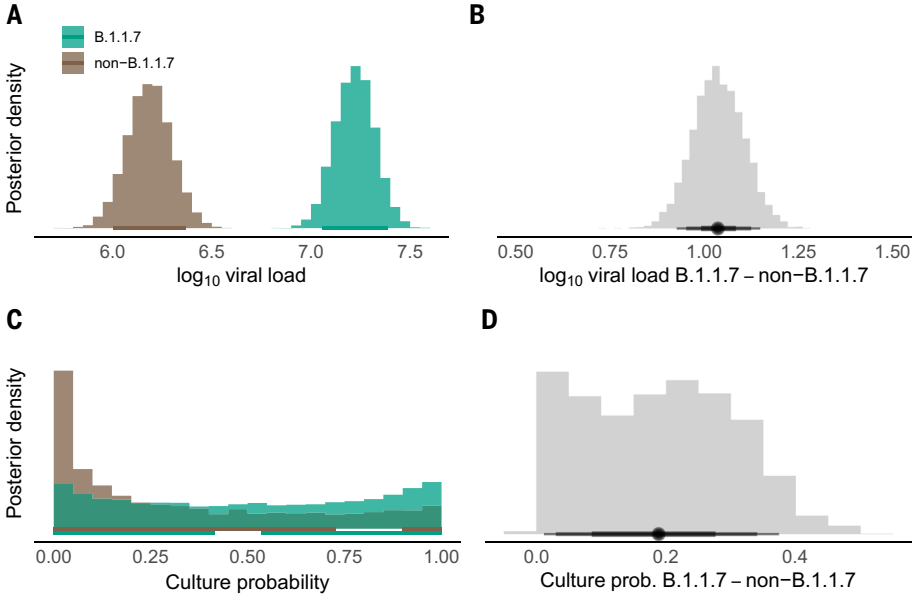

Fig. 3. Posterior distributions of estimated viral loads and culture probabilities for B.1.1.7 and non-B.1.1.7 subjects, and their differences. Viral loads and estimated culture probabilities of 1387 B.1.1.7 subjects and 977 non-B.1.1.7 subjects are represented. To select a comparable subset of non-B.1.1.7 viral loads for the comparison, we included only non-B.1.1.7 subjects from test centers that had detected a B.1.1.7 variant as well as at least one non-B.1.1.7 subject, and only if the non-B.1.1.7 infection was detected on the same day as a B.1.1.7 infection was detected, plus or minus 1 day. Similar differences exist when viral loads from larger, less restrictive, subsets of non-B.1.1.7 subjects are used in the comparison (table S2; see materials and methods). (**A**) Posterior distribution of viral load. (**B**) Posterior distribution of difference of average viral load between B.1.1.7 and non-B.1.1.7 cases. (**C**) Posterior distribution of the estimated culture probability. See also fig. S2. (**D**) Difference of mean culture probability between B.1.1.7 and non-B.1.1.7 cases. Horizontal lines indicate 90% credible intervals in (A), (B), and (D) and the highest posterior density intervals in (C).

where the viral loads fall on the viral load–culture probability curve. In our data, the viral loads involved in the difference between means in children and adults and the difference between means in B.1.1.7 and non-B.1.1.7 subjects result in quite different corresponding culture probabilities (see below).

A highly infectious minority and overdispersion

The bimodal distribution of culture probabilities (Fig. 2, D and E) shows a small group of 8.78% of highly infectious subjects. This qualitatively agrees with a model (*21*) and a study (*22*) concluding that 10% and 15% of index cases, respectively, may be responsible for 80% of transmission. Other studies reported that 8 to 9% of individuals harbored 90% of total viral load (*23*), and that in cases from India (*24*) and Hong Kong (*6*) ~70% of index cases had no secondary cases. PAMS subjects can be construed to pose a risk for several reasons: 36.1% of the highly infectious subjects in our study were PAMS at the time of the detection of their infection, their mean age was 37.6 years with a high standard deviation of 13.4 years (figs. S2 and S3), and we estimate that infectiousness peaks 1 to 3 days before onset of symptoms (if any).

Comparison with influenza virus

Without direct knowledge from a large number of SARS-CoV-2 transmission events, we could try to draw conclusions regarding infectiousness from studies of other respiratory viruses, such

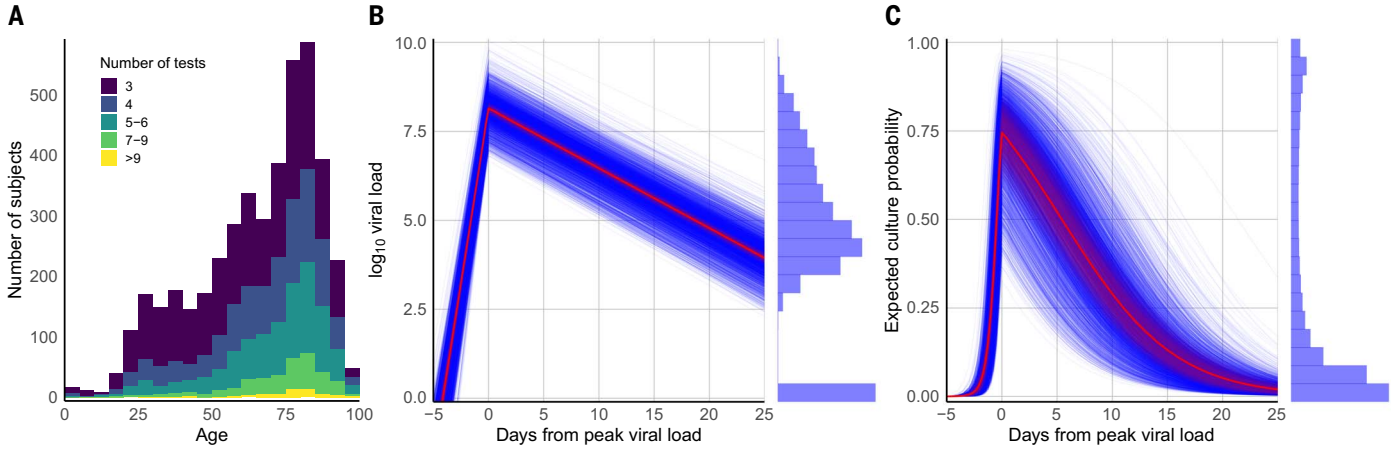

Fig. 4. Viral load and estimated infectious virus shedding time series. Of 25,381 positive subjects, 4344 had three or more RT-PCR test results available, and these were used in a viral load time-series analysis. Subjects with only one result cannot be placed in time because of inherent ambiguity (given that the model has both an increasing and a decreasing phase), and those with only two test results are excluded from the time-series analysis because of insufficient data for temporal placement (their number of data points is less than the number of model parameters being estimated). (**A**) Number of subjects with three or more RT-PCR test results available, at least two of which were positive, according to age. (**B**) Estimated time course of viral load for 18,136 RT-PCR results from the 4344 subjects with at least three RT-PCR results. Blue lines are expected complete time courses for individual cases. The sample mean is shown in red, with its 90% credible interval as a shaded area. The histogram at right shows the distribution of all observed viral loads. The histogram values at zero correspond to the initial and trailing negative tests in subject timelines. Figure S8 shows raw viral load time series, per subject and split by number of RT-PCR tests. (**C**) Estimated time course of positive cell culture probability, calculated by applying the results shown in Fig. 2C to the estimated viral load time courses in (B). Blue lines are expected time courses for individual subjects. The sample average is shown in red, with its 90% credible interval as a shaded area. The histogram at right shows the distribution of culture probabilities in the sample and was obtained by applying the curve in Fig. 2C to the data in the histogram in (B).

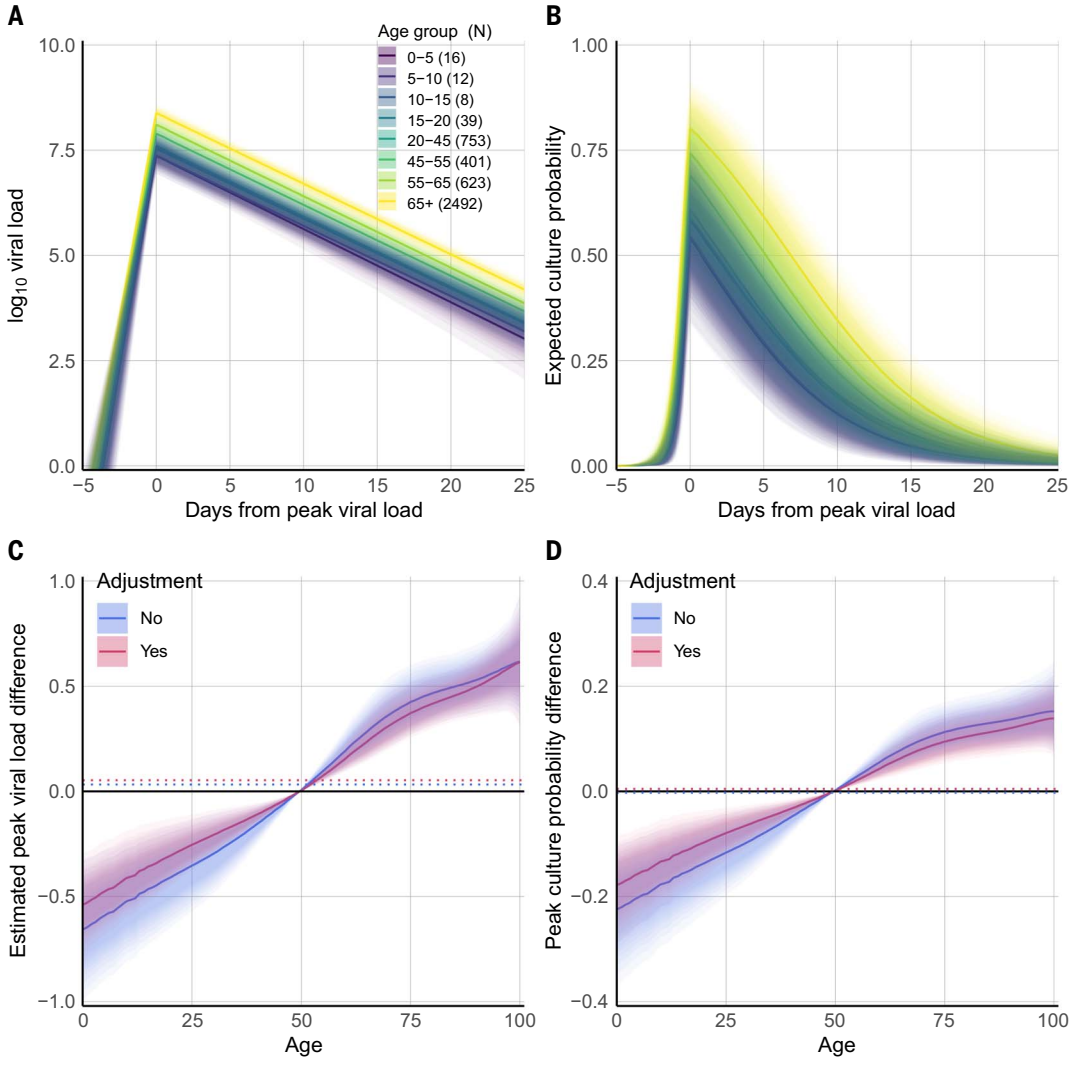

Fig. 5. Estimated expected viral load and culture probability for age groups by time. (**A**) Change in estimated viral load over time according to age group for 4344 subjects with at least three RT-PCR tests, at least two of which were positive. Shading indicates the 90% credible interval of the mean. (**B**) Change in estimated culture probability over time according to age. Age groups, coloring, and shading are as in (A). (**C**) Estimated age group differences in mean peak viral load, corresponding to the values at day zero in (A). (**D**) Estimated age group differences in mean peak culture probability, corresponding to the values at day zero in (B). In (C) and (D), adjusted differences account for variations by age in clinical status and gender. Dotted lines indicate grand means for the 4344 subjects.

as influenza. However, it has become clear that there are important differences and uncertainties that would cast doubt on such a comparison. Influenza may have later onset of viral shedding; shedding finishes earlier; there may be a lower secondary attack rate; viral loads are much lower; there is variation between virus subtypes; the role of asymptomatic subjects in transmission is uncertain or thought to be reduced; and the frequency of asymptomatic infections is uncertain, especially in children (*10*, *11*, *25*–*29*). Age-specific behavioral differences do, however, make a large contribution to the established higher shedding of children relative to adults in influenza. This should be an important consideration for SARS-CoV-2, as shown by studies indicating higher transmission between children of similar ages (*6*, *24*) and high transmission heterogeneity (*22*). Despite many decades of close study of influenza virus, the relationship between viral load and transmission is unclear (*10*, *11*). The situation with respiratory syncytial virus is even less clear (*30*). Understanding SARS-CoV-2 transmission will likely be at least as challenging, given the high frequency of transmission from PAMS subjects (*1*–*8*). This suggests an important role for clinical parameters, given the apparently strong association between viral load and transmission, independent of symptoms (*9*).

Estimated infectiousness in the young

The differences we observe in first-positive RT-PCR viral load between groups based on age are minor, as in other studies (*31*–*35*), and the viral loads in question—in the range of 5.9 to 6.6 (Table 1)—are in a region of the viral load–culture probability association where changes in viral load have relatively little impact on estimated culture probability (Fig. 2C). Comparisons between adult viral loads and those of children, and the relative infectious risks they pose, are impeded by the likely influence of nonviral factors. Nasopharyngeal swab samples, which often carry higher viral loads, are rarely taken from young children because they can be painful, and the sample volume carried by smaller pediatric swab devices is lower than in larger swabs used for adults (*36*). Infections in mildly symptomatic children may be initially missed and only detected later (*37*), resulting in lower first-positive viral loads. Our results of similar viral load trajectories for children and adults (Fig. 5), and the numeric range of the viral load values in question (Fig. 2C), suggest that viral load differences between children and adults are too small to be solely responsible for large differences in infectiousness. The impact on transmission of general age-related physiological differences, such as different innate immune responses (*38*), may be small relative to the impact of large differences in frequency of close contacts and transmission opportunities.

Timing of estimated peak infectiousness relative to onset of symptoms

We estimated the time from onset of shedding to peak viral load at 4.3 days. Previous studies

and reviews of COVID-19 report mean incubation times of 4.8 to 6.7 days (*4*, *39*–*44*), which suggests that, on average, a period of high infectivity can start several days before the onset of symptoms. Viral load rise may vary between individuals, and limitations of the available data suggest that our analysis may underestimate interindividual variation in viral load increase. The failure to isolate virus in cell culture beyond 10 days from symptom onset (*19*, *20*, *35*, *45*, *46*), together with our estimated slope of viral load decline, also suggest that peak viral load occurs 1 to 3 days before symptom onset (supplementary text). Data from 171 hospitalized patients from a Charité-Universitätsmedizin cohort suggest a figure of 4.3 days (fig. S15 and supplementary text).

Estimated infectiousness of the B.1.1.7 variant

We found that people infected with a B.1.1.7 virus had a first-positive viral load that was ~1 higher than in people infected with a wild-type virus. The scale of the viral load difference, and its presence in the comparison between B.1.1.7-infected and non–B.1.1.7-infected subjects drawn from the same test centers at the same times, argue that the difference is not due to a systematic difference in time of sampling. The higher B.1.1.7 viral load can be compared to the findings of two large and closely controlled UK studies, a mortality study (*47*) and a vaccine trial (*48*), which imply higher B.1.1.7 viral loads by a factor of 5 to 10 (based on RT-PCR cycle threshold differences of 2.3 and ~3, respectively). Several other studies also appear to point to a higher B.1.1.7 viral load (*49*–*52*) (supplementary text).

The mean B.1.1.7 viral load value in our study falls in a region of the viral load–culture probability curve with a steep gradient (Fig. 2C), resulting in an estimated culture probability considerably higher than for non-B.1.1.7 subjects. Although a strong correlation has been observed between SARS-CoV-2 viral load and transmission (*9*), here we are estimating infectivity probability from cell culture trials. Any impact of a change in viral load on transmission will be highly dependent on context, so the large difference in estimated culture probability in our data is only a proxy indication of potentially higher transmissibility of the B.1.1.7 strain. We estimate that B.1.1.7-infected subjects' mean culture probability is higher than that of non–B.1.1.7-infected subjects by a factor of 2.6. This can be compared to a UK study that found a factor of 1.3 relative increase in secondary attack rates for B.1.1.7 index cases in ~60,000 household contacts (*53*), a UK study estimating a factor of 1.7 to 1.8 increase in transmission (*54*), and an estimate of a 43% to 90% higher reproductive number (*55*).

Summary

Our results indicate that PAMS subjects in apparently healthy groups can be expected to be as infectious as hospitalized patients at the time of detection. The relative levels of expected infectious virus shedding of PAMS subjects (including children) is of high importance because these people are circulating in the community and it is clear that they can trigger and fuel outbreaks (*56*). The results from our time-series analysis, and their generally good agreement with results from studies based on other metrics (often epidemiological), show that accurate estimations can be directly obtained from two easily measured virological parameters, viral load and sample cell culture infectivity. Such results can be put to many uses: to estimate transmission risk from different groups (by age, gender, clinical status, etc.), to quantify variance, to show differences in virus variants, to highlight and quantify overdispersion, and to inform quarantine, containment, and elimination strategies. Our understanding of the timing and magnitude of change in viral load and infectiousness, including the impact of influencing factors, will continue to improve as data from large studies accumulate and are analyzed. A major ongoing challenge is to connect what we learn about estimated infectiousness from these clinical parameters to highly context-dependent in vivo transmission. On the basis of our estimates of infectiousness of PAMS subjects and the higher viral load found in subjects infected with the B.1.1.7 variant, we can safely assume that nonpharmaceutical interventions such as social distancing and mask wearing have been key in preventing many additional outbreaks. Such measures should be used in all social settings and across all age groups wherever the virus is present.

Materials and methods

Age ranges

Age categories for the analysis of the first-positive test results mentioned in the text indicate mathematically open-closed ranges of years (e.g., 0-5 signifies (0-5] years). We group subjects up to 20 years old into age categories spanning 5 years, subjects from 20 to 65 years into an adult group, and elderly subjects into a 65+ category. This categorization is motivated by the observed data and the Bayesian estimation of viral load differences between children of different ages and adults. The age groupings used in the viral load time-series analysis are broader in the younger categories to increase the cardinality of those groups, because few young people have at least three RT-PCR tests (Fig. 4A).

Viral loads

Viral load is semiquantitative, estimating RNA copies per entire swab sample, whereas only a fraction of the volume can reach the test tube. The quantification is based on a standard preparation tested in multiple diluted replicates to generate a standard curve and derive a formula in which RT-PCR cycle threshold values are converted to viral loads. This approach does not reflect inter-run variability or the variability in the sample preanalytic, such as type of swab or initial sample volume (varying between 2.0 and 4.3 ml). However, these variabilities apply to all age groups and do not affect the interpretation of data for the purpose of the present study.

Viral load figures are given as the logarithm base 10. Viral load is estimated from the cycle threshold (Ct) value using the empirical formulae $14.159 - (Ct \times 0.297)$ for the Roche Light Cycler 480 system and $15.043 - (Ct \times 0.296)$ for the Roche cobas 6800/8800 systems. The formulae are derived from testing standard curves and cannot be transferred to calculate viral load in other laboratory settings. Calibration of the systems and chemistries in actual use is required.

B.1.1.7 viral load analysis

No analysis regarding symptomatic status was made for B.1.1.7 subjects because of uncertainties regarding exact operational protocols at outbreak hospitals. B.1.1.7 assignment to samples was initially made according to typing RT-PCR tests that detect the N501Y and 69/70 deletion in the amino acid sequence of the virus spike protein. Examination of the complete viral genome of 49 samples confirmed that the subjects were in fact infected with the B.1.1.7 variant, with all variant-defining substitutions and deletions (*57*) found in all cases. No consistent additional mutations or deletions/insertions were found in the sequences.

Sequencing read mapping was performed with Bowtie, with alignment using MAFFT and visual inspection using Geneious Prime (all version numbers given below). For the statistical comparison of B.1.1.7 and non-B.1.1.7 subjects, we identified test centers (hospital departments or wards, or organizations outside hospitals) that reported B.1.1.7 cases, and chose as comparison groups non-B.1.1.7 cases that were detected in these test centers on the same day or 1 day earlier or later. By modeling random effects for test centers, we estimate the expected viral load difference as the average of the within-test center differences. The consistent effect of B.1.1.7 throughout a range of comparison scenarios is shown in table S2.

Sample type

An estimated 3% of our samples were from the lower respiratory tract. These were not removed from the dataset because of their low frequency and the fact that the first samples for patients are almost universally swab samples. Samples from the lower respiratory tract are generally taken from patients only after intubation, by which point viral loads have typically fallen.

PAMS status

Metadata needed to discriminate patients into subcohorts on the basis of underlying diseases,

outcome, or indications for diagnostic test application, including symptomatic status, were not always available. In the absence of subject-level data, we inferred PAMS status using the type of submitting test center as an indicator, classifying subjects as PAMS at the time of testing if their first-positive sample was taken from a walk-in COVID-19 test center and the subject had no later RT-PCR test done in a hospitalized context (e.g., in a ward or an intensive care unit). The correspondence between viral load and PAMS status derived herein may therefore be less accurate than in studies with subject-level symptom data. However, we make no formal claims regarding symptomatic status, and instead emphasize the fact that these PAMS subjects were healthy enough to be presenting at walk-in COVID-19 test centers, and were therefore capable to some extent, at that time, of circulating in the general community.

Bayesian analysis of age–viral load associations

We estimated associations of viral load and age with a thin-plate spline regression using the brms package (*58*, *59*) in R (*60*). Spline coefficients were allowed to vary between groups determined by the clinical status (PAMS, Hospitalized, or Other), and random intercepts captured effects of test centers. To reduce the impact of outliers, we used Student *t*–distributed error terms. The analysis additionally accounted for baseline differences between subject groups, B.1.1.7 status, gender, and for the effect of the RT-PCR system. We also estimated the association between viral load and culture probability in order to calculate the expected culture probability at different age levels. This analysis used weakly informative priors and was estimated using four chains with 1000 warm-up samples and 2000 post–warm-up samples. Convergence of MCMC chains was examined by checking that potential scale reduction factors (R-hat) values were below 1.1. All calculations of age averages and group differences are based on posterior predictions generated from estimated model parameters. Expected probabilities of positive cultures (and their differences) were calculated by applying the posterior distribution of model parameters from the culture probability model to posterior predictions from the age association model.

Combining culture probability data

To estimate the association between viral load and culture probability, we used data previously described by Wölfel (*19*) and Perera (*20*). Four other datasets could not be included because Ct values were not converted to viral loads (*35*, *46*, *61*, *62*). The data from the study by van Kampen *et al.* (*63*) were not included because they differed (by viral load of ~1.0) from the data used for the current analysis (*97*); this is likely due to a combination of factors including many patients who were in critical or immunocompromised condition, a high proportion of samples obtained from the lower respiratory tract (including late in the infectious course), and likely differences in cell culture trials. It is unsurprising that these data result in a shifted viral load/culture probability curve, and we excluded them because our focus was largely on first positive RT-PCR results from the upper respiratory tract, including from many subjects who were PAMS. [See (*97*) for a figure comparing the plot of the van Kampen dataset to the two we used.] To calculate the expected culture probability, by age (as in Fig. 2D) or by day from peak viral load (as in Fig. 4C), we combined the estimated viral loads (Figs. 2A and 4B) with the results of the regression of culture probability shown in Fig. 2C. We used posterior predictions from the age regression model, which reflect the variation of viral load within age groups, to estimate culture probabilities by age. For instance, to obtain the culture probability for a specific age and group, we look up the estimated (expected) viral load for that group, add an error term according to the estimated error variance, and, using the association shown in Fig. 2C, determine the expected culture probability. We used expected time courses (i.e., the model's best guess for a time course) to estimate culture probability time courses.

B.1.1.7 isolation data

The Institute of Virology at Charité–Universitätsmedizin Berlin routinely receives SARS-CoV-2–positive samples for confirmatory testing and sequencing. For this study we used anonymized remainder samples from a large laboratory in northern Germany, which were all stored in phosphate-buffered saline (PBS) and therefore suitable for cell culture isolation trials. Sample transport to the originating lab and later to Berlin was unrefrigerated, via road. As part of the routine testing, these samples were classified by typing RT-PCR and complete genome sequencing (*64*); 113 B.1.1.7 lineage samples and 110 B.1.177 lineage samples were selected, with approximately matched (pre-inoculation) SARS-CoV-2 RNA concentrations. Caco-2 (human colon carcinoma) cell cultures (*65*) were inoculated twice from each sample, once with undiluted material and once with a 1:10 dilution. The diluted inoculant was used to reduce the probability of culturing failure due to the possible presence of host immune factors (antibodies, cytokines, etc.) that might have a negative impact on isolation success, and to reduce the possibility of other unrelated agents (bacteria, fungi, etc.) resulting in cytopathic effect in the culture system. For cell culture isolation trials, 1.6×10^5 cells were seeded per well in a 24-well plate. Cells were inoculated with swab suspensions for 1 hour at 37°C, subsequently rinsed with PBS, and fed with 1 ml of fresh Dulbecco's modified Eagle's minimum essential medium (DMEM; ThermoFisher Scientific) supplemented with 2% fetal bovine serum (FBS; Gibco), penicillin and streptomycin (P/S; 100 U/ml and 100 μg/ml, respectively; ThermoFisher Scientific), and amphotericin B (2.5 μg/ml; Biomol), then incubated for 5 days before harvesting supernatant for RT-PCR testing. Positive cell culture isolation was defined by a minimum 10× higher SARS-CoV-2 RNA load in the supernatant compared to the inoculant and signs of a typical SARS-CoV-2 cytopathic effect. Culture isolation was successful for 22 B.1.1.7 and 61 B.1.177 samples. Because of uncertainty regarding sample handling before arrival at the originating diagnostic laboratory and the unrefrigerated transport, it was not possible to determine whether isolation failures were due to samples containing no infectious particles (due to sample degradation) or for other reasons. Such reasons could include systematic handling differences according to variant type or a difference in virion stability and durability regarding environmental factors such as temperature. Therefore, samples with negative isolation outcome were excluded from analysis. The strong likelihood of many cases of complete sample degradation is evident from the isolation failure of many samples with high pre-inoculation viral load, with the viral load in these cases merely indicating the presence of noninfectious SARS-CoV-2 RNA (fig. S4). Given this context, we were reduced to questioning whether there might be a difference in the range of viral loads that were able to result in isolation between B.1.1.7 and non-B.1.1.7 variants. Such a difference could result from a difference in the ratio of viral RNA to infectious particles produced by the variants, or from a difference other than viral load in the variants. We examined the distribution of pre-inoculation viral loads from isolation-positive samples from both variants for a difference. No statistically significant difference was found, but in the converse, the isolation-positive sample sizes are too low to support the assertion that the distributions do not differ.

Estimating viral load time course

Each RT-PCR test in our dataset has a date, but no information regarding the suspected date of subject infection or onset of symptoms (if any). Although determining the day of peak viral load for a single person based on a series of dated RT-PCR results would not in general be feasible because of individual variation, data from a large enough set of people would enable the inference of a clear and consistent model of viral load change over time with very few assumptions.

We included a single leading and/or trailing negative RT-PCR result, if dated within 7 days of the closest positive RT-PCR. To produce a model of typical viral load decline on a reasonable single-infection time scale, we excluded

subjects whose full time series contains positive RT-PCRs spread over a period exceeding 30 days. Such time series may be attributable to contamination, to later swabbing that picks up residual RNA fragments in tonsillar tissue (*66*), or to re-infection (*67*–*69*), or they may represent atypical infection courses (such as in immunocompromised or severely ill elderly patients) (*70*). We excluded data from subjects with an infection delimited by both an initial and a trailing negative test when there was only a single positive RT-PCR result between them.

We estimated the slopes for a model of linear increase and then decline of $\log_{10}$(viral load). To compensate for the absence of information regarding time of infection, we also estimated the number of days from infection to the first positive test for each participant, so as to position the observed time series relative to the day of peak viral load. The analysis was implemented in two ways. Initially, simulated annealing was used to find an optimized fit of the parameters, minimizing a least-squares error function. Second, a Bayesian hierarchical model estimated subject-specific time courses, imputed the viral load assigned to each initial or trailing negative test, and captured effects of age, gender, clinical status, and RT-PCR system with model parameters. We tested both methods on data subsets ranging from subjects with at least three to at least nine RT-PCR results. The two methods produced results that were in generally good agreement (table S5). The finer-grained Bayesian approach appears more sensitive than the simulated annealing; its results, for subjects with at least three RT-PCR results, are those described in the main text.

Simulated annealing approach: A simulated annealing optimization algorithm (*71*) was used to adjust the time series for each subject slightly earlier or later in time, by amounts drawn from a normal distribution with mean 0.0 and standard deviation 0.1 days. The error function was the sum of squares of distances of each viral load from a viral load decline line whose slope was also adjusted as part of the annealing process. In the error calculation, negative test results were assigned a viral load of 2.0, in accordance with our SARS-CoV-2 assay limit of detection and sample dilution (*19*). The initial slope of the decline line was set to –2.0 and was varied using $N(0, 0.01)$. A second, optional, increase line initialized with a slope of 2.0, adjusted using an $N(0, 0.01)$ random variable, was included in the error computation if the day of a RT-PCR test was moved earlier than day zero (the modeled day of peak viral load). The height of the intercept (i.e., the estimated peak viral load) between the increase line (if any) and the decline line was also allowed to vary randomly [starting value 10.0, varied using $N(0, 0.1)$]. The full time series for each subject was initialized with the first positive result positioned at day 2 + $N(0.0, 0.5)$ after peak viral load. The random-move step of the simulated annealing modified either of the two slopes or the intercept, each with probability 0.01, otherwise (with probability 0.97) one subject's time series was randomly chosen to be adjusted earlier or later in time. After the simulated annealing stage, each time series was adjusted to an improved fit (when possible) based on the optimized increase and decline lines. Linear regression lines were then fitted through the results occurring before and after the peak viral load ($x = 0$) and compared to the lines with slopes optimized by the simulated annealing alone. This final step helped to fine-tune the simulated annealing, in particular sometimes placing a time series much earlier or much later in time after it had stochastically moved initially in a direction that later (when the increase and decline line slopes had converged) proved to be suboptimal. The slopes of the lines fitted via linear regression after this final step were in all cases very similar (generally ±0.1) to those produced by the initial simulated annealing step. The final adjustments can be regarded as a last step in the optimization, using a steepest-descent movement operator instead of an uninformed random one. A representative optimization run for subjects with at least three RT-PCR results is shown in fig. S12.

Bayesian approach: The Bayesian analysis of viral load time course implements the same basic model, and additionally estimates associations of model parameters with covariates age, gender, B.1.1.7 status, and clinical status, estimates subject-level parameters (slope of $\log_{10}$ viral load increase, peak viral load, slope of $\log_{10}$ viral load decrease) as random effects, and accounts for effects of PCR system and test center types with random effects. To estimate the number of days from infection to the first test (henceforth "shift"), we constrained the possible shift values from –10 to 20 days and used a uniform prior on the support. In contrast to the other subject-level parameters, we estimated subject-level shifts independently (i.e., without a hierarchical structure). Figure S7 shows the placement in time of individual viral loads after shifting for subjects with RT-PCR results from at least 3 days. Model parameters changed gradually when subsets of subjects with an increasing minimum number of RT-PCR results, from three to nine, were examined (fig. S11 and table S5). The viral load assigned to negative test results (which may include viral loads below the level of detection) is estimated with a uniform prior on the support from –Inf to 3 (see also the caption of fig. S7). Using prior predictive simulations, we specified (weakly) informative priors for this analysis. This analysis was implemented in Stan (*72*), as described in (*97*).

Checking convergence of the model parameters showed that although 99.3% of all parameters converged with an R-hat value below 1.1, some subject-level parameters of 118 subjects (among 4344 subjects with at least three RT-PCR results) showed R-hat values between 1.1 and 1.74. Inspection of these parameters showed that these convergence difficulties were due to observed time courses that could arguably be placed equally well at the beginning or a later stage of the infection. Figure S16 shows a set of 81 randomly selected posterior predictions, to give an impression of time-series placement; fig. S17 shows the 49 participants with the parameters with the highest R-hat values. Although the high R-hat values could be removed by using a mixture approach to model shift for these participants, in light of their low frequency we retained the simpler model to avoid additional complexity. Alternatively, constraining the shift parameter to negative numbers would also improve R-hat values for these subjects, at the cost of the additional assumption that infections are generally not detected weeks after infection.

Sensitivity analysis: In addition to examining the viral load time series of subjects with RT-PCR results on at least 3 days, we tested both approaches on data from subjects with results from a minimum of 4 to 9 days. Given the degree of temporal viral load variation seen in other studies (*18*–*20*, *35*, *41*, *46*, *63*, *73*, *74*) and in our own data, our expectation was that a relatively high minimum number of results might be required before reliable parameter estimates with small variance would be obtained, but this proved not to be the case. The simulated annealing approach was tested with a wide range of initial slopes and intercept heights as well as seven different methods for the initial placement of time series. In general, maximum viral load and decline slopes were robust to data subset and initial time-series location, although there was variation in the length of the time to peak viral load, depending on how early in time the time series were initially positioned, the initial slopes of the increase and decrease lines and height of the maximum viral load. This is as expected, as the settings of these parameters can be used to bias the probability that a time series is initially positioned early or late in time and how difficult it is for it to subsequently move to the other side of the peak viral load at day zero. Table S5 shows parameter values for both approaches on the various data subsets.

Onset of shedding: We define the onset of shedding as the time point at which the increasing viral load crosses zero of the $\log_{10}$ y axis—that is, when just one viral particle was estimated to be present. Because the estimated time of infection depends on the estimated peak viral load and the slope with which viral load increases, the data should optimally include multiple pre-peak viral load test results for each individual. If, as in the

current dataset, only a subset of subjects have test results from pre-peak viral load, a hierarchical modeling approach still allows calculating subject-level estimates. Intuitively, this approach uses data from all subjects to calculate an average slope parameter for increasing viral load. In addition, it models subject-level parameters as varying around the group-level parameter. To further refine the estimation of slope parameters, the model also uses the age (see fig. S10), gender, and clinical status as covariates. Because negative test results could be false negatives, viral loads for these tests are imputed (with an upper bound of 3). Subject-level peak viral load and declining slope are modeled with the same approach. More generally, using a hierarchical model and shrinkage priors for the effects of covariates results in more accurate predictions in terms of expected squared error (*75*) compared to analyzing each subject in isolation, but the overall improvement introduces a slight bias toward the group mean, resulting in an underestimation of the true variability of subject-level parameters. This is especially the case if, as in the current dataset, subject-level data are sparse.

Onset of symptoms: The 317 onset-of-symptoms dates for hospitalized patients were collected as part of the Pa-COVID-19 study, a prospective observational cohort study at Charité–Universitätsmedizin Berlin (*76*, *77*), approved by the local ethics committee (EA2/066/20), conducted according to the Declaration of Helsinki and Good Clinical Practice principles (ICH 1996), and registered in the German and WHO international clinical trials registry (DRKS00021688).

Software

The following Python (version 3.8.2) software packages were used in the data analysis and in the production of figures: Scipy (version 1.4.1) (*78*), pandas (version 1.0.3) (*79*), statsmodels (version 0.11.1) (*80*), matplotlib (version 3.2.1) (*81*), numpy (1.18.3) (*82*), seaborn_sinaplot (*83*), simanneal (version 0.5.0) (*71*), and seaborn (version 0.10.1) (*84*). Sequence analysis used Bowtie2 (2.4.1) (*85*), bcftools and samtools (1.9) (*86*, *87*), Geneious Prime (2021.0.3) (*88*), ivar (1.2.2) (*89*), and MAFFT (4.475) (*90*). Analyses in R (4.0.2) (*60*) were conducted using the following main packages: brms (2.13.9) (*58*, *59*), rstanarm (2.21.1) (*91*), rstan (2.21.2) (*92*), data.table (1.13.3) (*93*), and ggplot2 (3.3.2) (*94*). Bayesian analysis in R was based on Stan (2.25) (*72*). Parallel execution was performed with GNU Parallel [20201122 ('Biden') (*95*)].

Data curation and anonymization

Research clearance for the use of routine data from anonymized subjects is provided under paragraph 25 of the Berlin *Landeskrankenhausgesetz*. All data are anonymized before processing to ensure that it is not possible to infer patient identity from any processing result. All patient information is securely combined into a token that is then replaced with a value from a strong one-way hash function prior to the distribution of data for analysis. Viral loads are calculated from RT-PCR cycle threshold values that have only one decimal place of precision.

REFERENCES AND NOTES

1. S. Lee *et al*., Clinical Course and Molecular Viral Shedding Among Asymptomatic and Symptomatic Patients With SARS-CoV-2 Infection in a Community Treatment Center in the Republic of Korea. *JAMA Intern. Med.* **180**, 1447–1452 (2020). doi: 10.1001/jamainternmed.2020.3862; pmid: 32780793
2. C. M. Szablewski *et al*., SARS-CoV-2 Transmission and Infection Among Attendees of an Overnight Camp - Georgia, June 2020. *MMWR Morb. Mortal. Wkly. Rep.* **69**, 1023–1025 (2020). doi: 10.15585/mmwr.mm6931e1; pmid: 32759921
3. Q.-X. Long *et al*., Clinical and immunological assessment of asymptomatic SARS-CoV-2 infections. *Nat. Med.* **26**, 1200–1204 (2020). doi: 10.1038/s41591-020-0965-6; pmid: 32555424
4. Q. Bi *et al*., Epidemiology and transmission of COVID-19 in 391 cases and 1286 of their close contacts in Shenzhen, China: A retrospective cohort study. *Lancet Infect. Dis.* **20**, 911–919 (2020). doi: 10.1016/S1473-3099(20)30287-5; pmid: 32353347
5. T. Waterfield *et al*., Seroprevalence of SARS-CoV-2 antibodies in children: A prospective multicentre cohort study. *Arch. Dis. Child.* 10.1136/archdischild-2020-320558 (2020). doi: 10.1136/archdischild-2020-320558; pmid: 33172887
6. D. C. Adam *et al*., Clustering and superspreading potential of SARS-CoV-2 infections in Hong Kong. *Nat. Med.* **26**, 1714–1719 (2020). pmid: 32943787
7. M. Hippich *et al*., A public health antibody screening indicates a six-fold higher SARS-CoV-2 exposure rate than reported cases in children. *Med* **2**, 149–163.e4 (2020). doi: 10.1038/s41586-020-2488-1; pmid: 32604404
8. E. Lavezzo *et al*., Suppression of a SARS-CoV-2 outbreak in the Italian municipality of Vo'. *Nature* **584**, 425–429 (2020). doi: 10.1038/s41586-020-2488-1; pmid: 32604404
9. M. Marks *et al*., Transmission of COVID-19 in 282 clusters in Catalonia, Spain: A cohort study. *Lancet Infect. Dis.* **21**, 629–636 (2021). doi: 10.1016/S1473-3099(20)30985-3; pmid: 33545090
10. L. L. H. Lau *et al*., Viral shedding and clinical illness in naturally acquired influenza virus infections. *J. Infect. Dis.* **201**, 1509–1516 (2010). doi: 10.1086/652241; pmid: 20377412
11. T. K. Tsang *et al*., Individual Correlates of Infectivity of Influenza A Virus Infections in Households. *PLOS ONE* **11**, e0154418 (2016). doi: 10.1371/journal.pone.0154418; pmid: 27153194
12. E. A. Meyerowitz, A. Richterman, I. I. Bogoch, N. Low, M. Cevik, Towards an accurate and systematic characterisation of persistently asymptomatic infection with SARS-CoV-2. *Lancet Infect. Dis.* S1473-3099(20)30837-9 (2020). doi: 10.1016/S1473-3099(20)30837-9; pmid: 33301725
13. A. Fontanet *et al*., SARS-CoV-2 infection in schools in a northern French city: A retrospective serological cohort study in an area of high transmission, France, January to April 2020. *Euro Surveill.* **26**, 2001695 (2021). doi: 10.2807/1560-7917.ES.2021.26.15.2001695
14. C. Stein-Zamir *et al*., A large COVID-19 outbreak in a high school 10 days after schools' reopening, Israel, May 2020. *Euro Surveill.* **25**, (2020). doi: 10.2807/1560-7917.ES.2020.25.29.2001352; pmid: 32720636
15. I. W. Pray *et al*., COVID-19 Outbreak at an Overnight Summer School Retreat - Wisconsin, July-August 2020. *MMWR Morb. Mortal. Wkly. Rep.* **69**, 1600–1604 (2020). doi: 10.15585/mmwr.mm6943a4; pmid: 33119558
16. J. P. Torres *et al*., SARS-CoV-2 antibody prevalence in blood in a large school community subject to a Covid-19 outbreak: A cross-sectional study. *Clin. Infect. Dis.* ciaa955 (2020). doi: 10.1093/cid/ciaa955; pmid: 32649743
17. M. H. Ebell, C. Chupp, M. Bentivegna, A high proportion of SARS-CoV-2-infected university students are asymptomatic. *J. Fam. Pract.* **69**, 428–429 (2020). pmid: 33176345
18. S. M. Kissler *et al*., Viral dynamics of SARS-CoV-2 infection and the predictive value of repeat testing. medRxiv 20217042 [preprint]. 23 October 2020. pmid: 20217042
19. R. Wölfel *et al*., Virological assessment of hospitalized patients with COVID-2019. *Nature* **581**, 465–469 (2020). doi: 10.1038/s41586-020-2196-x; pmid: 32235945
20. R. A. P. M. Perera *et al*., SARS-CoV-2 Virus Culture and Subgenomic RNA for Respiratory Specimens from Patients with Mild Coronavirus Disease. *Emerg. Infect. Dis.* **26**, 2701–2704 (2020). doi: 10.3201/eid2611.203219; pmid: 32749957
21. A. Endo, S. Abbott, A. J. Kucharski, S. Funk, Centre for the Mathematical Modelling of Infectious Diseases COVID-19 Working Group, Estimating the overdispersion in COVID-19 transmission using outbreak sizes outside China. *Wellcome Open Res.* **5**, 67 (2020). doi: 10.12688/wellcomeopenres.15842.3; pmid: 32685698
22. K. Sun *et al*., Transmission heterogeneities, kinetics, and controllability of SARS-CoV-2. *Science* **371**, eabe2424 (2021). pmid: 33234698
23. N. J. Lennon *et al*., Comparison of viral levels in individuals with or without symptoms at time of COVID-19 testing among 32,480 residents and staff of nursing homes and assisted living facilities in Massachusetts. *Open Forum Infect. Dis.* **7** (suppl. 1), 848–849 (2020). doi: 10.1093/ofid/ofaa515.1908
24. R. Laxminarayan *et al*., Epidemiology and transmission dynamics of COVID-19 in two Indian states. *Science* **370**, 691–697 (2020). doi: 10.1126/science.abd7672; pmid: 33154136
25. T. Suess *et al*., Comparison of shedding characteristics of seasonal influenza virus (sub)types and influenza A(H1N1)pdm09; Germany, 2007-2011. *PLOS ONE* **7**, e51653 (2012). doi: 10.1371/journal.pone.0051653; pmid: 23240050
26. M. Loeb *et al*., Longitudinal study of influenza molecular viral shedding in Hutterite communities. *J. Infect. Dis.* **206**, 1078–1084 (2012). doi: 10.1093/infdis/jis450; pmid: 22837493
27. B. J. Cowling *et al*., Comparative epidemiology of pandemic and seasonal influenza A in households. *N. Engl. J. Med.* **362**, 2175–2184 (2010). doi: 10.1056/NEJMoa0911530; pmid: 20558368
28. D. K. M. Ip *et al*., Viral Shedding and Transmission Potential of Asymptomatic and Paucisymptomatic Influenza Virus Infections in the Community. *Clin. Infect. Dis.* **64**, 736–742 (2017). pmid: 28011603
29. N. H. L. Leung, C. Xu, D. K. M. Ip, B. J. Cowling, The Fraction of Influenza Virus Infections That Are Asymptomatic: A Systematic Review and Meta-analysis. *Epidemiology* **26**, 862–872 (2015). doi: 10.1097/EDE.0000000000000340; pmid: 26133025
30. L. P. Moreira *et al*., Respiratory syncytial virus evaluation among asymptomatic and symptomatic subjects in a university hospital in Sao Paulo, Brazil, in the period of 2009-2013. *Influenza Other Respir. Viruses* **12**, 326–330 (2018). doi: 10.1111/irv.12518; pmid: 29078028
31. D. Jacot, G. Greub, K. Jaton, O. Opota, Viral load of SARS-CoV-2 across patients and compared to other respiratory viruses. *Microbes Infect.* **22**, 617–621 (2020). doi: 10.1016/j.micinf.2020.08.004; pmid: 32911086
32. T. Heald-Sargent *et al*., Age-Related Differences in Nasopharyngeal Severe Acute Respiratory Syndrome Coronavirus 2 (SARS-CoV-2) Levels in Patients With Mild to Moderate Coronavirus Disease 2019 (COVID-19). *JAMA Pediatr.* **174**, 902–903 (2020). doi: 10.1001/jamapediatrics.2020.3651; pmid: 32745201
33. L. M. Yonker *et al*., Pediatric SARS-CoV-2: Clinical Presentation, Infectivity, and Immune Responses. *J. Pediatr.* **227**, 45–52.e5 (2020). doi: 10.1016/j.jpeds.2020.08.037; pmid: 32827525
34. S. Baggio *et al*., SARS-CoV-2 viral load in the upper respiratory tract of children and adults with early acute COVID-19. *Clin. Infect. Dis.* ciaa1157 (2020). doi: 10.1093/cid/ciaa1157; pmid: 32761228
35. A. Singanayagam *et al*., Duration of infectiousness and correlation with RT-PCR cycle threshold values in cases of COVID-19, England, January to May 2020. *Euro Surveill.* **25**, (2020). doi: 10.2807/1560-7917.ES.2020.25.32.2001483; pmid: 32794447
36. V. M. Corman *et al*., Comparison of seven commercial SARS-CoV-2 rapid point-of-care antigen tests: a single-centre

laboratory evaluation study. *Lancet Microbe* 10.1016/S2666-5247(21)00056-2 (2021). doi: 10.1001/jamapediatrics.2020.3988; pmid: 32857112
37. M. S. Han *et al*., Clinical Characteristics and Viral RNA Detection in Children With Coronavirus Disease, 2019 in the Republic of Korea. *JAMA Pediatr.* **175**, 73–80 (2021). doi: 10.1001/jamapediatrics.2020.3988; pmid: 32857112
38. C. A. Pierce *et al*., Natural mucosal barriers and COVID-19 in children. *JCI Insight* **6**, e148694 (2021). doi: 10.1172/jci.insight.148694; pmid: 33822777
39. Q. Li *et al*., Early Transmission Dynamics in Wuhan, China, of Novel Coronavirus-Infected Pneumonia. *N. Engl. J. Med.* **382**, 1199–1207 (2020). doi: 10.1056/NEJMoa2001316; pmid: 31995857
40. L. Ferretti *et al*., The timing of COVID-19 transmission. medRxiv [preprint]. 7 September 2020. pmid: 20188516
41. X. He *et al*., Temporal dynamics in viral shedding and transmissibility of COVID-19. *Nat. Med.* **26**, 672–675 (2020). doi: 10.1038/s41591-020-0869-5; pmid: 32296168
42. C. McAloon *et al*., Incubation period of COVID-19: A rapid systematic review and meta-analysis of observational research. *BMJ Open* **10**, e039652 (2020). doi: 10.1136/bmjopen-2020-039652; pmid: 32801208
43. P. Banka, C. Comiskey, The incubation period of COVID-19: A scoping review and meta-analysis to aid modelling and planning. MedRxiv 20216143 [preprint]. 3 November 2020.
44. B. Rai, A. Shukla, L. K. Dwivedi, Incubation period for COVID-19: A systematic review and meta-analysis. *J. Public Health* 10.1007/s10389-021-01478-1 (2021). doi: 10.1007/s10389-021-01478-1; pmid: 33643779
45. J. Bullard *et al*., Predicting infectious SARS-CoV-2 from diagnostic samples. *Clin. Infect. Dis.* **71**, 2663–2666 (2020). doi: 10.1093/cid/ciaa638
46. M. M. Arons *et al*., Presymptomatic SARS-CoV-2 Infections and Transmission in a Skilled Nursing Facility. *N. Engl. J. Med.* **382**, 2081–2090 (2020). doi: 10.1056/NEJMoa2008457; pmid: 32329971
47. R. Challen *et al*., Risk of mortality in patients infected with SARS-CoV-2 variant of concern 202012/1: Matched cohort study. *BMJ* **372**, n579 (2021). pmid: 33687922
48. K. R. W. Emary, T. Golubchik, Efficacy of ChAdOx1 nCoV-19 (AZD1222) vaccine against SARS-CoV-2 VOC 202012/01 (B.1.1.7). SSRN [preprint]. 4 February 2021; https://ssrn.com/abstract=3779160.
49. M. D. Parker *et al*., Altered subgenomic RNA expression in SARS-CoV-2 B.1.1.7 infections. bioRxiv 433156 [preprint]. 4 March 2021. pmid: 433156
50. M. Kidd *et al*., S-variant SARS-CoV-2 lineage B1.1.7 is associated with significantly higher viral loads in samples tested by TaqPath Polymerase Chain Reaction. *J. Infect. Dis.* jiab082 (2021). doi: 10.1093/infdis/jiab082; pmid: 33580259
51. T. Golubchik *et al*., COVID-19 Genomics UK (COG-UK) Consortium, Early analysis of a potential link between viral load and the N501Y mutation in the SARS-COV-2 spike protein. medRxiv 20249080 [preprint]. 15 January 2021. pmid: 20249080
52. S. Kissler *et al*., "Densely sampled viral trajectories suggest longer duration of acute infection with B.1.1.7 variant relative to non-B.1.1.7 SARS-CoV-2" (Harvard T. H. Chan School of Public Health, 2021); https://dash.harvard.edu/handle/1/37366884.
53. Public Health England, "Investigation of novel SARS-CoV-2 Variant of Concern 202012/01: Technical briefing 5" (2021).
54. K. Leung, M. H. Shum, G. M. Leung, T. T. Lam, J. T. Wu, Early transmissibility assessment of the N501Y mutant strains of SARS-CoV-2 in the United Kingdom, October to November 2020. *Euro Surveill.* **26**, (2021). doi: 10.2807/1560-7917.ES.2020.26.1.2002106; pmid: 33413740
55. N. G. Davies *et al*., Estimated transmissibility and impact of SARS-CoV-2 lineage B.1.1.7 in England. *Science* **372**, eabg3055 (2021). doi: 10.1126/science.abg3055; pmid: 33658326
56. R. Li *et al*., Substantial undocumented infection facilitates the rapid dissemination of novel coronavirus (SARS-CoV-2). *Science* **368**, 489–493 (2020). doi: 10.1126/science.abb3221; pmid: 32179701
57. Public Health England, "Investigation of novel SARS-CoV-2 Variant of Concern 202012/01: Technical briefing 1" (2020).
58. P.-C. Bürkner, brms: An R Package for Bayesian Multilevel Models Using Stan. *J. Stat. Softw.* **80**, (2017). doi: 10.18637/jss.v080.i01
59. P.-C. Bürkner, Advanced Bayesian Multilevel Modeling with the R Package brms. *R J.* **10**, 395 (2018). doi: 10.32614/RJ-2018-017
60. R Core Team, *R: A Language and Environment for Statistical Computing* (R Foundation for Statistical Computing, 2020); www.R-project.org/.
61. K. Basile *et al*., Cell-based culture of SARS-CoV-2 informs infectivity and safe de-isolation assessments during COVID-19. *Clin. Infect. Dis.* ciaa1579 (2020). doi: 10.1093/cid/ciaa1579; pmid: 33098412
62. B. La Scola *et al*., Viral RNA load as determined by cell culture as a management tool for discharge of SARS-CoV-2 patients from infectious disease wards. *Eur. J. Clin. Microbiol. Infect. Dis.* **39**, 1059–1061 (2020). doi: 10.1007/s10096-020-03913-9; pmid: 32342252
63. J. J. A. van Kampen *et al*., Duration and key determinants of infectious virus shedding in hospitalized patients with coronavirus disease-2019 (COVID-19). *Nat. Commun.* **12**, 267 (2021). doi: 10.1038/s41467-020-20568-4; pmid: 33431879
64. M. Widera *et al*., Surveillance of SARS-CoV-2 in Frankfurt am Main from October to December 2020 Reveals High Viral Diversity Including Spike Mutation N501Y in B.1.1.70 and B.1.1.7. *Microorganisms* **9**, 748 (2021). doi: 10.3390/microorganisms9040748; pmid: 33918332
65. T. Toptan *et al*., Evaluation of a SARS-CoV-2 rapid antigen test: Potential to help reduce community spread? *J. Clin. Virol.* **135**, 104713 (2021). doi: 10.1016/j.jcv.2020.104713; pmid: 33352470
66. S. Herberhold, A.-M. Eis-Hübinger, M. Panning, Frequent detection of respiratory viruses by real-time PCR in adenoid samples from asymptomatic children. *J. Clin. Microbiol.* **47**, 2682–2683 (2009). doi: 10.1128/JCM.00899-09; pmid: 19494063
67. F. M. Liotti *et al*., Assessment of SARS-CoV-2 RNA Test Results Among Patients Who Recovered From COVID-19 With Prior Negative Results. *JAMA Intern. Med.* **181**, 702–704 (2021). doi: 10.1001/jamainternmed.2020.7570; pmid: 33180119
68. R. L. Tillett *et al*., Genomic evidence for reinfection with SARS-CoV-2: A case study. *Lancet Infect. Dis.* **21**, 52–58 (2021). doi: 10.1016/S1473-3099(20)30764-7; pmid: 33058797
69. K. K.-W. To *et al*., Coronavirus Disease 2019 (COVID-19) Re-infection by a Phylogenetically Distinct Severe Acute Respiratory Syndrome Coronavirus 2 Strain Confirmed by Whole Genome Sequencing. *Clin. Infect. Dis.* **9**, 1664 (2020).
70. P. Simmonds, S. Williams, H. Harvala, Understanding the outcomes of COVID-19 – does the current model of an acute respiratory infection really fit? *J. Gen. Virol.* **102**, 10.1099/jgv.0.001545 (2020). doi: 10.1099/jgv.0.001545; pmid: 33331810
71. M. Perry, simanneal: A Python Module for Simulated Annealing Optimization; https://github.com/perrygeo/simanneal.
72. Stan Development Team, Stan Modeling Language Users Guide and Reference Manual (version 2.25); https://mc-stan.org.
73. Y. Liu *et al*., Viral dynamics in mild and severe cases of COVID-19. *Lancet Infect. Dis.* **20**, 656–657 (2020). doi: 10.1016/S1473-3099(20)30232-2; pmid: 32199493
74. K. K.-W. To *et al*., Temporal profiles of viral load in posterior oropharyngeal saliva samples and serum antibody responses during infection by SARS-CoV-2: An observational cohort study. *Lancet Infect. Dis.* **20**, 565–574 (2020). doi: 10.1016/S1473-3099(20)30196-1; pmid: 32213337
75. S. Greenland, Principles of multilevel modelling. *Int. J. Epidemiol.* **29**, 158–167 (2000). doi: 10.1093/ije/29.1.158; pmid: 10750618
76. F. Kurth *et al*., Studying the pathophysiology of coronavirus disease 2019: A protocol for the Berlin prospective COVID-19 patient cohort (Pa-COVID-19). *Infection* **48**, 619–626 (2020). doi: 10.1007/s15010-020-01464-x; pmid: 32535877
77. C. Thibeault *et al*., Clinical and virological characteristics of hospitalised COVID-19 patients in a German tertiary care centre during the first wave of the SARS-CoV-2 pandemic: A prospective observational study. *Infection* 10.1007/s15010-021-01594-w (2021). doi: 10.1007/s15010-021-01594-w; pmid: 33890243
78. P. Virtanen *et al*., SciPy 1.0: Fundamental algorithms for scientific computing in Python. *Nat. Methods* **17**, 261–272 (2020). doi: 10.1038/s41592-019-0686-2; pmid: 32015543
79. W. McKinney, Data Structures for Statistical Computing in Python. In *Proceedings of the 9th Python in Science Conference* (2010). doi: 10.25080/majora-92bf1922-00a
80. S. Seabold, J. Perktold, Statsmodels: Econometric and Statistical Modeling with Python. In *Proceedings of the 9th Python in Science Conference* (2010). doi: 10.25080/majora-92bf1922-011
81. J. D. Hunter, Matplotlib: A 2D Graphics Environment. *Comput. Sci. Eng.* **9**, 90–95 (2007). doi: 10.1109/MCSE.2007.55
82. T. Oliphant, *Guide to NumPy* (CreateSpace, ed. 2, 2015).
83. M. Parker, seaborn_sinaplot; https://github.com/mparker2/seaborn_sinaplot.
84. M. Waskom *et al*., seaborn: v0.5.0 (2014); DOI: 10.5281/zenodo.12710.
85. B. Langmead, S. L. Salzberg, Fast gapped-read alignment with Bowtie 2. *Nat. Methods* **9**, 357–359 (2012). doi: 10.1038/nmeth.1923; pmid: 22388286
86. P. Danecek *et al*., Twelve years of SAMtools and BCFtools. *Gigascience* **10**, giab008 (2021). doi: 10.1093/gigascience/giab008; pmid: 33590861
87. J. K. Bonfield *et al*., HTSlib: C library for reading/writing high-throughput sequencing data. *Gigascience* **10**, giab007 (2021). doi: 10.1093/gigascience/giab007; pmid: 33594436
88. G. Dick, *Genomic Approaches in Earth and Environmental Sciences* (Wiley, 2018).
89. N. D. Grubaugh *et al*., An amplicon-based sequencing framework for accurately measuring intrahost virus diversity using PrimalSeq and iVar. *Genome Biol.* **20**, 8 (2019). doi: 10.1186/s13059-018-1618-7; pmid: 30621750
90. K. Katoh, D. M. Standley, MAFFT multiple sequence alignment software version 7: Improvements in performance and usability. *Mol. Biol. Evol.* **30**, 772–780 (2013). doi: 10.1093/molbev/mst010; pmid: 23329690
91. B. Goodrich, J. Gabry, I. Ali, S. Brilleman, rstanarm: Bayesian applied regression modeling via Stan (2020); https://mc-stan.org/rstanarm.
92. B. Carpenter *et al*., Stan: A Probabilistic Programming Language. *J. Stat. Softw.* **76**, (2017). doi: 10.18637/jss.v076.i01
93. M. Dowle, A. Srinivasan, data.table: Extension of 'data.frame' (2020).
94. H. Wickham, *ggplot2: Elegant Graphics for Data Analysis* (Springer, 2016).
95. O. Tange, GNU Parallel 20201122 ('Biden') (2020); www.gnu.org/software/parallel/.
96. H. B. Mann, D. R. Whitney, On a Test of Whether One of Two Random Variables is Stochastically Larger than the Other. *Ann. Math. Stat.* **18**, 50–60 (1947). doi: 10.1214/aoms/1177730491
97. Additional statistical information and the R code and data to reproduce the results, figures, and tables are available at https://doi.org/10.5281/zenodo.4774226.

ACKNOWLEDGMENTS

Computation was performed on the HPC for Research/Clinic cluster of the Berlin Institute of Health, supported by D. Beule, M. Holtgrewe, and O. Stolpe. We thank U. Gieraths and L. Meiners for careful commentary on the manuscript, T. D. Best for compiling cell culture isolation data, the Charité–Universitätsmedizin Pa-COVID-19 collaborative study group for providing additional onset of symptoms data, and S. Kissler for providing additional details regarding their NBA study. The conditions allowing the work to be done with no need for consent are given at https://gesetze.berlin.de/bsbe/document/jlr-KHGBE2011V4P25. **Funding:** Work at Charité–Universitätsmedizin Institute of Virology is funded by European Commission via project ReCoVer, German Federal Ministry of Education and Research (Bundesministerium für Bildung und Forschung) through projects DZIF (301-4-7-01.703) to C.D.; VARIPath (01KI2021) to V.M.C.; PROVID (FKZ 01KI20160C) to C.D., V.M.C., and L.E.S.; and NaFoUniMedCovid19 (NUM)–COVIM (FKZ 01KX2021) to C.D., V.M.C., and L.E.S. The Pa-COVID 19 Study is supported by grants from the Berlin Institute of Health. This study was supported in part by the German Ministry of Health (Konsiliarlabor für Coronaviren and SeCoV) to C.D. and V.M.C. T.C.J. is in part funded through NIAID-NIH CEIRS contract HHSN272201400008C. **Author contributions:** T.C.J., G.B., B.M.: bioinformatic processing, statistical analysis, interpretation of results, writing of original draft and final text; T.V.: statistical analysis, interpretation of results, writing of original draft and final text, next-generation sequencing; J.S., J.B.-S., T.B., J.T., M.L.S.: sample preparation, virus isolation and culturing, RT-PCR, next-generation sequencing; L.E.S., F.K.: collection of symptom onset data; P.M., R.S., M.Z., J.H., A.K., A.S., A.E.: diagnostic work and collection of raw data; V.M.C.: diagnostic data collection, viral load calibration, supervision of laboratory work, interpretation of results; C.D.: project concept, interpretation of results, writing of original draft and final text. **Competing interests:** The authors declare that they have no

competing interests. **Data and materials availability:** Additional statistical information and the R code and data to reproduce the results, figures, and tables are available (*97*).

SUPPLEMENTARY MATERIALS

science.sciencemag.org/content/373/6551/eabi5273/suppl/DC1
Supplementary Text
Figs. S1 to S17
Tables S1 to S5
References (*98*–*102*)
MDAR Reproducibility Checklist

15 March 2021; accepted 21 May 2021
Published online 25 May 2021
10.1126/science.abi5273

Science

Estimating infectiousness throughout SARS-CoV-2 infection course

Terry C. Jones, Guido Biele, Barbara Mühlemann, Talitha Veith, Julia Schneider, Jörn Beheim-Schwarzbach, Tobias Bleicker, Julia Tesch, Marie Luisa Schmidt, Leif Erik Sander, Florian Kurth, Peter Menzel, Rolf Schwarzer, Marta Zuchowski, Jörg Hofmann, Andi Krumbholz, Angela Stein, Anke Edelmann, Victor Max Corman and Christian Drosten

Science **373** (6551), eabi5273.
DOI: 10.1126/science.abi5273originally published online May 25, 2021

Correlates of infectiousness

The role that individuals with asymptomatic or mildly symptomatic severe acute respiratory syndrome coronavirus 2 have in transmission of the virus is not well understood. Jones *et al.* investigated viral load in patients, comparing those showing few, if any, symptoms with hospitalized cases. Approximately 400,000 individuals, mostly from Berlin, were tested from February 2020 to March 2021 and about 6% tested positive. Of the 25,381 positive subjects, about 8% showed very high viral loads. People became infectious within 2 days of infection, and in hospitalized individuals, about 4 days elapsed from the start of virus shedding to the time of peak viral load, which occurred 1 to 3 days before the onset of symptoms. Overall, viral load was highly variable, but was about 10-fold higher in persons infected with the B.1.1.7 variant. Children had slightly lower viral loads than adults, although this difference may not be clinically significant.

Science, abi5273, this issue p. eabi5273

Science (print ISSN 0036-8075; online ISSN 1095-9203) is published by the American Association for the Advancement of Science, 1200 New York Avenue NW, Washington, DC 20005. The title *Science* is a registered trademark of AAAS.

Virological and serological kinetics of SARS-CoV-2 Delta variant vaccine-breakthrough infections: a multi-center cohort study

Po Ying Chia, MBBS[1,2,4]; Sean Wei Xiang Ong, MBBS[1,2]; Calvin J Chiew, MPH[1,3]; Li Wei Ang, MSc[1]; Jean-Marc Chavatte PhD[1]; Tze-Minn Mak, PhD[1]; Lin Cui, PhD[1]; Shirin Kalimuddin, MPH[5,6]; Wan Ni Chia, PhD[6]; Chee Wah Tan, PhD[6]; Louis Yi Ann Chai, PhD[7,8]; Seow Yen Tan, MBBS[9]; Shuwei Zheng, MBBS[10]; Raymond Tzer Pin Lin, MBBS[1]; Linfa Wang, PhD[6], Yee-Sin Leo, MPH[1,2,4,8]; Vernon J Lee, PhD[3]; David Chien Lye, MBBS[1,2,4,8]; Barnaby Edward Young, MB BChir[1,2,4]

[1] National Centre for Infectious Diseases, Singapore
[2] Tan Tock Seng Hospital, Singapore
[3] Ministry of Health, Singapore
[4] Lee Kong Chian School of Medicine, Nanyang Technological University, Singapore
[5] Singapore General Hospital, Singapore
[6] Duke-NUS Medical School, National University of Singapore, Singapore
[7] National University Health System, Singapore
[8] Yong Loo Lin School of Medicine, National University of Singapore, Singapore
[9] Changi General Hospital, Singapore
[10] Sengkang General Hospital, Singapore

Running title: Delta VOC: Viral Kinetics for Vaccinated

Corresponding Author:

Barnaby Young, National Centre for Infectious Diseases, 16 Jln Tan Tock Seng, Singapore 308442

E-mail: Barnaby_young@ncid.sg; Telephone: (+65) 6256 6011

Keywords: COVID-19; SARS-CoV-2; breakthrough infection; delta; variants of concern; vaccine breakthrough; vaccination

Objectives

Highly effective vaccines against severe acute respiratory syndrome coronavirus 2 (SARS-CoV-2) have been developed but variants of concerns (VOCs) with mutations in the spike protein are worrisome, especially B.1.617.2 (Delta) which has rapidly spread across the world. We aim to study if vaccination alters virological and serological kinetics in breakthrough infections.

Methods

We conducted a multi-centre retrospective cohort study of patients in Singapore who had received a licensed mRNA vaccine and been admitted to hospital with B.1.617.2 SARS-CoV-2 infection. We compared the clinical features, virological and serological kinetics (anti-nucleocapsid, anti-spike and surrogate virus neutralization titres) between fully vaccinated and unvaccinated individuals.

Results

Of 218 individuals with B.1.617.2 infection, 84 had received a mRNA vaccine of which 71 were fully vaccinated, 130 were unvaccinated and 4 received a non-mRNA. Despite significantly older age in the vaccine breakthrough group, the odds of severe COVID-19 requiring oxygen supplementation was significantly lower following vaccination (adjusted odds ratio 0.07 95%CI: 0.015-0.335, p=0.001). PCR cycle threshold (Ct) values were similar between both vaccinated and unvaccinated groups at diagnosis, but viral loads decreased faster in vaccinated individuals. Early, robust boosting of anti-spike protein antibodies was observed in vaccinated patients, however, these titers were significantly lower against B.1.617.2 as compared with the wildtype vaccine strain.

Conclusion

The mRNA vaccines are highly effective at preventing symptomatic and severe COVID-19 associated with B.1.617.2 infection. Vaccination is associated with faster decline in viral RNA load and a robust serological response. Vaccination remains a key strategy for control of COVID-19 pandemic.

Background

Availability of effective vaccines against severe acute respiratory syndrome coronavirus 2 (SARS-CoV-2) within one year of the first report of coronavirus disease 2019 (COVID-19) is remarkable. Phase 3 clinical trials of messenger RNA (mRNA) vaccines have demonstrated 92-95% efficacy in preventing symptomatic infection and severe disease [1-4] and intensive vaccination programs have reduced infection and mortality rates in multiple settings [5-7].

Emerging variants of concern (VOCs), such as B.1.1.7 (Alpha in the World Health Organization classification), B.1.351 (Beta), P.1 (Gamma), and B.1.617.2 (Delta) exhibit varied sequence changes and alteration of amino acid sequences of the spike protein. This has led to concerns of viral immune evasion and decreased vaccine effectiveness. Furthermore, these VOCs have been shown to be more transmissible [8-10], and B.1.1.7 and B.1.617.2 has been associated with increased disease severity and hospitalization [11, 12]. B.1.617.2 has rapidly spread outside India, becoming the most frequently sequenced lineage worldwide by end of June 2021 [13]. Case series of vaccine-breakthrough infections have reported an over-representation by these VOCs [14, 15].

Understanding vaccine effectiveness in the context of VOCs requires granular data: which vaccines were administered, at what time point prior to infection, number of doses, and particularly which VOC has caused the infection. Important VOC-specific vaccination outcomes include severity of infection and vaccine effects on transmission.

The COVID-19 vaccination program was initiated in Singapore on 30 December 2020, with free vaccinations provided to all Singapore residents in phases, beginning with the elderly and those in high-risk occupations such as healthcare workers. Vaccines used are mRNA vaccines, Pfizer/BioNTech BNT162b2 and Moderna mRNA-1273. As of 19 July 2021, 6,837,200 vaccine doses had been administered and ~2,792,430 individuals (47% of the total population) had completed the vaccination course [16]. In May 2021, B.1.617.2 became the dominant circulating variant based on local sequencing data.

In this multi-center cohort study, we characterize the clinical features, virological and serological kinetics of patients with vaccine-breakthrough PCR-confirmed B.1.617.2 infection and compared them with unvaccinated patients.

Methods

Patient Recruitment

Adults aged ≥18 years with COVID-19 confirmed by positive SARS-CoV-2 PCR and admitted to any of the five study sites from 1 April to 14 June 2021 were screened. Patients with B.1.617.2 infection (identification methods delineated below) were included in this analysis. Vaccine-breakthrough infection was defined as PCR-confirmed COVID-19 with symptom onset or first positive PCR (whichever was earlier) ≥14 days following a second dose of BNT162b2 or mRNA-1273 vaccine. Incomplete vaccination was defined as receipt of one dose of these vaccines ≥14 days prior to symptom onset or first positive PCR. Patients who received non-mRNA vaccines or developed infection within 14 days after the first dose were excluded from this analysis. B.1.617.2 vaccine-breakthrough infections were compared with a retrospective cohort of unvaccinated patients with B.1.617.2 infection admitted to one study site.

Data Collection

Clinical and laboratory data were collected from electronic medical records using a standardized data-collection form [17]. Laboratory data including cycle threshold (Ct) values from SARS-CoV-2 RT-PCR assays and serological results from Elecsys® (Roche, Basel, Switzerland) Anti-SARS-CoV-2 chemiluminescent immunoassays [anti-nucleocapsid (anti-N) and anti-spike protein (anti-S)] and surrogate virologic neutralization test (sVNT) cPass™ (Genscript, NJ, USA) were recorded. cPass™ detects total neutralizing antibodies targeting the viral spike protein receptor-binding domain [18]. These tests were performed as part of routine clinical care.

Additional Serologic testing

Serum samples from a subset of vaccine-breakthrough patients who had separately consented for specimen collection were additionally tested with a newly developed multiplex-sVNT assay using the Luminex platform. Further details can be found in the supplementary information.

Viral RNA sequencing and VOC determination

SARS-CoV-2 PCR was performed using various commercially available assays in different clinical laboratories. As part of active genomic surveillance, whole genome sequencing (WGS) by National Public Health Laboratory is performed for all patients in Singapore with SARS-CoV-2 detected by RT-PCR with a Ct value less than 30. Pangolin COVID-19 Lineage Assigner and CoVsurver were used to assign lineage to each sequence. For individuals with PCR confirmed infection without available sequencing results, lineage was inferred based on epidemiological investigations by the Singapore Ministry of Health (MOH), and likely B.1.617.2 infections were included (i.e., clear epidemiologic link with patients with sequencing confirmed B.1.617.2 infection).

Clinical Management

All individuals with confirmed COVID-19 (including asymptomatic cases) in Singapore are admitted to hospital for inpatient evaluation and isolation. Individuals with pneumonia requiring supplemental oxygen are treated with intravenous remdesivir, while dexamethasone and other agents were reserved for progressive infections per national guidelines [19]. Disease severity was stratified into asymptomatic, mild (no pneumonia on chest radiography), moderate (presence of pneumonia on chest radiography), severe (requiring supplemental oxygen), or critical (requiring intensive care unit [ICU] admission or mechanical ventilation). Collection of clinical data was censored on discharge from hospital.

Statistical Analysis

For descriptive analysis, data were presented as median (interquartile range (IQR)) for continuous parameters and frequency (percentage) for categorical variables. Chi-square and Fisher's exact tests

were used to compared categorical variables, while for continuous variables, t-test was used for normal data and Mann-Whitney U test for non-normal data. For asymptomatic patients, the day of confirmatory COVID-19 diagnosis was denoted as day one of illness. For symptomatic patients, the day of symptom onset or the day of confirmatory COVID-19 diagnosis, whichever earlier, was denoted as day one of illness.

Previously reported risk factors for disease severity [20] were evaluated and included in a multivariate logistic regression model [21]. For serial Ct values, we fitted a generalized additive mixed model (GAMM) with a random intercept by patient. To investigate the effect of vaccination status on rate of increase of Ct value, we included fixed factors of vaccination status and day of illness with smoothing terms and interaction between these two fixed factors. We plotted Ct values with marginal effect of day of illness by vaccination status and 95% confidence intervals (CI) from the GAMM.

For analysis of cPass™ and anti-S titres we fitted a GAMM to serial titres with random intercept by patient in addition to fixed factor of day of illness with smoothing terms, separately for vaccine-breakthrough and unvaccinated patients infected with Delta variant. We plotted cPass™/anti-S titres with marginal effect of day of illness and 95%CI from GAMM for each group of vaccine-breakthrough and unvaccinated patients.

P-values less than 0.05 were considered statistically significant, and all tests were 2-tailed. Data analyses were performed using Stata Release 15 (StataCorp, College Station, TX) and R version 3.6.2 (R Foundation for Statistical Computing, Vienna, Austria).

Ethical approval

Written informed consent was obtained from study participants of the multi-centre study approved by National Healthcare Group Domain Specific Review Board (NHG-DSRB) (Study Reference

2012/00917). Informed consent for retrospective data collection at National Centre for Infectious Diseases (NCID) was waived (NHG-DSRB reference number 2020/01122).

Results

218 B.1.617.2 infections were identified across the five study sites (Supplementary Figure S1). Of these, 71 met the definition for vaccine-breakthrough. An additional 13 only received one dose ≥14 days prior to disease onset or received both doses but within 14 days of disease onset, while four had received a non-mRNA vaccine overseas. Majority of participants meeting study definition for vaccine-breakthrough had received two doses of BNT162b2 (n=66, 93%).

Clinical Features

In line with Singapore's national vaccination strategy wherein older adults were prioritized for vaccination, our vaccine-breakthrough cohort was of significantly older age; median age of 56 years (IQR:39-64) versus 39.5 (IQR:30-58) ($p<0.001$) (Table 1). Other baseline demographics were similar.

Vaccine-breakthrough patients were significantly more likely to be asymptomatic (28.2% versus 9.2%, $p<0.001$); and if symptomatic, had fewer number of symptoms (Table 1). Unvaccinated individuals had worse levels of known biomarkers associated with increased COVID-19 severity including lymphocyte count, C-reactive protein [CRP], lactate dehydrogenase [LDH] and alanine transferase [ALT]. Correspondingly, a higher proportion of the unvaccinated cohort had pneumonia, required supplementary oxygen and ICU admission compared with the vaccinated cohort. A broader analysis comparing unvaccinated versus those who had received at least one dose of vaccine (i.e. both vaccine-breakthrough and incomplete vaccination) demonstrated similar findings (Supplementary Table T1).

Multivariate logistic regression analysis for development of severe COVID-19 (defined by supplementary oxygen requirement) demonstrated that vaccination was protective with an adjusted odds ratio (aOR) of 0.073 (95% confidence interval [CI]):0.016-0.343) ($p=0.001$) (Table 2). Analysis

comparing unvaccinated versus those who had received at least one dose of vaccine demonstrated similar findings (Supplementary Table T2). Multivariate logistic regression analysis for development of moderately severe COVID-19 (defined by development of pneumonia) also demonstrated that vaccination was protective with aOR of 0.069 (95%CI:0.027-0.180) (p<0.001) (Supplementary Table T3).

Virologic kinetics

Serial Ct values of individuals were analyzed as a surrogate marker for the viral load. The initial median initial Ct value did not differ between unvaccinated and fully vaccinated patients (unvaccinated median Ct 18.8 (14.9-22.7), vaccinated 19.2 (15.2-22.2), p=0.929). However, fully vaccinated patients had a faster rate of increase in Ct value over time compared with unvaccinated individuals, suggesting faster viral load decline (coefficient estimates for interaction terms ranged from 9.12 (standard error 3.75) to 12.06 (standard error 3.03); p-value <0.05 for each interaction terms) (Figure 1).

Serologic data

69 fully vaccinated individuals and 45 unvaccinated had serologic data available on record. 66/66 (100%) of vaccinated individuals had detectable S antibodies in week 1 of illness, while 7/45 (16%) of unvaccinated individuals did (Supplementary Figure S2). There was no difference in the proportion of individuals who seroconverted with the anti-N assay in week 1 (vaccinated 7/68 (10%) vs unvaccinated 11/107 (10%)) or week 2 (vaccinated 2/11 (18%), unvaccinated 4/20 (20%).

Analysis of sVNT with cPass indicated very high inhibition among vaccinated individuals in week 1 of illness (median 98.3% (IQR:91.0-99.4%)) which increased to 99.6% (IQR 99.3-99.9%) in week 2 (Figure 2A, 2B). Among unvaccinated individuals, median inhibition was below the 20% threshold at both week 1 and week 2. Among the 37 vaccinated individuals with a serum sample available for

193 testing by the multiplex sVNT assay, titres were significantly higher against wildtype virus compared
194 with B.1.617.2 and other VOCs (Figure 3). sVNT titres were lowest against B.1.617.2 and P.1 VOCs.

195 **Discussion**

196 In this study, we found that fully vaccinated patients had significantly lower odds of moderate or
197 severe outcomes following infection by the SARS-CoV-2 VOC B.1.617.2. Vaccination was associated
198 with lower peak measures of systemic inflammation, fewer symptoms, including more asymptomatic
199 infection, and better clinical outcomes. Notably, in contrast to existing studies that showed lower
200 viral load in vaccinated patients [22], initial viral load indicated by PCR Ct values was similar between
201 vaccinated and unvaccinated patients with B.1.617.2. However, vaccinated patients appeared to
202 clear viral load at a faster rate. Our serologic data suggest an early rapid rise in neutralizing and
203 binding antibodies indicated by C-Pass and Roche anti-S antibodies, which may be evidence of
204 memory immunity to COVID-19 vaccination on challenge with a breakthrough infection with
205 B.1.617.2.

206 As part of active case finding and surveillance in Singapore, all patients with fever or respiratory
207 symptoms, close contacts of confirmed cases, and newly arrived travelers are screened for COVID-19
208 using PCR. Additionally, high-risk individuals in frontline occupations or congregate settings are
209 tested as part of routine surveillance. All confirmed COVID-19 cases are reported to MOH and
210 admitted to a hospital for initial evaluation. As such, our hospitalized cohort uniquely captures the
211 entire spectrum of disease severity of COVID-19 infection and provides granular data even for mild
212 and asymptomatic vaccine-breakthrough infections, giving us the opportunity to analyze virologic
213 and serologic kinetics of these patients.

214 The finding of diminished severity with B.1.617.2 infection in vaccinated individuals is reassuring and
215 corroborates emerging data from the United Kingdom which have found that mRNA vaccination
216 remains protective against symptomatic and severe disease[12, 23]. An observational cohort study
217 conducted in Scotland suggested that ≥14 days after the second dose, BNT162b2 vaccine offered

92% vaccine effectiveness against presumptive non-B.1.617.2 infection and 79% protection against presumptive B.1.617.2 [24]. Protection associated with the ChAdOx1 nCoV-19 vaccine was 73% and 60% respectively. Although vaccine-breakthrough infections are increasingly reported, with the largest series to date in the United States reporting 10,262 breakthrough infections, a majority of these were mild (27% asymptomatic, 10% hospitalization, 2% mortality)[25]. Vaccine-breakthrough infections will continue to be observed, especially with genetic drift and selection pressures resulting in emergence of newer VOCs; however, it is likely that there will be a shift toward milder disease spectrum with more widespread implementation of vaccination programs.

To our knowledge, we provide the first data characterizing impact of vaccination on virologic kinetics by the B.1.617.2 variant. While initial Ct values were similar; the effect of vaccination with a more rapid decline in viral load (and hence shorter duration of viral shedding) has implications on transmissibility and infection control policy. A shorter duration of infectivity may allow a shorter duration of isolation for vaccinated individuals. Based on our data, it seems likely that vaccination reduces secondary transmission, though this needs to be further studied in larger community surveillance studies. Other studies found similar impact of vaccination on other variants. Pritchard and colleagues found that vaccinated individuals had higher Ct values compared with unvaccinated individuals in B.1.1.7 infections [7], while Levine-Tiefenbaum and colleagues similarly found a reduction in viral loads after BNT162b2 vaccine, though no data was provided on variant type [26].

There are several limitations to our study. Firstly, we only compared vaccine-breakthrough infections with unvaccinated COVID-19 patients. We did not study vaccinated individuals who had similar exposure risk but did not develop COVID-19 infection. We thus could not evaluate vaccine efficacy against asymptomatic infection. We also did not have detailed epidemiologic data to study the effect of vaccination on preventing secondary transmission.

Secondly, we could only obtain serologic tests after infection since patients were recruited after confirmation of infection. While active contact tracing and case finding in Singapore resulted in early

identification of most COVID-19 cases, the first available serologic result was at a median of 2 (IQR:1-3) days of illness and antibody levels are likely to already have been boosted by natural infection. We thus could not evaluate the underlying immunologic mechanisms behind vaccine-breakthrough infection, e.g., diminished neutralizing antibody level or impaired cellular immunity. Further study should compare similarly exposed vaccinated individuals who develop breakthrough infection with those who do not, to elucidate the underlying drivers of susceptibility, which may enlighten us on how to optimize protection (e.g., through enhanced/boosted dosing schedules).

Thirdly, PCR testing was not standardized in a centralized laboratory, and instead conducted at each centre using different validated commercial assays. Ct values are only a surrogate measure of viral load and shedding. We did not evaluate viability of shed virus via viral culture. In addition, we only evaluated participants with mRNA vaccination, and thus our findings are restricted to mRNA vaccines and not all COVID-19 vaccines.

Conclusion

mRNA vaccines against COVID-19 are protective against symptomatic infection and severe disease by the B.1.617.2 variant. Vaccinated individuals had a more rapid decline in viral load, which has implications on secondary transmission and public health policy. Rapid and widespread implementation of vaccination programs remains a key strategy for control of COVID-19 pandemic. Further studies should elucidate immunologic features driving vaccine-breakthrough infection to improve vaccine-induced protection.

Conflict of Interest Disclosures

BEY reports personal fees from Roche and Sanofi, outside the submitted work. All other authors declare no competing interests.

Acknowledgments

We thank all clinical and nursing staff who provided care for the patients and staff in the Infectious Disease Research and Training Office of the National Centre for Infectious Diseases who assisted with data collection. We will also like to thank Jeremy Cutter at the National Public Health and Epidemiology Unit of National Centre for Infectious Diseases who assisted with data management on Ct values.

Funding

This study was funded by grants from the Singapore National Medical Research Council (COVID19RF-001, COVID19RF-008). The funders had no role in the design and conduct of the study; collection, management, analysis and interpretation of the data; preparation, review or approval of the manuscript; and decision to submit the manuscript for publication.

287

288

	Unvaccinated n = 130	Vaccinated n = 71	*p*-value
Median age (IQR), years	39.5 (30-58)	56 (39-64)	<0.001
Male (%)	67 (51.5)	27 (38)	0.067
Median Charlson Comorbidity Index (IQR)	0 (0-1)	0 (0-0)	0.125
Diabetes mellitus (%)	28 (21.5)	5 (7.0)	0.008
Hypertension (%)	28 (21.5)	14 (19.7)	0.762
Hyperlipidaemia (%)	32 (24.6)	18 (25.4)	0.908
Median Ct value on diagnosis (IQR)*	18.8 (14.9-22.7)	19.2 (15.2-22.2)	0.929
Asymptomatic	12 (9.2)	20 (28.2)	<0.001
Symptom onset after Diagnosis (%)	11 (9.3)	11 (21.6)	0.030
Median day of illness symptoms start (IQR)	2 (2-3)	3 (2-3)	0.715
Median Ct values for Symptom Onset After (IQR)	21.87 (18.8-31.2)	19.2 (16.6-21.5)	0.279
Median Sum of Symptoms Reported (IQR)	2 (1-3)	1 (0-2)	<0.001
Fever (%)	96 (73.9)	29 (40.9)	<0.001
Cough (%)	79 (60.8)	27 (38)	0.002
Shortness of Breath (%)	17 (13.1)	1 (1.4)	0.004
Runny Nose (%)	31 (23.9)	27 (38)	0.034
Sore Throat (%)	43 (33.1)	18 (25.4)	0.255
Diarrhoea (%)	8 (6.2)	0	0.052
Median highest Neutrophil (IQR) $\times 10^9$/L	4.50 (3.07-5.92)	4.33 (3.52-5.43)	0.117
Median lowest Lymphocyte (IQR) $\times 10^9$/L	0.95 (0.65-1.50)	1.36 (1.02-1.87)	<0.001
Median highest C-Reactive Protein (IQR), mg/L	24.7 (6.9-84.8)	12.6 (6.5-22.5)	<0.001
Median highest Lactate Dehydrogenase (IQR), U/L	486 (365-672)	373 (314-421)	0.062
Median highest Alanine Transferase (IQR), U/L	35	19	<0.001

	(18-74)	(13-34)	
Disease Outcome			
Pneumonia (%)	69 (53.1)	9 (21.7)	<0.001
Supplementary O2 required (%)	27 (20.8)	2 (2.8)	<0.001
ICU admission required (%)	7 (5.4)	0	0.053
Median days of ICU admission required (IQR)	4 (3-9)	-	-
Intubation (%)	2 (1.5)	0	0.541
Median days of Intubation (IQR)	7 (3-11)	-	-
COVID-19 specific treatment (%)	39 (30)	5 (7)	<0.001
Mortality	2 (1.54)	0	0.541

289

290 Table 1: Baseline characteristics and disease outcome between unvaccinated and completed mRNA

291 vaccination COVID-19 B1.617.2 infected patients

292

	Univariable model		Multivariable model	
	Crude OR (95% CI)	***p*-value**	**Adjusted OR (95% CI)**	***p*-value**
Vaccinated	0.111 (0.025-0.480)	0.003	0.073 (0.016-0.343)	0.001
Age group				
<45 years old	1	-	1	-
45-64 years old	6.19 (1.90-20.2)	0.003	8.29 (2.29-30.0)	0.001
>64 years old	13 (3.90-42.9)	<0.001	13.5 (2.66-68.8)	0.002
Male	0.913 (0.414-2.01)	0.821	1.09 (0.418-2.85)	0.857
Diabetes	6.18 (2.59-14.7)	<0.001	2.24 (0.785-6.41)	0.132
Hypertension	4.8 (2.09-11.0)	<0.001	1.62 (0.509-5.18)	0.413
Presence of other comorbidities, if any	3.96 (1.66-9.44)	0.002	0.897 (0.262-3.07)	0.862

293

294 **Table 2:** Odds ratio of candidate risk factors for development of severe COVID-19 for completed

295 mRNA vaccination COVID-19 B1.617.2 infected patients. CI, confidence interval; OR, odds ratio

296

297

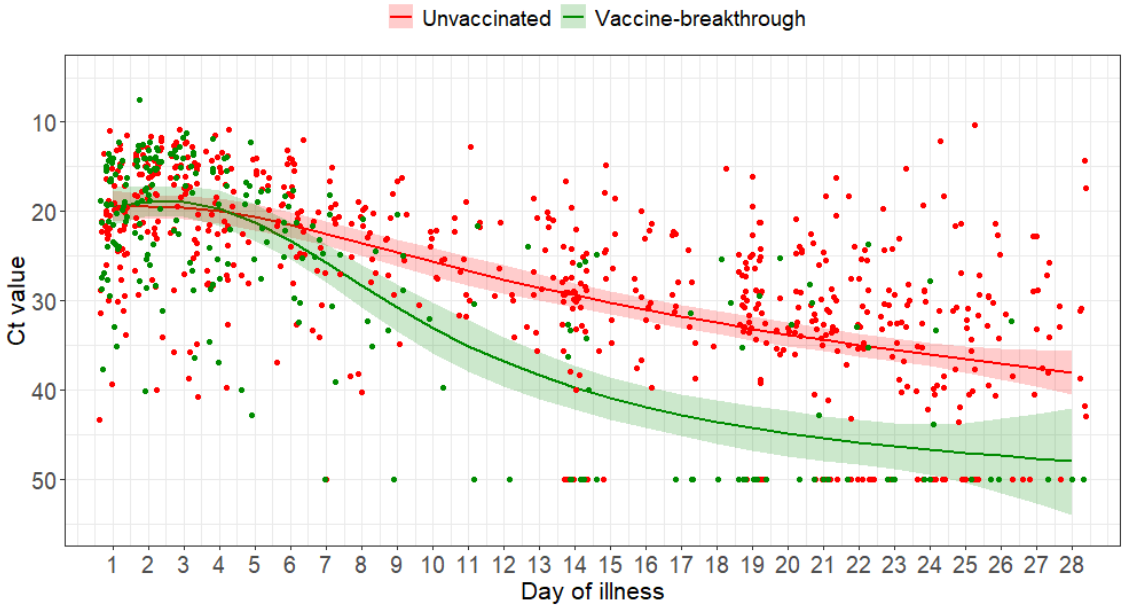

298

299 **Figure 1:** Scatterplot of Ct values and marginal effect of day of illness of COVID-19 B1.617.2 infected

300 patients with 95% confidence intervals from generalized additive mixed model with interaction term

301 between vaccination status and day of illness

302

303

304

305

306

307

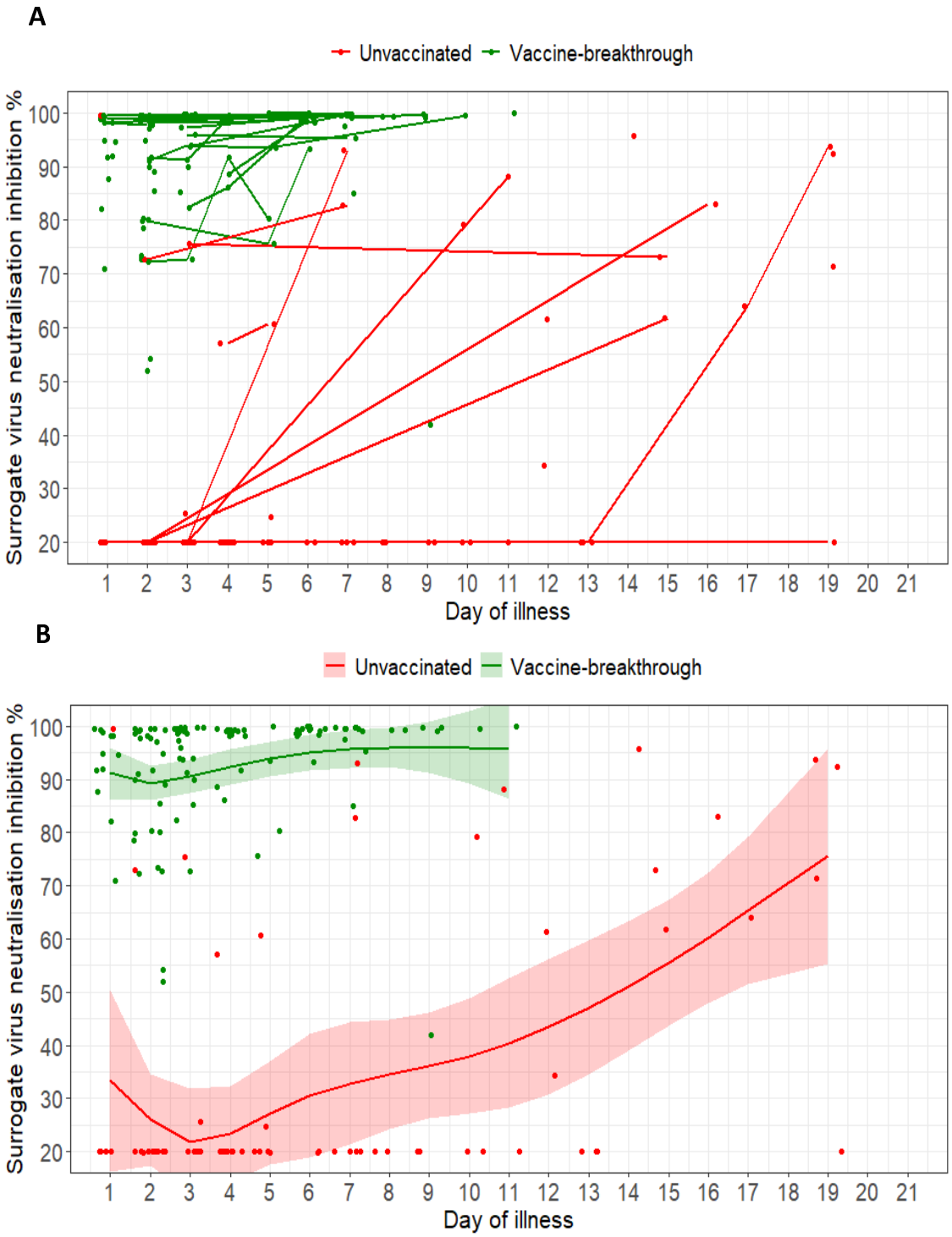

308

309

310 **Figure 2:** (A) Spaghetti plot of surrogate virus neutralisation (sVNT) inhibition % as measured by

311 cPass; (B) Scatterplot of sVNT inhibition % and marginal effect of day of illness by vaccine-

312 breakthrough and unvaccinated groups of COVID-19 B1.617.2 infected patients with 95% confidence

313 intervals from generalized additive mixed models. For both plots, n=127; vaccine-breakthrough = 67,

314 unvaccinated = 60

315

316

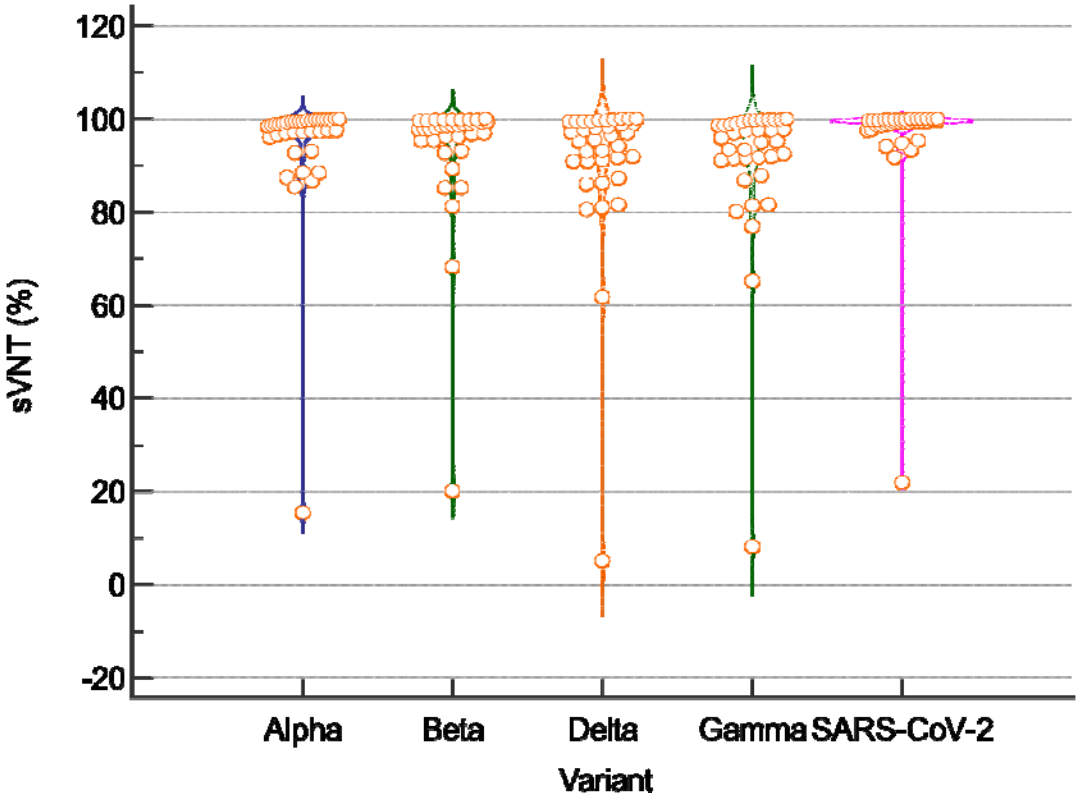

317

318 **Figure 3:** Violin plots of of surrogate virus neutralisation (sVNT) inhibition % against wildtype SARS-

319 CoV-2 and the B.1.617.2 variant for 36 patients with vaccine-breakthrough infection (median day of

320 sample collection from infection onset 6 days (inter-quartile range (IQR) 3-7). Titres against the four

321 variants were significantly lower than against wildtype SARS-CoV-2 [median sVNT, B.1.1.7 98.5%

322 (IQR: 96.3-99.5); B.1.351 98.2% (IQR: 95.3-99.5); B.1.617.2 96.0% (IQR: 90.9-99.3); P.1 95.5% (IQR:

323 91.3-98.9); Wildtype 99.4% (IQR: 98.5-99.7), Kruskal-Walis p-value = 0.00055, Post-hoc pairwise

324 comparison (Conover) Wildtype versus each variant $p<0.05$]

References

[1] F.P. Polack, S.J. Thomas, N. Kitchin, J. Absalon, A. Gurtman, S. Lockhart, J.L. Perez, G. Perez Marc, E.D. Moreira, C. Zerbini, R. Bailey, K.A. Swanson, S. Roychoudhury, K. Koury, P. Li, W.V. Kalina, D. Cooper, R.W. Frenck, Jr., L.L. Hammitt, O. Tureci, H. Nell, A. Schaefer, S. Unal, D.B. Tresnan, S. Mather, P.R. Dormitzer, U. Sahin, K.U. Jansen, W.C. Gruber, C.C.T. Group, Safety and Efficacy of the BNT162b2 mRNA Covid-19 Vaccine, N Engl J Med 383(27) (2020) 2603-2615.

[2] N. Dagan, N. Barda, E. Kepten, O. Miron, S. Perchik, M.A. Katz, M.A. Hernan, M. Lipsitch, B. Reis, R.D. Balicer, BNT162b2 mRNA Covid-19 Vaccine in a Nationwide Mass Vaccination Setting, N Engl J Med 384(15) (2021) 1412-1423.

[3] Y. Angel, A. Spitzer, O. Henig, E. Saiag, E. Sprecher, H. Padova, R. Ben-Ami, Association Between Vaccination With BNT162b2 and Incidence of Symptomatic and Asymptomatic SARS-CoV-2 Infections Among Health Care Workers, JAMA (2021).

[4] L.R. Baden, H.M. El Sahly, B. Essink, K. Kotloff, S. Frey, R. Novak, D. Diemert, S.A. Spector, N. Rouphael, C.B. Creech, J. McGettigan, S. Khetan, N. Segall, J. Solis, A. Brosz, C. Fierro, H. Schwartz, K. Neuzil, L. Corey, P. Gilbert, H. Janes, D. Follmann, M. Marovich, J. Mascola, L. Polakowski, J. Ledgerwood, B.S. Graham, H. Bennett, R. Pajon, C. Knightly, B. Leav, W. Deng, H. Zhou, S. Han, M. Ivarsson, J. Miller, T. Zaks, C.S. Group, Efficacy and Safety of the mRNA-1273 SARS-CoV-2 Vaccine, N Engl J Med 384(5) (2021) 403-416.

[5] E.J. Haas, F.J. Angulo, J.M. McLaughlin, E. Anis, S.R. Singer, F. Khan, N. Brooks, M. Smaja, G. Mircus, K. Pan, J. Southern, D.L. Swerdlow, L. Jodar, Y. Levy, S. Alroy-Preis, Impact and effectiveness of mRNA BNT162b2 vaccine against SARS-CoV-2 infections and COVID-19 cases, hospitalisations, and deaths following a nationwide vaccination campaign in Israel: an observational study using national surveillance data, Lancet 397(10287) (2021) 1819-1829.

[6] E. Vasileiou, C.R. Simpson, T. Shi, S. Kerr, U. Agrawal, A. Akbari, S. Bedston, J. Beggs, D. Bradley, A. Chuter, S. de Lusignan, A.B. Docherty, D. Ford, F.R. Hobbs, M. Joy, S.V. Katikireddi, J. Marple, C. McCowan, D. McGagh, J. McMenamin, E. Moore, J.L. Murray, J. Pan, L. Ritchie, S.A. Shah, S. Stock, F. Torabi, R.S. Tsang, R. Wood, M. Woolhouse, C. Robertson, A. Sheikh, Interim findings from first-dose mass COVID-19 vaccination roll-out and COVID-19 hospital admissions in Scotland: a national prospective cohort study, Lancet 397(10285) (2021) 1646-1657.

[7] E. Pritchard, P.C. Matthews, N. Stoesser, D.W. Eyre, O. Gethings, K.D. Vihta, J. Jones, T. House, H. VanSteenHouse, I. Bell, J.I. Bell, J.N. Newton, J. Farrar, I. Diamond, E. Rourke, R. Studley, D. Crook, T.E.A. Peto, A.S. Walker, K.B. Pouwels, Impact of vaccination on new SARS-CoV-2 infections in the United Kingdom, Nat Med (2021).

[8] N.G. Davies, S. Abbott, R.C. Barnard, C.I. Jarvis, A.J. Kucharski, J.D. Munday, C.A.B. Pearson, T.W. Russell, D.C. Tully, A.D. Washburne, T. Wenseleers, A. Gimma, W. Waites, K.L.M. Wong, K. van Zandvoort, J.D. Silverman, C.C.-W. Group, C.-G.U. Consortium, K. Diaz-Ordaz, R. Keogh, R.M. Eggo, S. Funk, M. Jit, K.E. Atkins, W.J. Edmunds, Estimated transmissibility and impact of SARS-CoV-2 lineage B.1.1.7 in England, Science (2021).

[9] H. Tegally, E. Wilkinson, M. Giovanetti, A. Iranzadeh, V. Fonseca, J. Giandhari, D. Doolabh, S. Pillay, E.J. San, N. Msomi, K. Mlisana, A. von Gottberg, S. Walaza, M. Allam, A. Ismail, T. Mohale, A.J. Glass, S. Engelbrecht, G. Van Zyl, W. Preiser, F. Petruccione, A. Sigal, D. Hardie, G. Marais, N.Y. Hsiao, S. Korsman, M.A. Davies, L. Tyers, I. Mudau, D. York, C. Maslo, D. Goedhals, S. Abrahams, O. Laguda-Akingba, A. Alisoltani-Dehkordi, A. Godzik, C.K. Wibmer, B.T. Sewell, J. Lourenco, L.C.J. Alcantara, S.L. Kosakovsky Pond, S. Weaver, D. Martin, R.J. Lessells, J.N. Bhiman, C. Williamson, T. de Oliveira, Detection of a SARS-CoV-2 variant of concern in South Africa, Nature 592(7854) (2021) 438-443.

[10] R. Pung, T.M. Mak, A.J. Kucharski, V.J. Lee, Serial intervals observed in SARS-CoV-2 B.1.617.2 variant cases, medRxiv (2021) 2021.06.04.21258205.

[11] N.G. Davies, C.I. Jarvis, C.C.-W. Group, W.J. Edmunds, N.P. Jewell, K. Diaz-Ordaz, R.H. Keogh, Increased mortality in community-tested cases of SARS-CoV-2 lineage B.1.1.7, Nature (2021).

[12] A. Sheikh, J. McMenamin, B. Taylor, C. Robertson, SARS-CoV-2 Delta VOC in Scotland: demographics, risk of hospital admission, and vaccine effectiveness, Lancet 397(10293) (2021) 2461-2462.
[13] Á. O'Toole, Hill, V., and Rambaut Group, PANGO lineages International Lineage Report B.1.617.2 Report <https://cov-lineages.org/global_report_B.1.617.2.html>, (accessed 8 July 2021.).
[14] T. Kustin, N. Harel, U. Finkel, S. Perchik, S. Harari, M. Tahor, I. Caspi, R. Levy, M. Leshchinsky, S. Ken Dror, G. Bergerzon, H. Gadban, F. Gadban, E. Eliassian, O. Shimron, L. Saleh, H. Ben-Zvi, E. Keren Taraday, D. Amichay, A. Ben-Dor, D. Sagas, M. Strauss, Y. Shemer Avni, A. Huppert, E. Kepten, R.D. Balicer, D. Netzer, S. Ben-Shachar, A. Stern, Evidence for increased breakthrough rates of SARS-CoV-2 variants of concern in BNT162b2-mRNA-vaccinated individuals, Nat Med (2021).
[15] A.E. McEwen, S. Cohen, C. Bryson-Cahn, C. Liu, S.A. Pergam, J. Lynch, A. Schippers, K. Strand, E. Whimbey, N.S. Mani, A.J. Zelikoff, V.A. Makarewicz, E.R. Brown, S.A.M. Bakhash, N.R. Baker, J. Castor, R.J. Livingston, M.L. Huang, K.R. Jerome, A.L. Greninger, P. Roychoudhury, Variants of concern are overrepresented among post-vaccination breakthrough infections of SARS-CoV-2 in Washington State, Clin Infect Dis (2021).
[16] Updates on COVID-19 (Coronavirus Disease 2019) Local Situation. <https://www.moh.gov.sg/covid-19>, 2021 (accessed June 10 2021.).
[17] COVID-19 therapies and vaccine landscape, Nat Mater 19(8) (2020) 809.
[18] C.W. Tan, W.N. Chia, X. Qin, P. Liu, M.I. Chen, C. Tiu, Z. Hu, V.C. Chen, B.E. Young, W.R. Sia, Y.J. Tan, R. Foo, Y. Yi, D.C. Lye, D.E. Anderson, L.F. Wang, A SARS-CoV-2 surrogate virus neutralization test based on antibody-mediated blockage of ACE2-spike protein-protein interaction, Nat Biotechnol 38(9) (2020) 1073-1078.
[19] Treatment Guidelines for COVID-19. <https://www.ncid.sg/Health-Professionals/Diseases-and-Conditions/Pages/COVID-19.aspx>, 2021 (accessed 1 June 2021.).
[20] J.J.Y. Zhang, K.S. Lee, L.W. Ang, Y.S. Leo, B.E. Young, Risk Factors for Severe Disease and Efficacy of Treatment in Patients Infected With COVID-19: A Systematic Review, Meta-Analysis, and Meta-Regression Analysis, Clin Infect Dis 71(16) (2020) 2199-2206.
[21] J. Coveney, FIRTHLOGIT: Stata module to calculate bias reduction in logistic regression. Statistical Software Components S456948, Boston College Department of Economics, revised 25 Apr 2021., (2008).
[22] M.G. Thompson, J.L. Burgess, A.L. Naleway, H. Tyner, S.K. Yoon, J. Meece, L.E.W. Olsho, A.J. Caban-Martinez, A.L. Fowlkes, K. Lutrick, H.C. Groom, K. Dunnigan, M.J. Odean, K. Hegmann, E. Stefanski, L.J. Edwards, N. Schaefer-Solle, L. Grant, K. Ellingson, J.L. Kuntz, T. Zunie, M.S. Thiese, L. Ivacic, M.G. Wesley, J. Mayo Lamberte, X. Sun, M.E. Smith, A.L. Phillips, K.D. Groover, Y.M. Yoo, J. Gerald, R.T. Brown, M.K. Herring, G. Joseph, S. Beitel, T.C. Morrill, J. Mak, P. Rivers, B.P. Poe, B. Lynch, Y. Zhou, J. Zhang, A. Kelleher, Y. Li, M. Dickerson, E. Hanson, K. Guenther, S. Tong, A. Bateman, E. Reisdorf, J. Barnes, E. Azziz-Baumgartner, D.R. Hunt, M.L. Arvay, P. Kutty, A.M. Fry, M. Gaglani, Prevention and Attenuation of Covid-19 with the BNT162b2 and mRNA-1273 Vaccines, New England Journal of Medicine (2021).
[23] J.L. Bernal, N. Andrews, C. Gower, E. Gallagher, R. Simmons, S. Thelwall, J. Stowe, E. Tessier, N. Groves, G. Dabrera, R. Myers, C. Campbell, G. Amirthalingam, M. Edmunds, M. Zambon, K. Brown, S. Hopkins, M. Chand, M. Ramsay, Effectiveness of COVID-19 vaccines against the B.1.617.2 variant, medRxiv (2021) 2021.05.22.21257658.
[24] A. Sheikh, J. McMenamin, B. Taylor, C. Robertson, SARS-CoV-2 Delta VOC in Scotland: demographics, risk of hospital admission, and vaccine effectiveness, The Lancet 397(10293) (2021) 2461-2462.
[25] CDC COVID-19 Vaccine Breakthrough Case Investigations Team. COVID-19 Vaccine Breakthrough Infections Reported to CDC — United States, January 1–April 30, 2021. MMWR Morb Mortal Wkly Rep 2021;70:792–793. .

423 [26] M. Levine-Tiefenbrun, I. Yelin, R. Katz, E. Herzel, Z. Golan, L. Schreiber, T. Wolf, V. Nadler, A.
424 Ben-Tov, J. Kuint, S. Gazit, T. Patalon, G. Chodick, R. Kishony, Initial report of decreased SARS-CoV-2
425 viral load after inoculation with the BNT162b2 vaccine, Nat Med 27(5) (2021) 790-792.

426
427